UNIVERSITY OF WASHINGTON
DEPARTMENT OF
OCEANOGRAPHY

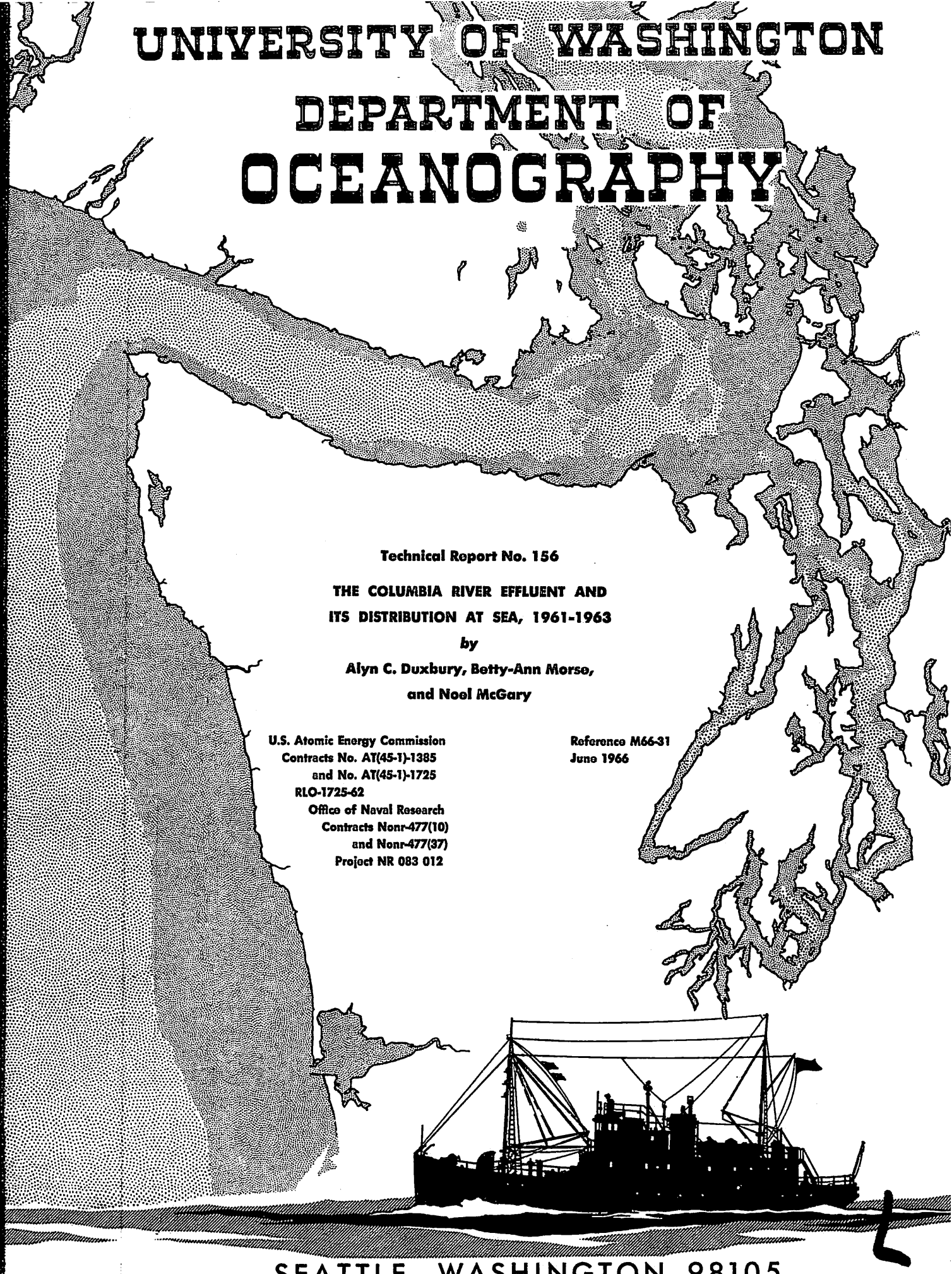

Technical Report No. 156

THE COLUMBIA RIVER EFFLUENT AND ITS DISTRIBUTION AT SEA, 1961-1963

by

Alyn C. Duxbury, Betty-Ann Morse, and Noel McGary

U.S. Atomic Energy Commission
Contracts No. AT(45-1)-1385
and No. AT(45-1)-1725
RLO-1725-62
Office of Naval Research
Contracts Nonr-477(10)
and Nonr-477(37)
Project NR 083 012

Reference M66-31
June 1966

SEATTLE, WASHINGTON 98105

UNIVERSITY OF WASHINGTON
DEPARTMENT OF OCEANOGRAPHY
Seattle, Washington 98105

Technical Report No. 156

THE COLUMBIA RIVER EFFLUENT AND ITS DISTRIBUTION AT SEA, 1961-1963

by

Alyn C. Duxbury, Betty-Ann Morse,

and Noel McGary

U.S. Atomic Energy Commission
Contracts No. AT(45-1)-1385
and No. AT(45-1)-1725
RLO-1725-62

Office of Naval Research
Contracts Nonr-477(10)
and Nonr-477(37)
Project NR 083 012

RICHARD H. FLEMING
CHAIRMAN

CLIFFORD A. BARNES
PRINCIPAL INVESTIGATOR

Reference M66-31
June 1966

ABSTRACT

Surveys off the Washington-Oregon coast by the Department of Oceanography, University of Washington, from 1961 through 1963 have provided salinity data for describing the Columbia River effluent in the Northeast Pacific Ocean. The data also have provided insight into the interactions between the observed distributions and the meteorological systems. Each salinity distribution is categorized into one of four distinct seasonal patterns, mainly influenced by river discharge and winds. The salinity distributions delineate the extent of the influence of the Columbia River effluent in the Northeast Pacific Ocean both horizontally with distance and vertically with depth. Also shown and discussed are the mean wind patterns for the area during this time period, their influence on the river outflow and their role in the transport of the dilute surface waters. A method is described for the prediction of the salinity distribution of the effluent from surface wind data.

TABLE OF CONTENTS

LIST OF FIGURES

Vertical Salinity Sections

Generalized Surface Salinity Distributions

LIST OF TABLES

INTRODUCTION

Since January 1961, the Department of Oceanography, University of Washington, has been directing a research program to determine the distribution of Columbia River water in the Northeast Pacific Ocean. The salinity data from most of the cruises during 1961 through 1963 have been analyzed and selected features are presented here to describe the observed distributions of the river effluent at sea and to establish generalized seasonal patterns based on these distributions. Salinity is convenient for defining the effluent distribution because it is easily and precisely determined and the river effluent at all seasons depresses the salinity of the seawater contiguous to the river below that of the coastal and offshore ocean waters. The distribution of this river water at sea is influenced in part by winds and river discharge rates.

The area of study, the physical characteristics of the ambient water structure, and other background information have been discussed in detail by Budinger, Coachman, and Barnes (1964) in Technical Report No. 99, hereafter referred to as T.R. 99. Additional data, beyond the material presented here, in the areas of biological, geological, chemical, and physical oceanography and meteorology recorded during the same period are available in the data summations of each cruise. Other sources of data and information related to the cruises are listed in the Appendix. The observations and descriptions presented in this report are based primarily on 35 Columbia River cruises (Table 1) conducted by this department on the RV Brown Bear and the CNAV Oshawa in conjunction with the Pacific Naval Laboratory and the Pacific Oceanographic Group of Canada. Some additional data used in the interpretation were obtained by Oregon State University's RV Acona and the MV John N. Cobb of the U.S. Fish and Wildlife Service. Listed for each cruise in Table 1 are the time periods covered, distances traveled, number of oceanographic stations sampled, and subject areas of primary interest. Most cruises of the Department of Oceanography have multiple objectives involving various subfields in oceanography. These subfields are tabulated in sequence of decreasing emphasis. Table 2 lists the technical reports containing the original oceanographic station data from these cruises.

The presentation of a detailed analysis of the observed salinity distributions for each cruise is considered beyond the scope and purpose of this report. The salinity distributions are discussed, however, in terms of four generalized seasonal patterns that largely are controlled by wind and river runoff, and each cruise has been related to one of the four seasonal patterns. The interpreted data incorporated in this report are displayed by seasonal groupings rather than in sequence of occurrence.

Table 1. Columbia River Cruises, 1961-1963

Columbia River cruise number	Ship cruise number	Period	Nautical miles[a]	Number of oceanographic stations	Major purpose by rank
		1961			
1	BB 275	10-27 January	1685	67	Physical-chemical-biological
2	BB 280	7-24 March	1585	74	Physical-chemical
3	BB 282	3-7 April	765	6	Cobb Seamount buoy test, physical-chemical-biological
4	BB 287	8-24 May	1762	82	Physical-chemical-biological
5	BB 288	9-19 June	960	53	Physical-chemical-biological-geological
6	BB 290	6-25 July	2300	77	Physical-chemical-biological
7	BB 291	28 July - 13 August	1700	28	Geological-biological-physical-chemical
8	BB 292	14-29 August	700	9	Drogue measurements, physical-chemical-biological
9	BB 293	14 September - 20 October	4155	131	Physical-chemical-biological-geological
10	BB 297	28 November - 18 December	2122	73	Physical-chemical-biological
		1962			
11	BB 299	23 January - 7 February	1644	97	Physical-chemical-biological
12	BB 304	27 March - 12 April	1775	89	Physical-chemical-biological
13	BB 308	7-19 June	959	79	Geological-physical-chemical-biological
14	BB 309	20 June - 9 July	702	89	Biological-physical-chemical
15	BB 310	10-23 July	1506	31	Physical-chemical-biological
16	BB 311	24 July - 14 August	2300	15	Geological-physical-chemical
17	BB 312	14 September - 9 October	3840	158	Physical-chemical-biological-geological

Table 1. (continued)

Columbia River cruise number	Ship cruise number	Period	Nautical miles[a]	Number of oceanographic stations	Major purpose by rank
		1963			
18	BB 318	27 February - 20 March	1965	106	Physical-chemical-biological
19	OSH 001	12-26 March	2240	70	Physical-chemical-biological
20	BB 320	28 March - 10 April	1430	39	Physical-chemical-biological
21	BB 322	16 April - 1 May	1767	97	Physical-chemical-biological
22	BB 323	13-19 May	760	27	Physical-chemical-biological
23	BB 324	21 May - 4 June	1486	140	Physical-chemical
24	OSH 002	22 May - 12 June	3383	84	Physical-chemical-biological
25	BB 326	13-23 June	791	76	Physical-chemical-biological-geological
26	OSH 003	17-30 June	2280	52	Physical-chemical-biological
27	BB 327	24 June - 1 July	634	7	Cobb Seamount buoy test, physical-chemical
28	BB 329	8-19 July	1204	38	Biological-physical-chemical
29	HH 073	7-25 August	1457	11	Joint survey with BB 331
30	BB 331	12-24 August	956	63	Inshore survey-radionuclide measurements, physical-chemical-biological-geological
31	BB 332	24-28 August	625	10	Biological-physical-chemical
32	BB 333	28 August - 14 September	1366	41	Geological-physical-chemical
33	BB 335	20 September - 26 October	3385	225	Physical-chemical-biological
34	BB 339	3-12 December	1033	67	Physical-chemical
35	OSH 004	10-20 December	1775	26	Biological-physical-chemical

[a]One nautical mile = 1.85 km.

Table 2. Original Data Sources by Cruise

Ship cruise	Department of Oceanography Technical Report number	Date of reference
Brown Bear 275	86	July 1963
Brown Bear 280	86	July 1963
Brown Bear 282	86	July 1963
Brown Bear 287	86	July 1963
Brown Bear 288	86	July 1963
Brown Bear 290	112	October 1964
Brown Bear 291	112	October 1964
Brown Bear 292	112	October 1964
Brown Bear 293	115 Vol. I	December 1964
Brown Bear 297	115 Vol. II	December 1964
Brown Bear 299	119 Vol. I	August 1965
Brown Bear 304	119 Vol. II	August 1965
Brown Bear 308	119 Vol. III	August 1965
Brown Bear 309	119 Vol. IV	August 1965
Brown Bear 310	119 Vol. III	August 1965
Brown Bear 311	119 Vol. III	August 1965
Brown Bear 312	119 Vol. V	August 1965
Brown Bear 318	134 Vol. I	March 1966
Acona 6301-E (Biol. only)	134 Vol. I	March 1966
Oshawa 001	134 Vol. II	March 1966
Brown Bear 320	134 Vol. II	March 1966
Brown Bear 322	134 Vol. III	March 1966
Betty A 001 (Biol. only)	134 Vol. III	March 1966
Brown Bear 323	134 Vol. III	March 1966
Brown Bear 324	134 Vol. IV	March 1966
Oshawa 002	134 Vol. V	March 1966
Brown Bear 326	134 Vol. VI	March 1966
Oshawa 003	134 Vol. VI	March 1966
Brown Bear 327	134 Vol. V	March 1966
Brown Bear 329	159 Vol. I	
Hoh 073	159 Vol. I	
Brown Bear 331	159 Vol. I	
Brown Bear 332	159 Vol. I	
Brown Bear 333	159 Vol. I	
Brown Bear 335 I	159 Vol. II	
Brown Bear 335 II	159 Vol. III	
Brown Bear 339	159 Vol. IV	
Oshawa 004	159 Vol. IV	

DESCRIPTION OF AREA

Columbia River Drainage Basin

The drainage basin of the 1930-km (1200-mile) long Columbia River covers approximately 670,000 km^2 (259,000 statute mi^2) (Fig. 1). The 85% of this basin within the United States constitutes 7% of the nation's continental area. The crest of the Cascade Mountains divides the watershed into two parts. The area west of the mountains discharges its water primarily during the winter and supplies most of the water contributing to the winter discharge peaks in the river flow observed at Astoria, Oregon (Fig. 2). The higher mountains and the interior plateau, comprising the major portion of the drainage basin, retain the winter precipitation as snow until the spring thaw and then release the water to produce the principal annual discharge peak of the river.

River Gaging

The volume of discharge of the Columbia River at The Dalles, Oregon, is monitored and the resulting figures are published in The Weekly Runoff Report for the Pacific Northwest by the Water Resources Division of the U.S. Geological Survey. Several of the major tributaries of the Columbia River below The Dalles are also gaged and reported in the same source. A technique for estimating the contribution of the ungaged rivers below The Dalles from their watersheds, and the gaged rivers and their watersheds, has been reported previously in T.R. 99. The following equation was taken from this report and was used in the computation of the discharge curves in Fig. 2.

$$\text{Astoria discharge} = \text{The Dalles discharge} + F_1 \left\{\begin{matrix}\text{Willamette and} \\ \text{Cowlitz discharges}\end{matrix}\right\} + F_2 \left\{\begin{matrix}\text{Hood and} \\ \text{Klickitat} \\ \text{discharges}\end{matrix}\right\}, \quad (1)$$

where F_1 and F_2 are:

	Jan.	Feb.	Mar.	Apr.	May	June	July	Aug.	Sept.	Oct.	Nov.	Dec.
F_1	1.95	2.05	1.85	2.12	1.87	1.80	1.79	1.72	1.60	2.06	1.88	1.87
F_2	2.20	2.13	1.68	1.92	1.84	2.07	2.08	2.06	1.95	1.97	1.91	1.93

Comparisons of the calculated Astoria, Oregon, discharge of the Columbia River from the preceding equation with discharge calculations made by the U.S. Army Corps of Engineers (1960) indicate that the derived discharge, equation (1), is in close agreement with the Corps of Engineers data (T.R. 99). D. V. Hansen, Department of Oceanography, University of Washington, has found that results from equation (1) also compare favorably with discharge estimates made by the U.S. Public Health Service.

Effluent Area

Surveys to determine the extent of the river effluent have covered an ocean area of approximately 420,000 km^2. Within this area the 32.5°/$_{oo}$

salinity isopleth has been taken as a practical boundary of Columbia River outflow water (T.R. 99). The typical locations of this limiting salinity isopleth during the four seasons are shown in Fig. 1.

SALINITY DISTRIBUTION

Horizontal and Vertical Structure

The station locations sampled for seawater analyses are presented in Fig. 3-22. These figures show the field of coverage and density of stations used in sampling for each cruise, and indicate the adequacy of points on which the salinity isopleths are based.

Salinity (Fig. 23-42 and 45-79) is a practical parameter for distinguishing the Columbia River effluent from the ambient oceanic and coastal waters of the northeastern Pacific. The temperature differential between the river water and the oceanic water seldom is great enough to show clearly the extent of the influence of the river effluent in the oceanic environment. Figures 23-42 depict the horizontal distributions of salinity at 0, 10, and 20 m for each of the cruises that produced enough physical and chemical data to warrant contouring. These three depths represent the average depth zones in which major changes in the salinity patterns of the water column proximal to the river occur. The surface charts (0 m) generally show the maximum horizontal changes in salinity associated with the river effluent. The 10-m charts depict the horizontal distributions of salinity at the approximate depth where the stability (primarily salinity dependent) of the water column is maximum. The 20-m charts show the horizontal distribution of salinity below the zone of maximum stability and give an indication of the extent of influence of the river water in decreasing the salinity of the oceanic water below the reference value of $32.5^{\circ}/_{oo}$. The increase of salinity with depth is slight near the surface, maximum at approximately 10 m, and low again near 20 m. The zone of maximum stability deepens with increasing distance from the river mouth to a maximum of about 40 m. The isopleth interval of salinity used in these figures is $1^{\circ}/_{oo}$ except where excessive crowding, usually at the river mouth, requires a larger interval or where nonuniformity in the salinity gradients requires an additional $0.5^{\circ}/_{oo}$ interval to clarify the distribution. The limiting $32.5^{\circ}/_{oo}$ salinity isopleth is shown as a dotted line; long dashes in the isopleths represent uncertain location because of insufficient data. All isopleths have been appropriately truncated in agreement with the field of data points.

Figures 43 and 44 show the location and orientation of the vertical salinity sections (Fig. 45-79), which are based on the same cruise data used for the horizontal plots. The interval between the solid lines is always $1^{\circ}/_{oo}$. Where crowding of the isopleths occurs near the river mouth, the salinity minimum has been indicated. The vertical distribution of salinity is shown to 140 m which is well below the river halocline, and indicates some of the salinity structure associated with the prevailing regional halocline.

Seasonal Distributions

The plan and profile diagrams of salinity have been arranged in groups possessing similar "seasonal" characteristics. Four distinctive salinity distributions occur during the year corresponding roughly to the seasonal periods: spring, summer, autumn, and winter. These periods are more indicative of general meteorological conditions and river stage rather than of precisely fixed times in the calendar year. During spring the river discharge of snow melt increases, the winds change from southerly to northerly, and a well-defined plume of river water develops and extends southwest of the river mouth. A band of upwelled water develops along the Oregon coast inshore from the river effluent.

In summer the river discharge decreases rapidly and the persistent northerly winds extend the plume to the southwest. In the autumn period the river discharge is still low but the winds shift to a southerly quarter and increase over the area, reducing the size of the offshore plume. During winter short periods of high river runoff accompany coastal precipitation peaks and the effluent moves northward along the Washington coast under the influence of predominant strong southerly winds. The period of transition between the winter distribution and the spring distribution of the plume is usually very brief and is considered part of the spring group. Table 3 shows groupings of the cruises based on these four periods during the year.

Table 3. Cruises Categorized by Season

Spring	Summer	Autumn	Winter
BB 287	BB 288	BB 293	BB 275
BB 304	BB 290	BB 312	BB 280
BB 318	BB 291	BB 335 II	BB 297
OSH 001	BB 308		BB 299
BB 320	BB 324		
BB 322	OSH 002		
BB 323	BB 326		
	OSH 003		
	BB 335 I		

The groupings in Table 3 form the basis for the four generalized salinity distributions of the Columbia River effluent shown in Fig. 80-83. These interpretative composite figures were derived from data of many cruises and do not represent particular cruise distributions. Each figure serves as a stylized base against which observed distributions can be compared. Such comparison should be helpful in determining the meteorological, tidal, or river-discharge factors that cause distributions on an individual cruise to vary from the generalized figures.

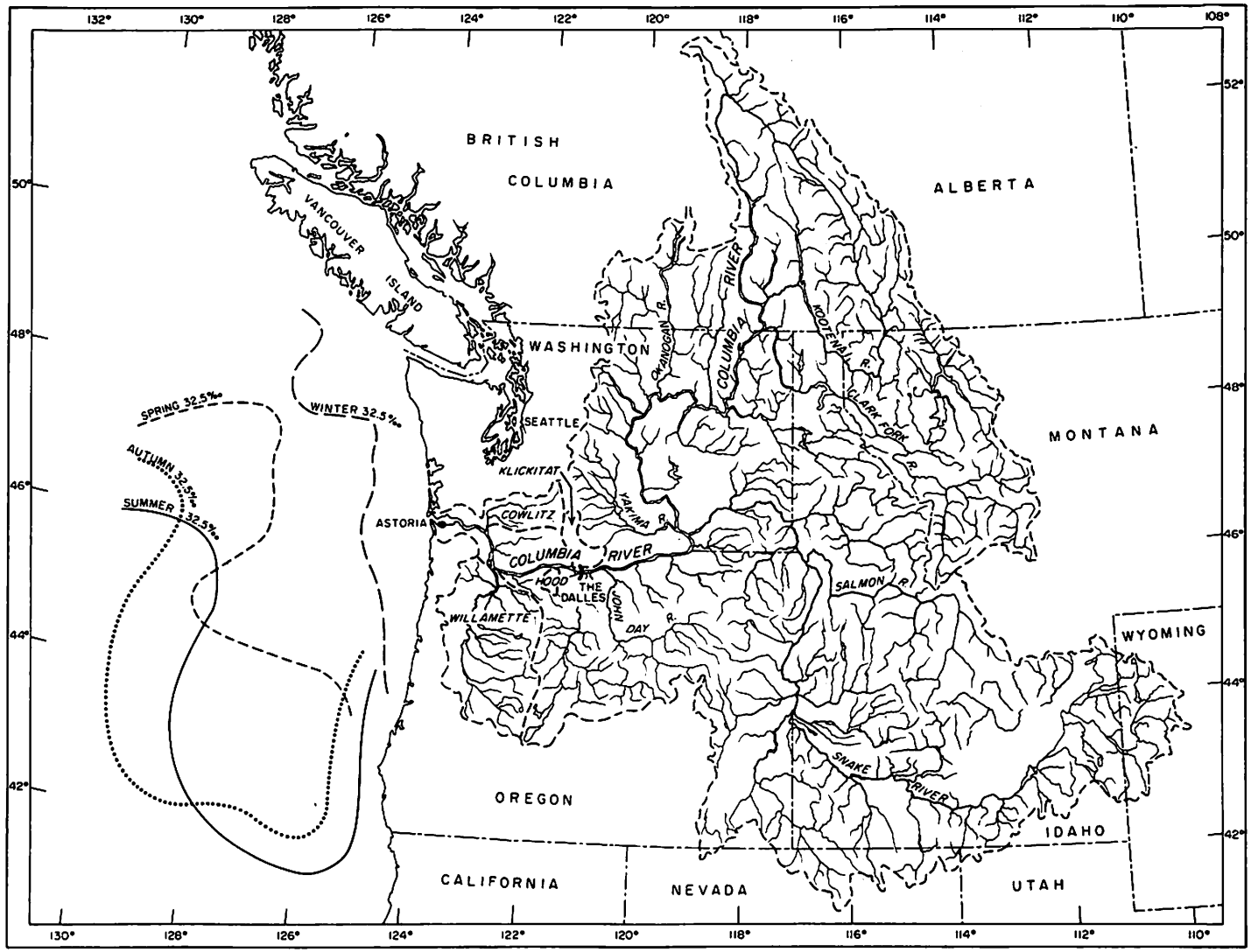

Fig. 1. Columbia River drainage basin and average seasonal extent of the Columbia River effluent shown by the 32.5°/oo salinity isopleth.

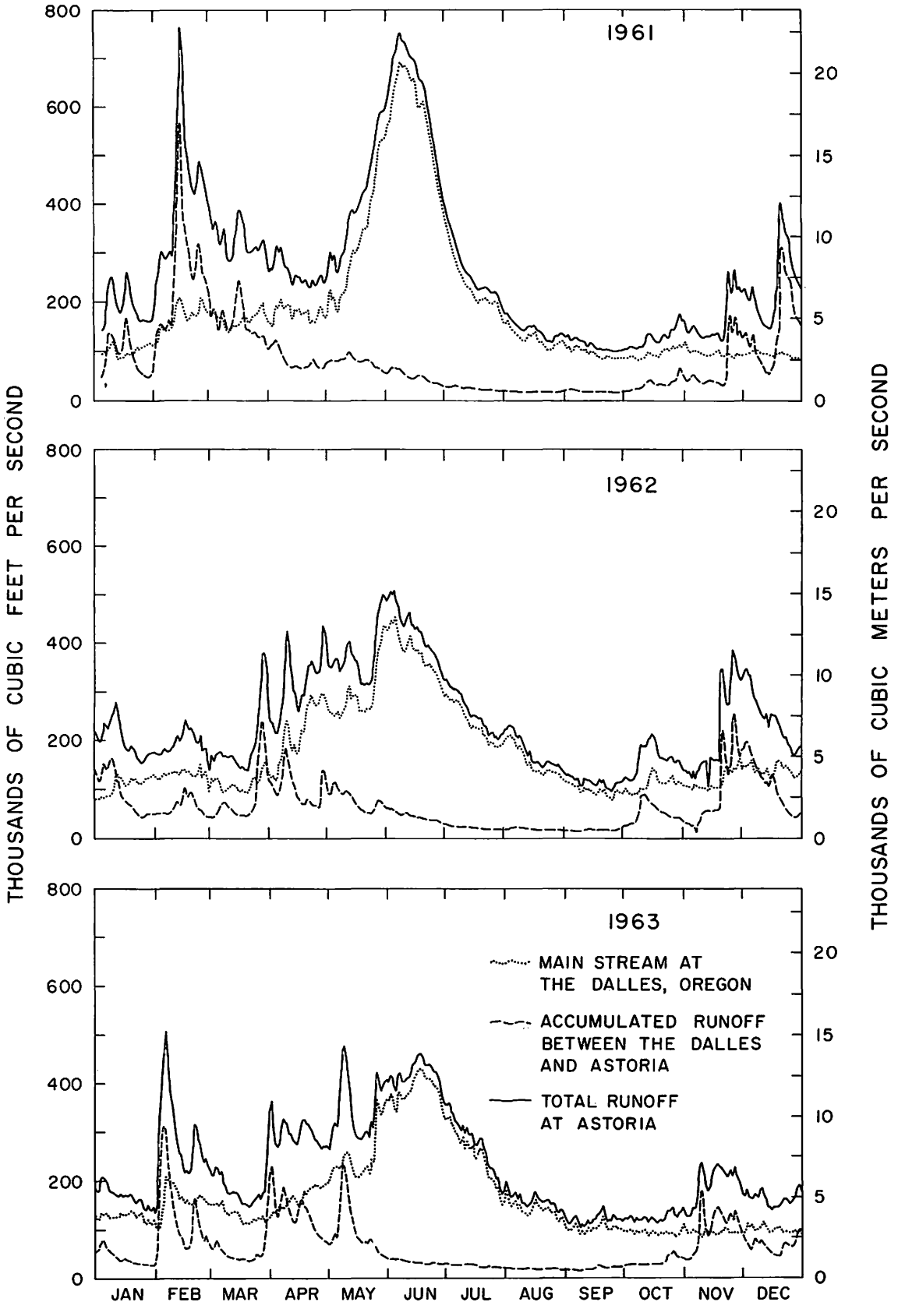

Fig. 2. Columbia River discharge curves, 1961-1963.

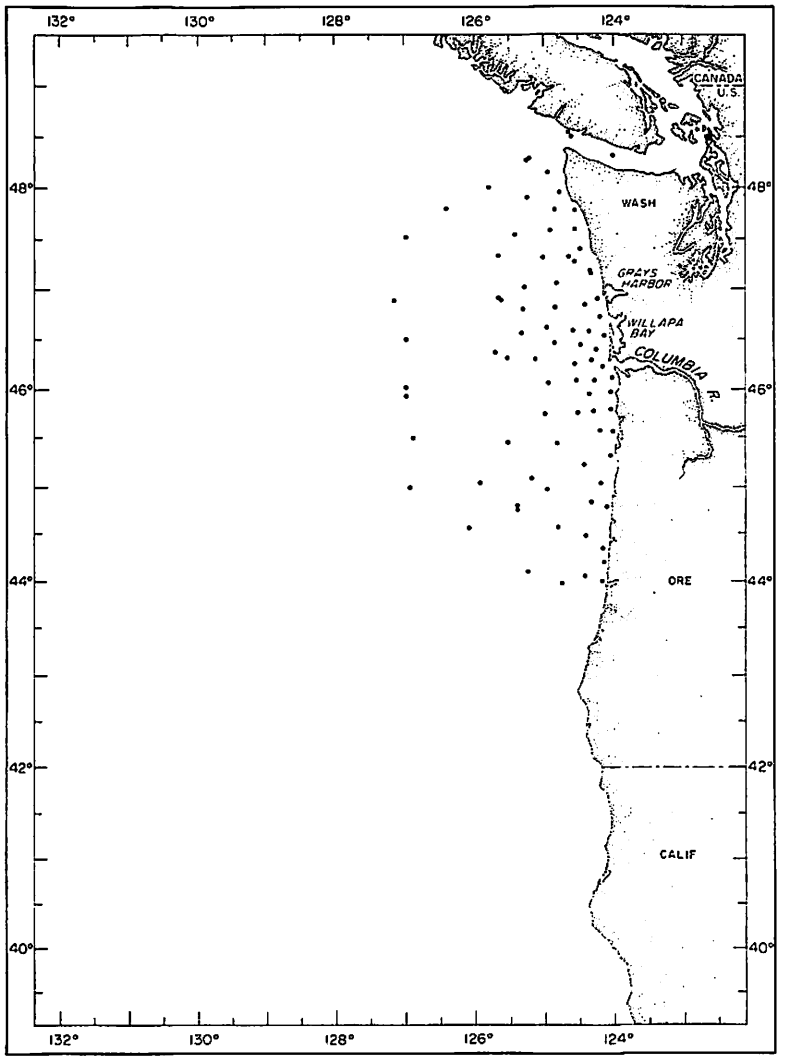

Fig. 3. Station locations for Brown Bear Cruise 287, 8-24 May 1961.

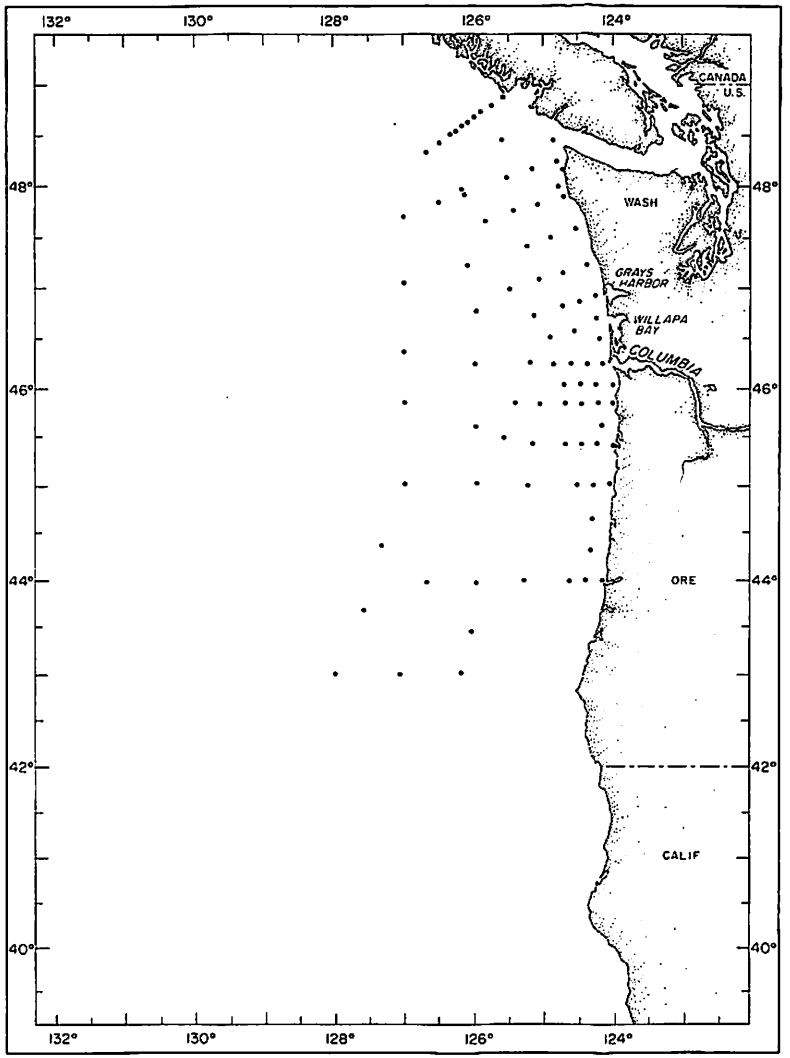

Fig. 4. Station locations for Brown Bear Cruise 304, 27 March - 12 April 1962.

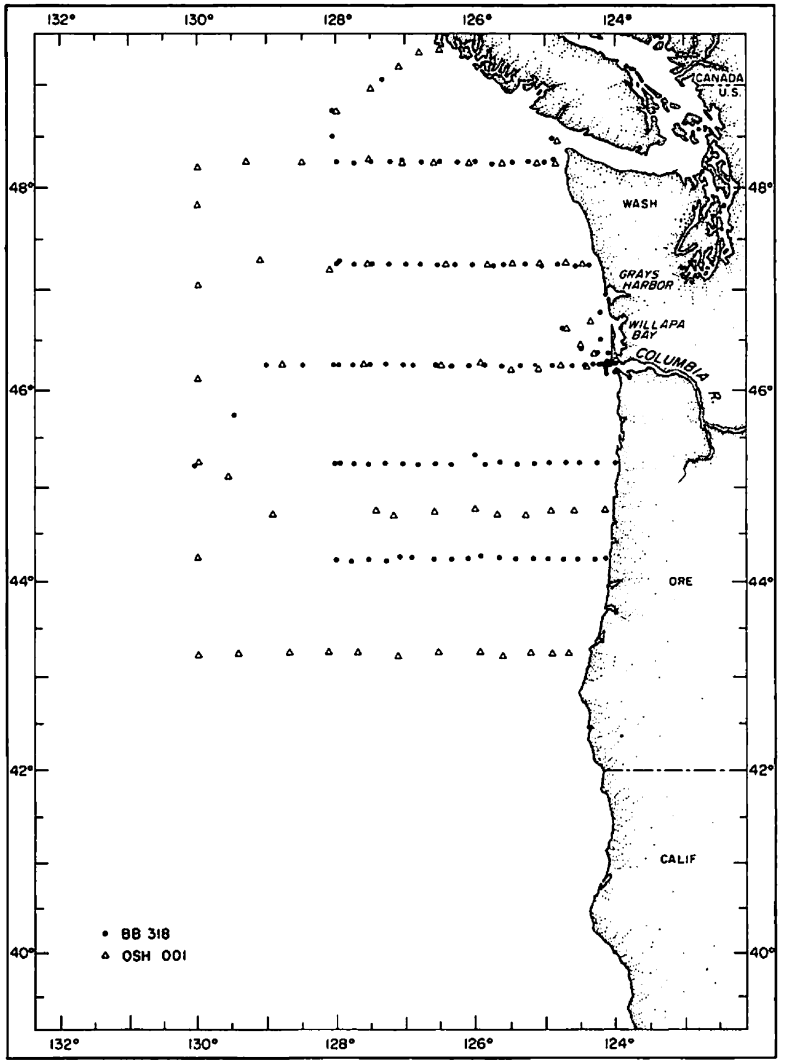

Fig. 5. Station locations for Brown Bear Cruise 318, 27 February - 20 March 1963 and Oshawa Cruise 001, 12-26 March 1963.

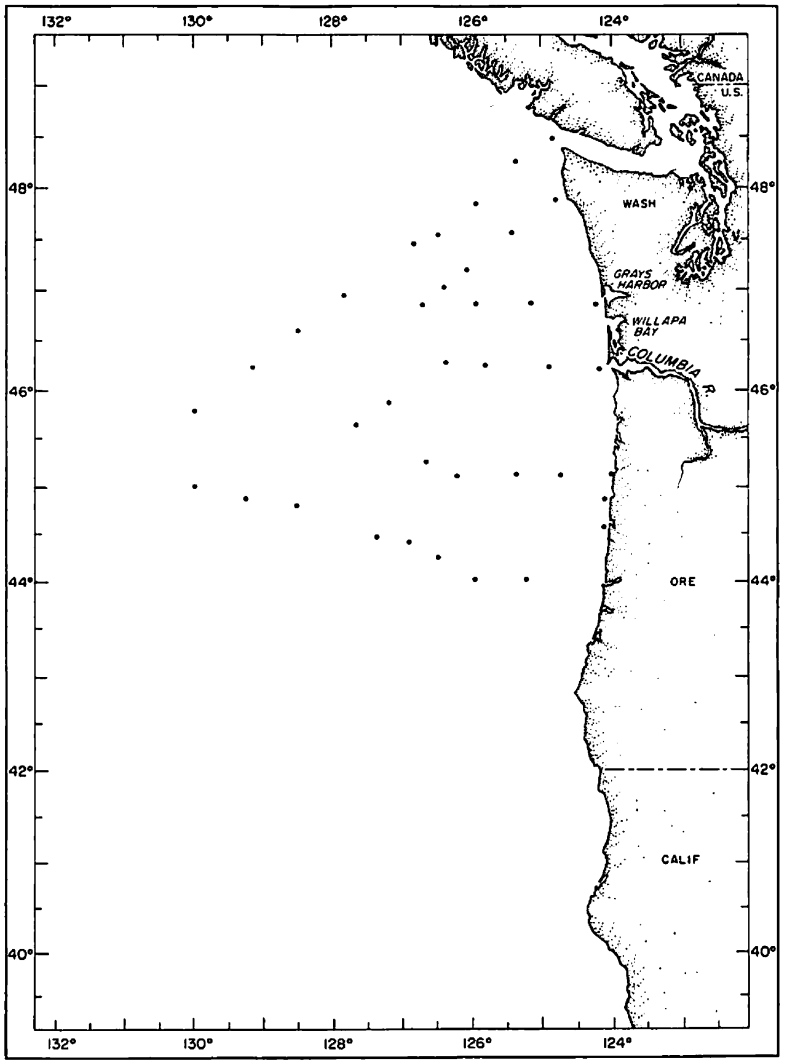

Fig. 6. Station locations for Brown Bear Cruise 320, 28 March - 10 April 1963.

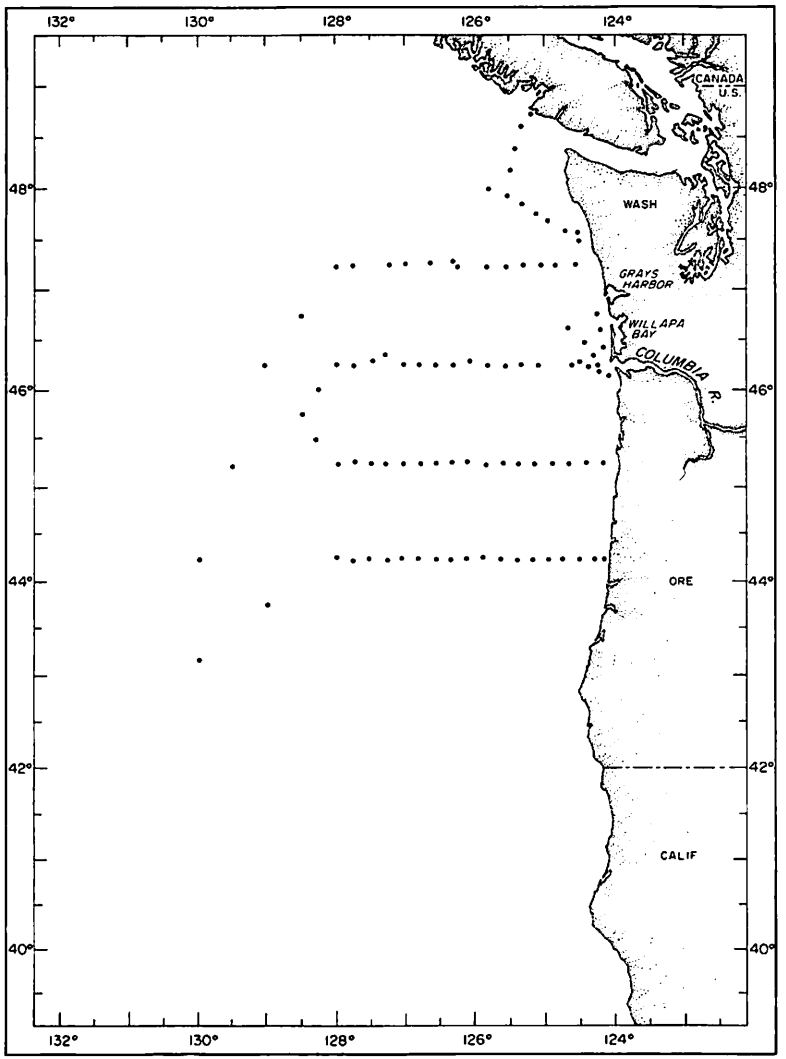

Fig. 7. Station locations for Brown Bear Cruise 322, 16 April - 1 May 1963.

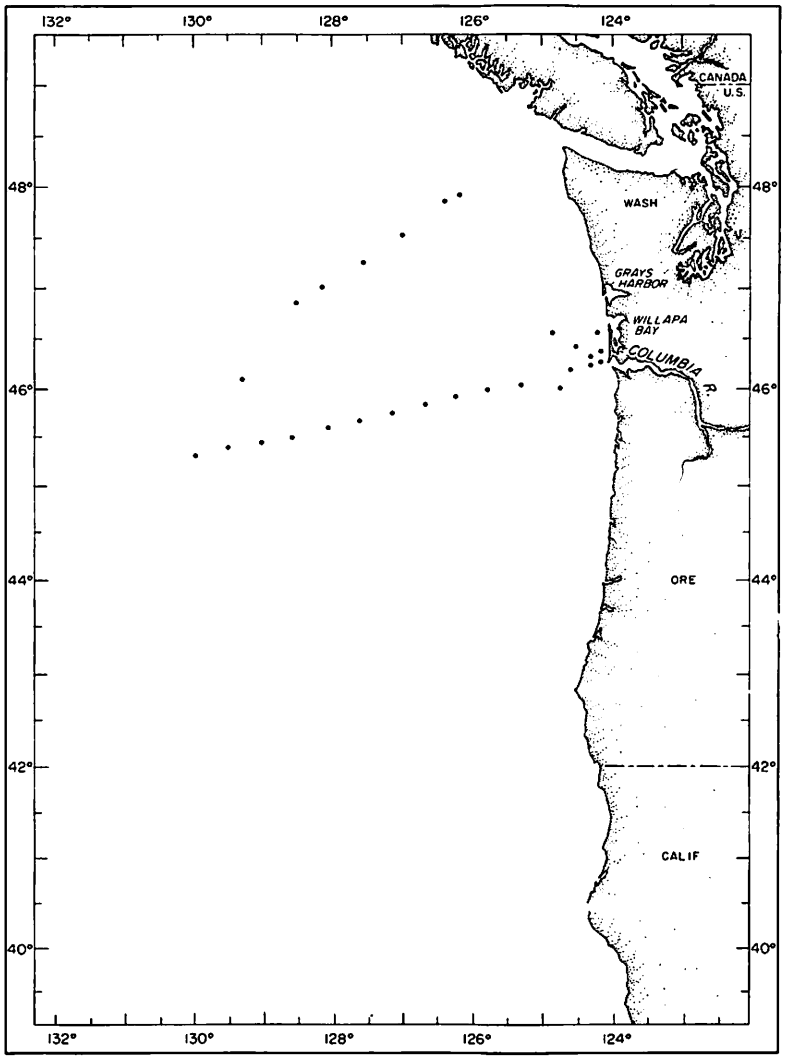

Fig 8. Station locations for Brown Bear Cruise 323, 13-19 May 1963.

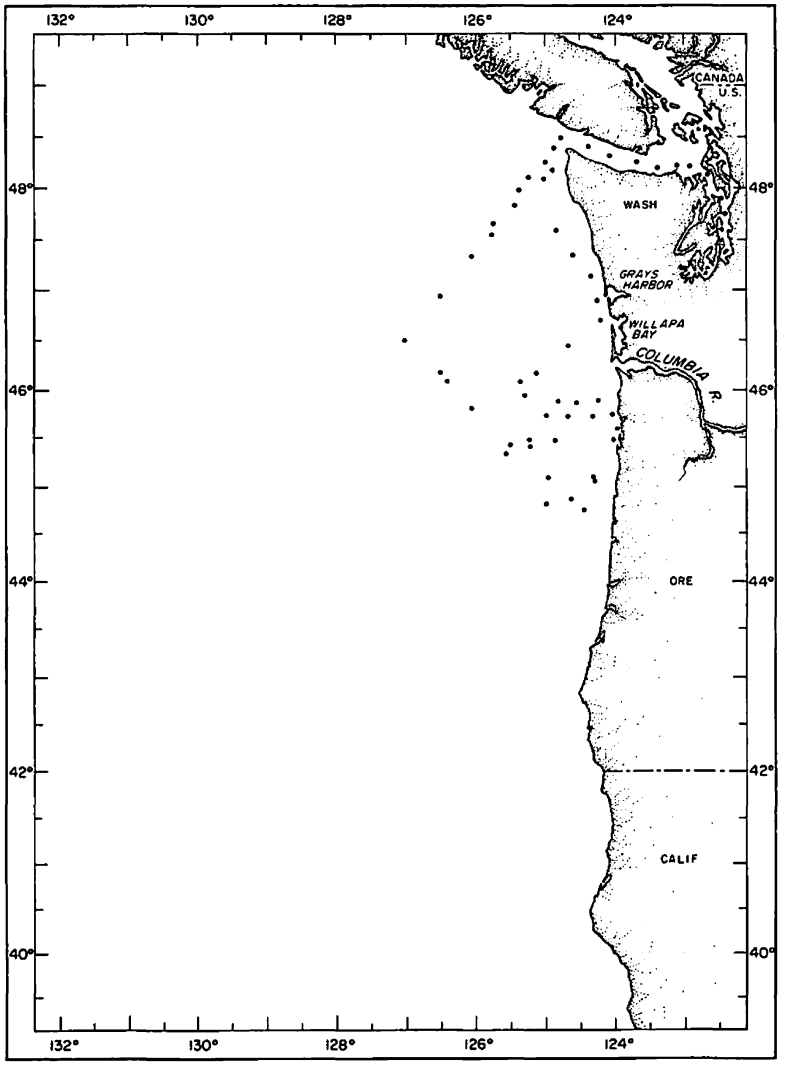

Fig. 9. Station locations for Brown Bear Cruise 288, 9-19 June 1961.

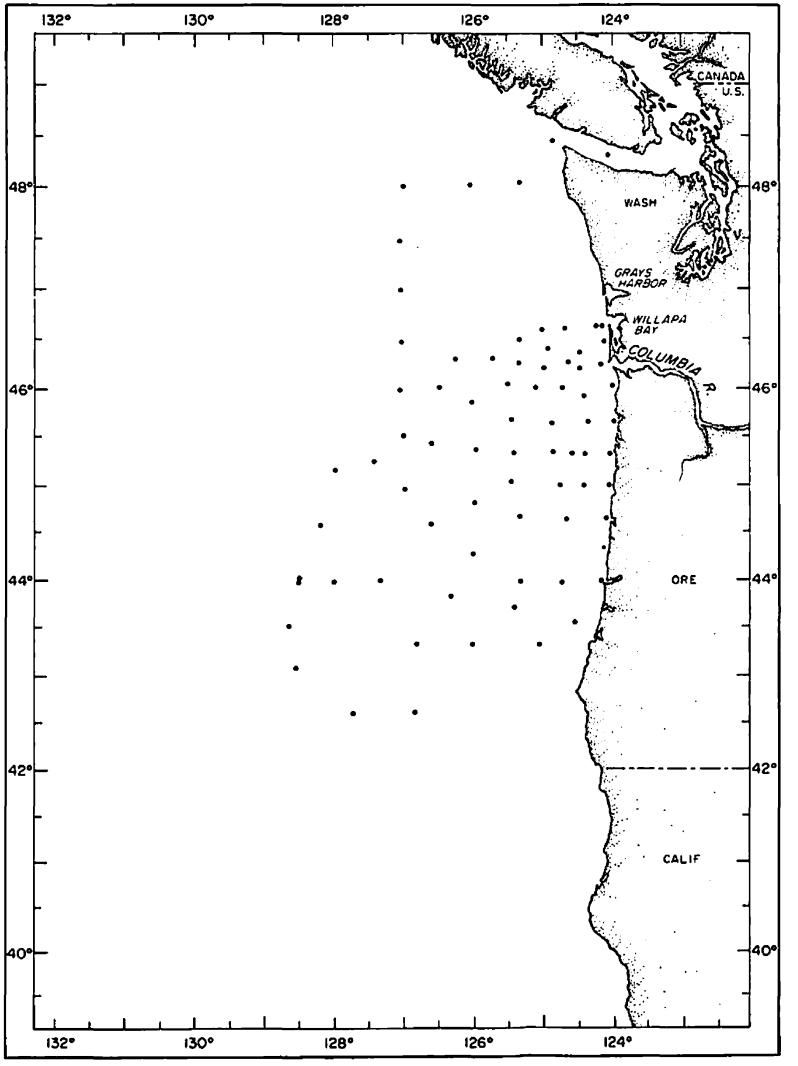

Fig. 10. Station locations for Brown Bear Cruise 290, 6-25 July 1961.

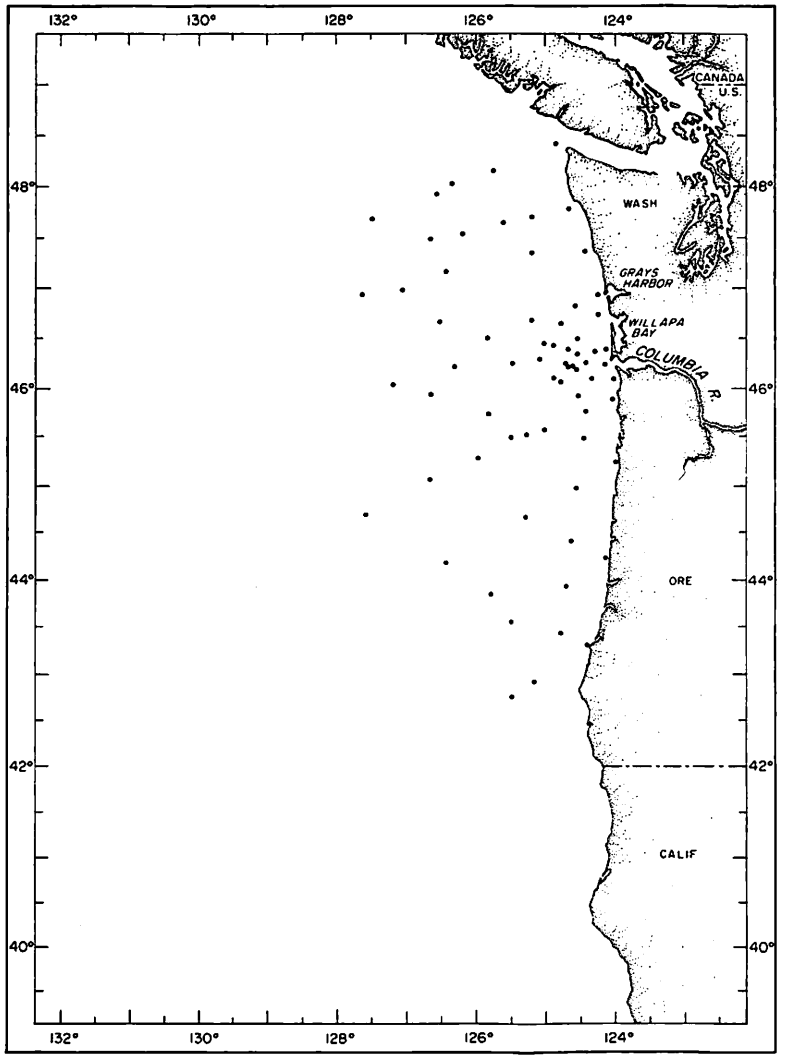

Fig. 11. Station locations for Brown Bear Cruise 291, 28 July - 13 August 1961.

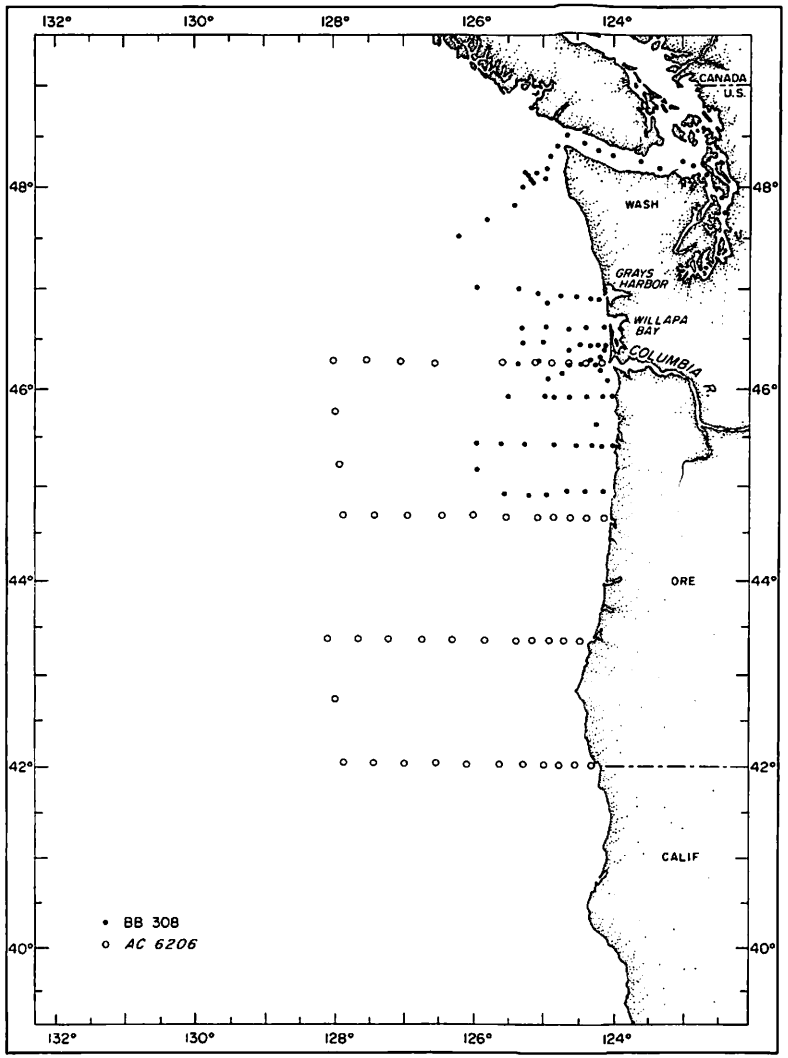

Fig. 12. Station locations for Brown Bear Cruise 308, 7-19 June 1962 and Acona Cruise 6206, 4-17 June 1962.

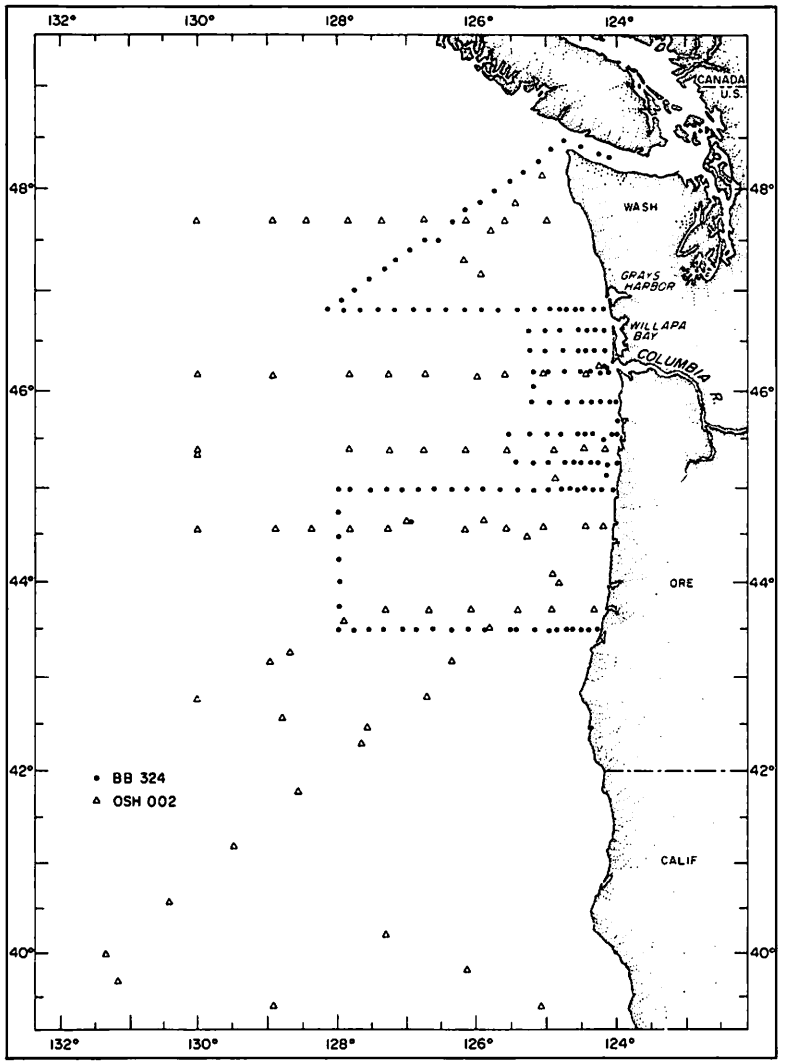

Fig. 13. Station locations for Brown Bear Cruise 324, 21 May - 4 June 1963 and Oshawa Cruise 002, 22 May - 12 June 1963.

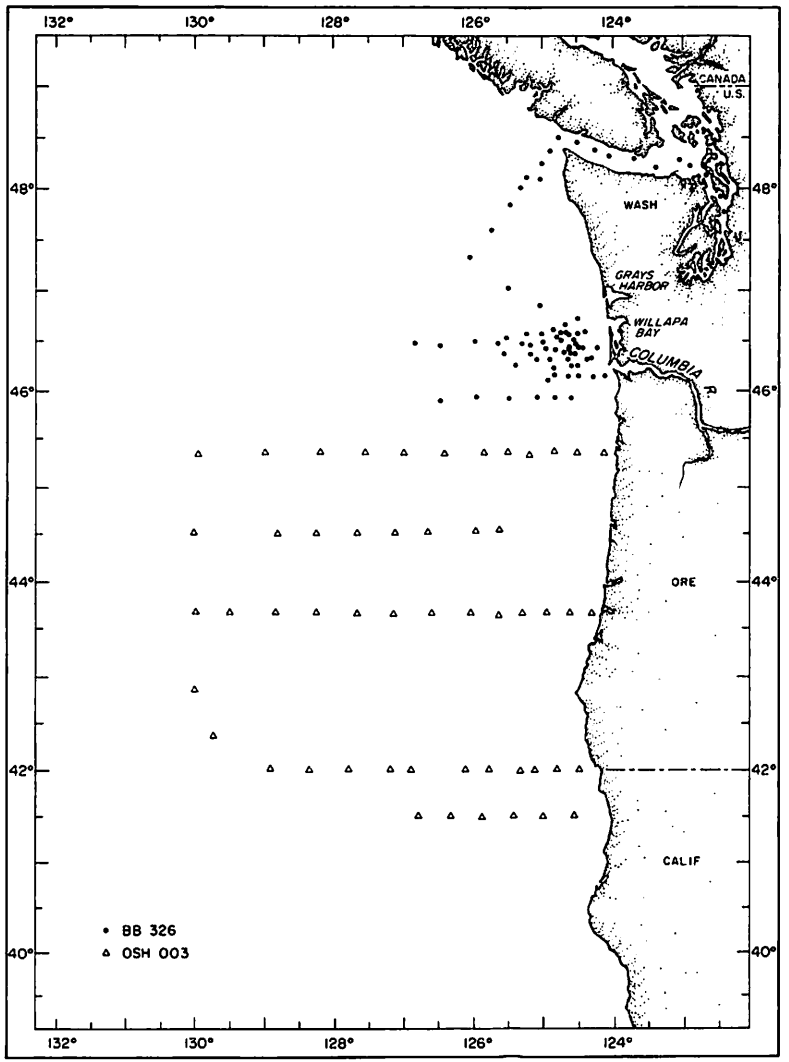

Fig. 14. Station locations for Brown Bear Cruise 326, 13-23 June 1963 and Oshawa Cruise 003, 17-30 June 1963.

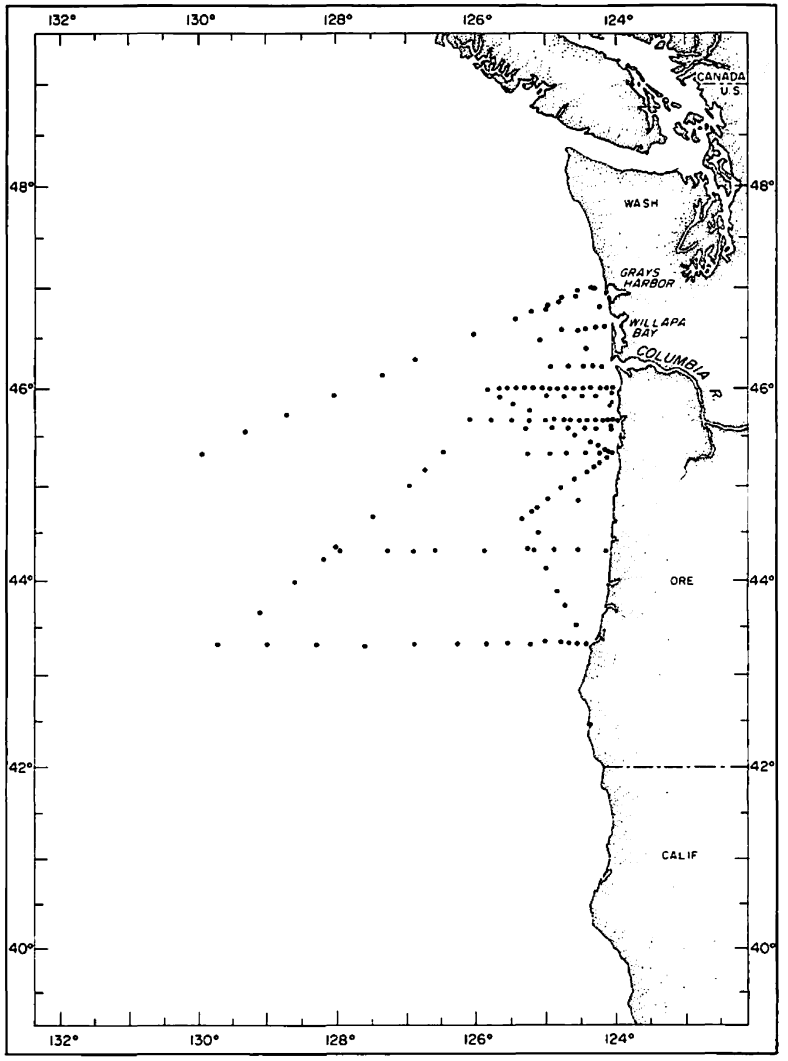

Fig. 15. Station locations for Brown Bear Cruise 335 I, 20 September - 12 October 1963.

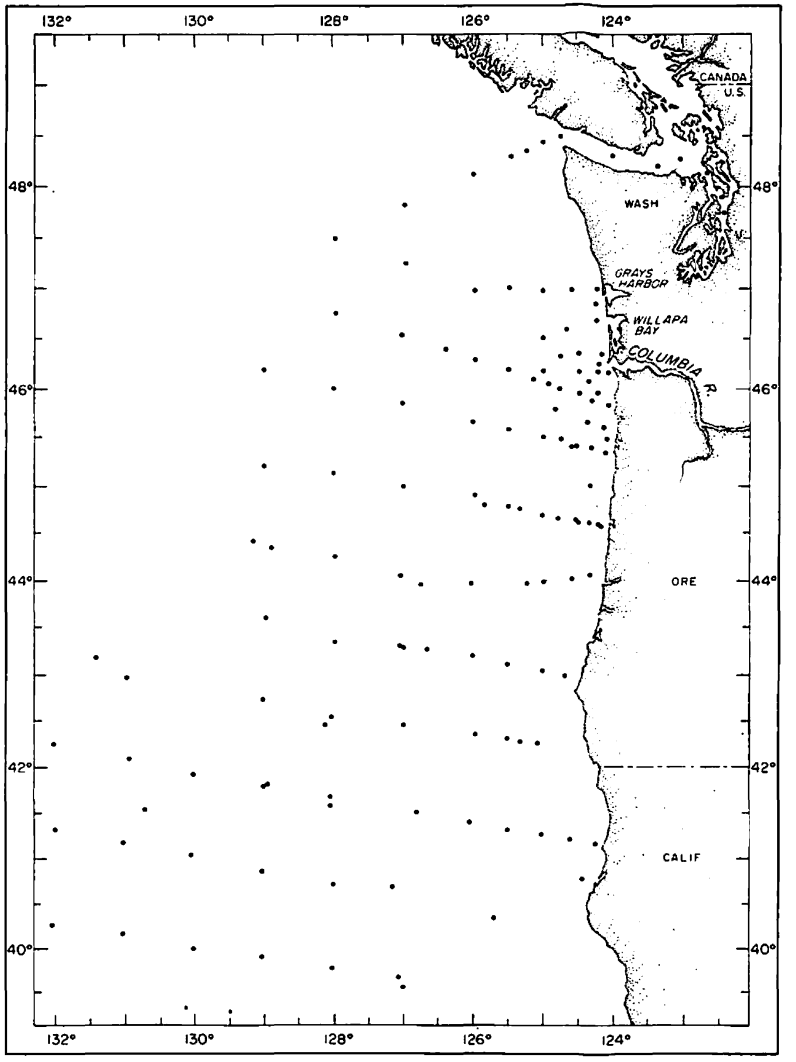

Fig. 16. Station locations for Brown Bear Cruise 293, 14 September - 20 October 1961.

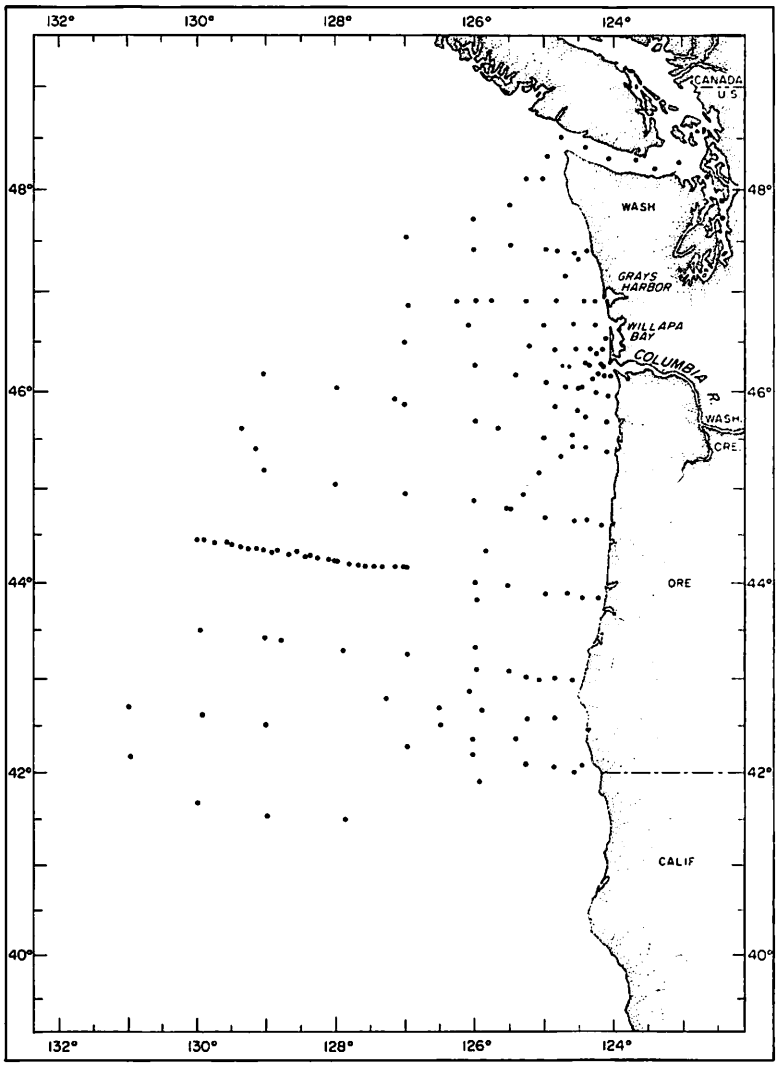

Fig. 17. Station locations for Brown Bear Cruise 312, 14 September - 9 October 1962.

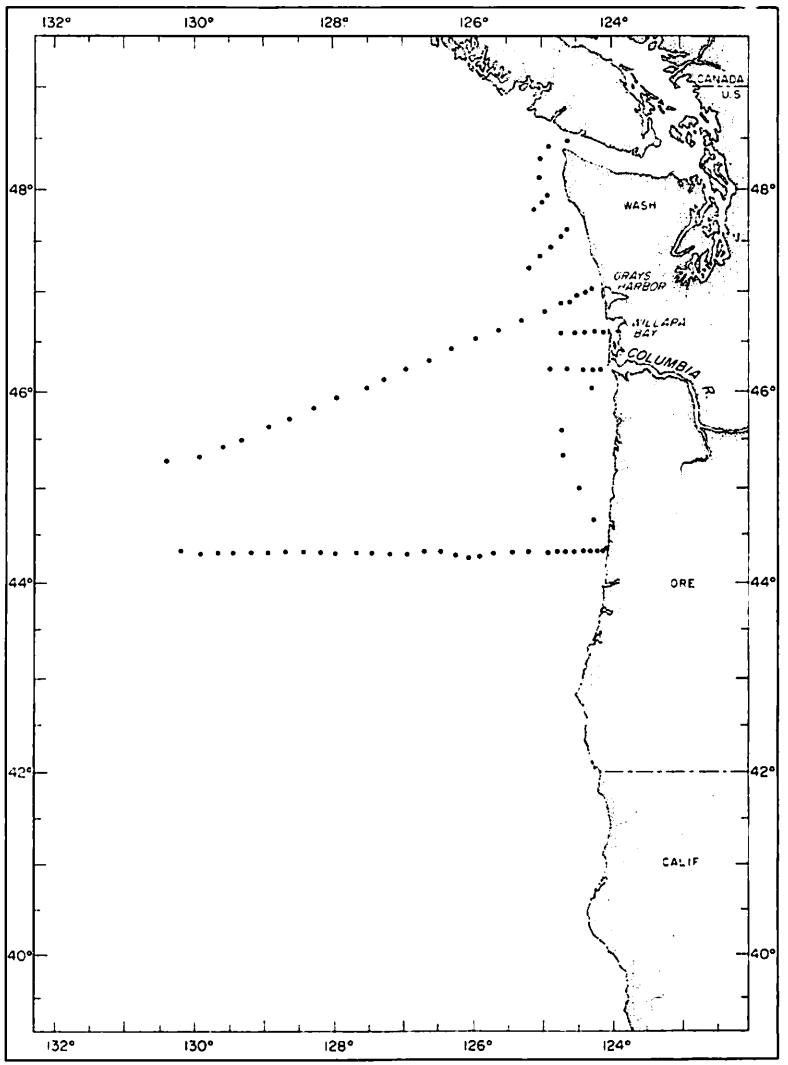

Fig. 18. Station locations for Brown Bear Cruise 335 II, 15-25 October 1963.

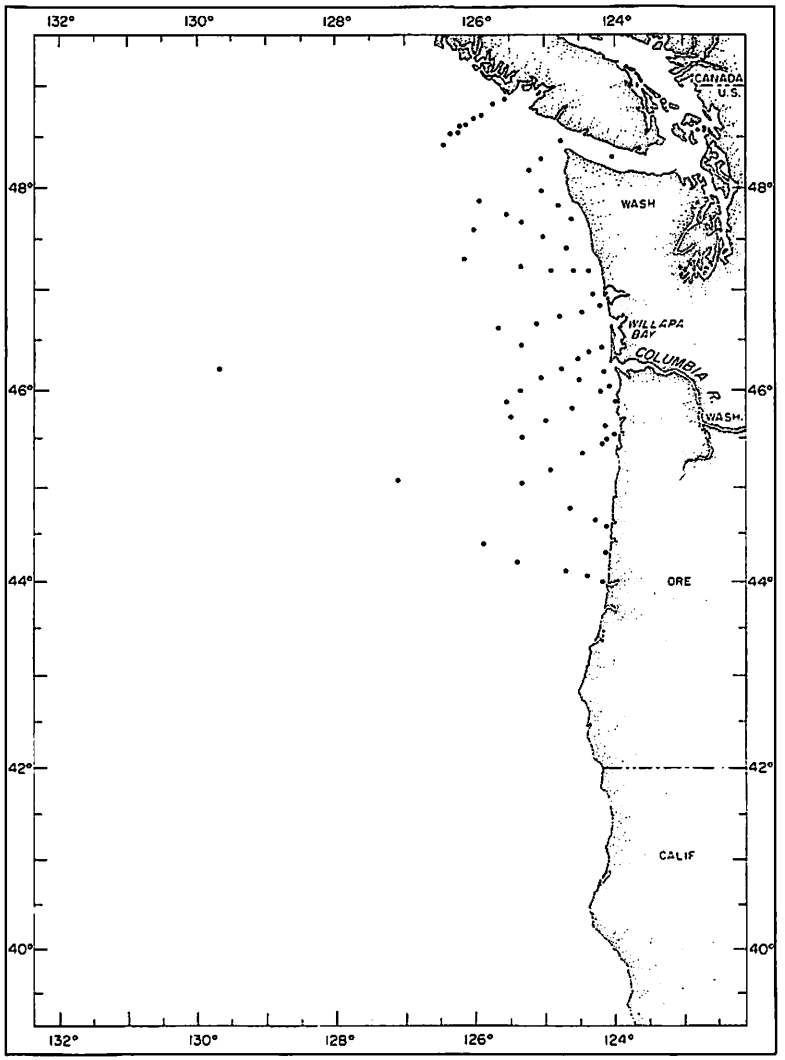

Fig. 19. Station locations for Brown Bear Cruise 275, 10-27 January 1961.

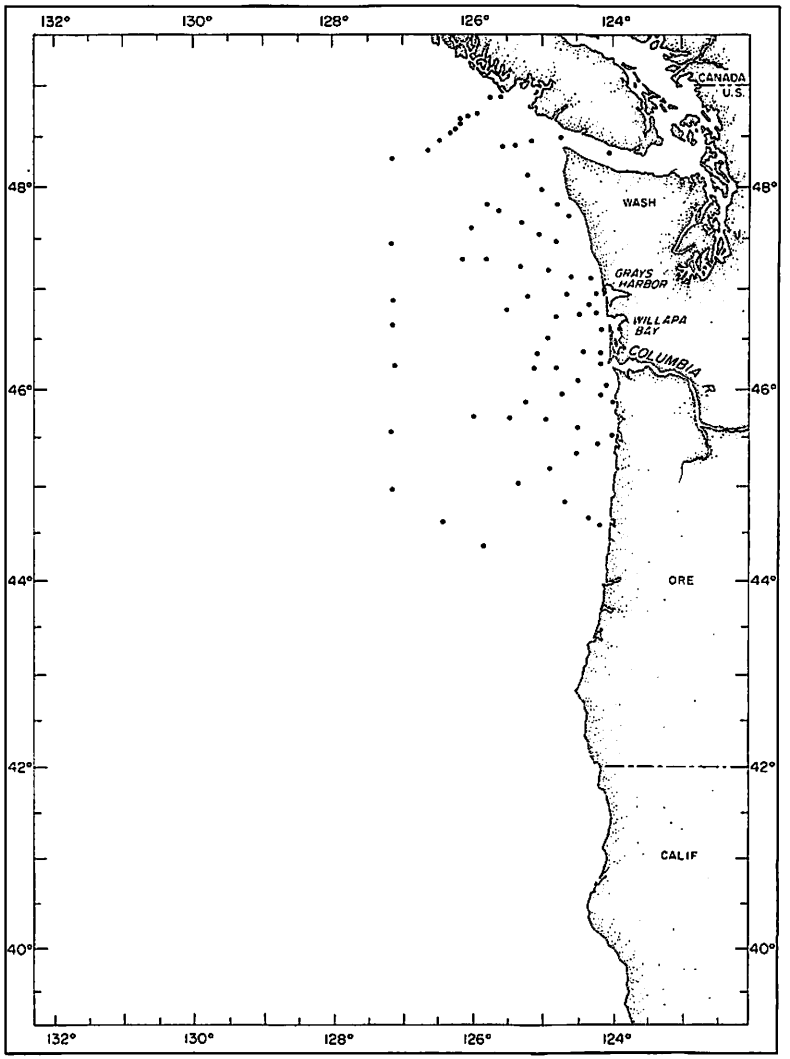

Fig. 20. Station locations for Brown Bear Cruise 280, 7-24 March 1961.

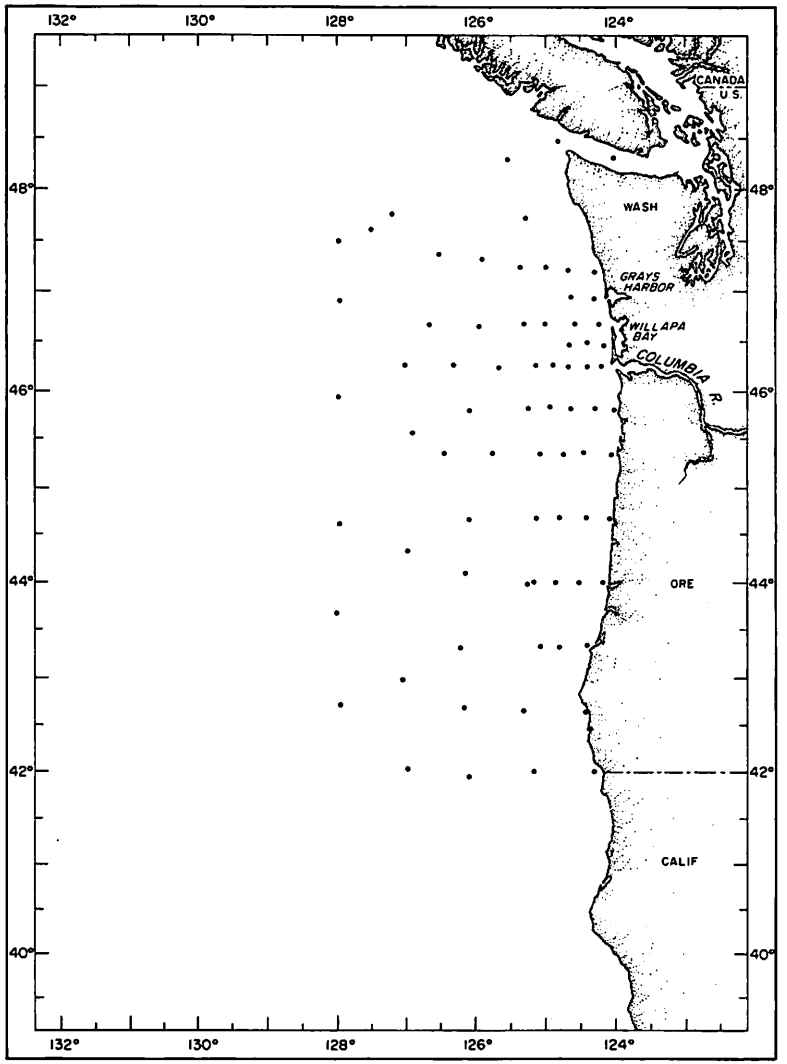

Fig. 21. Station locations for Brown Bear Cruise 297, 28 November - 18 December 1961.

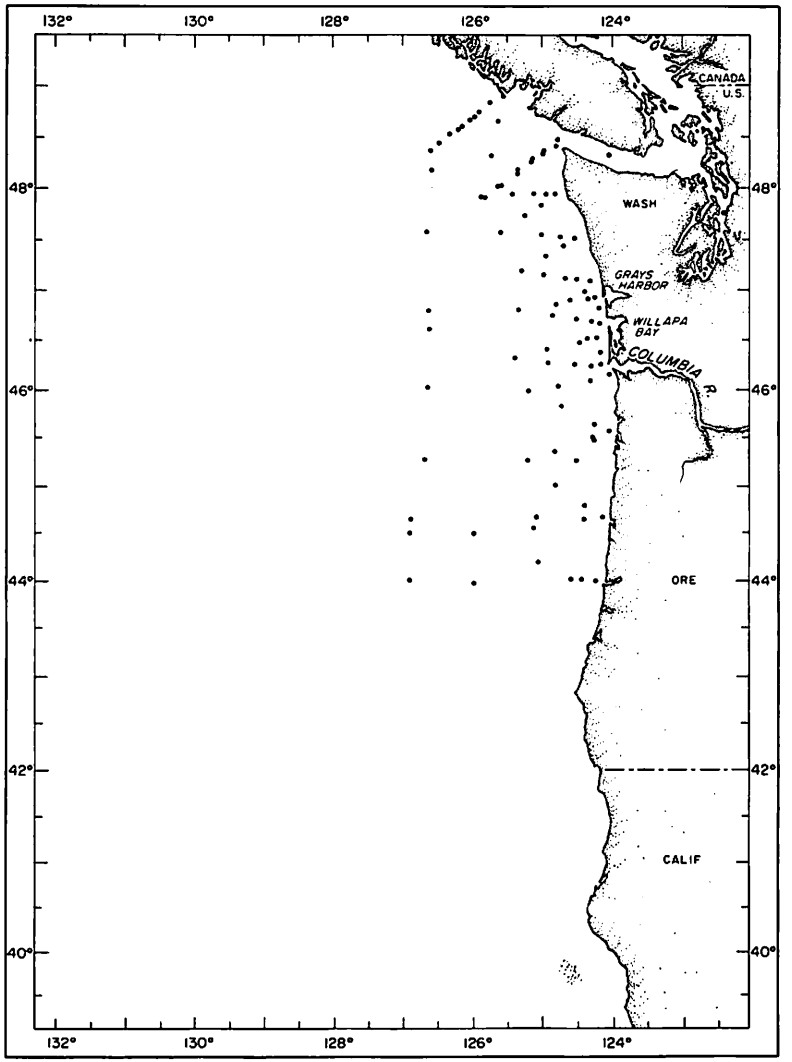

Fig. 22. Station locations for Brown Bear Cruise 299, 23 January - 7 February 1962.

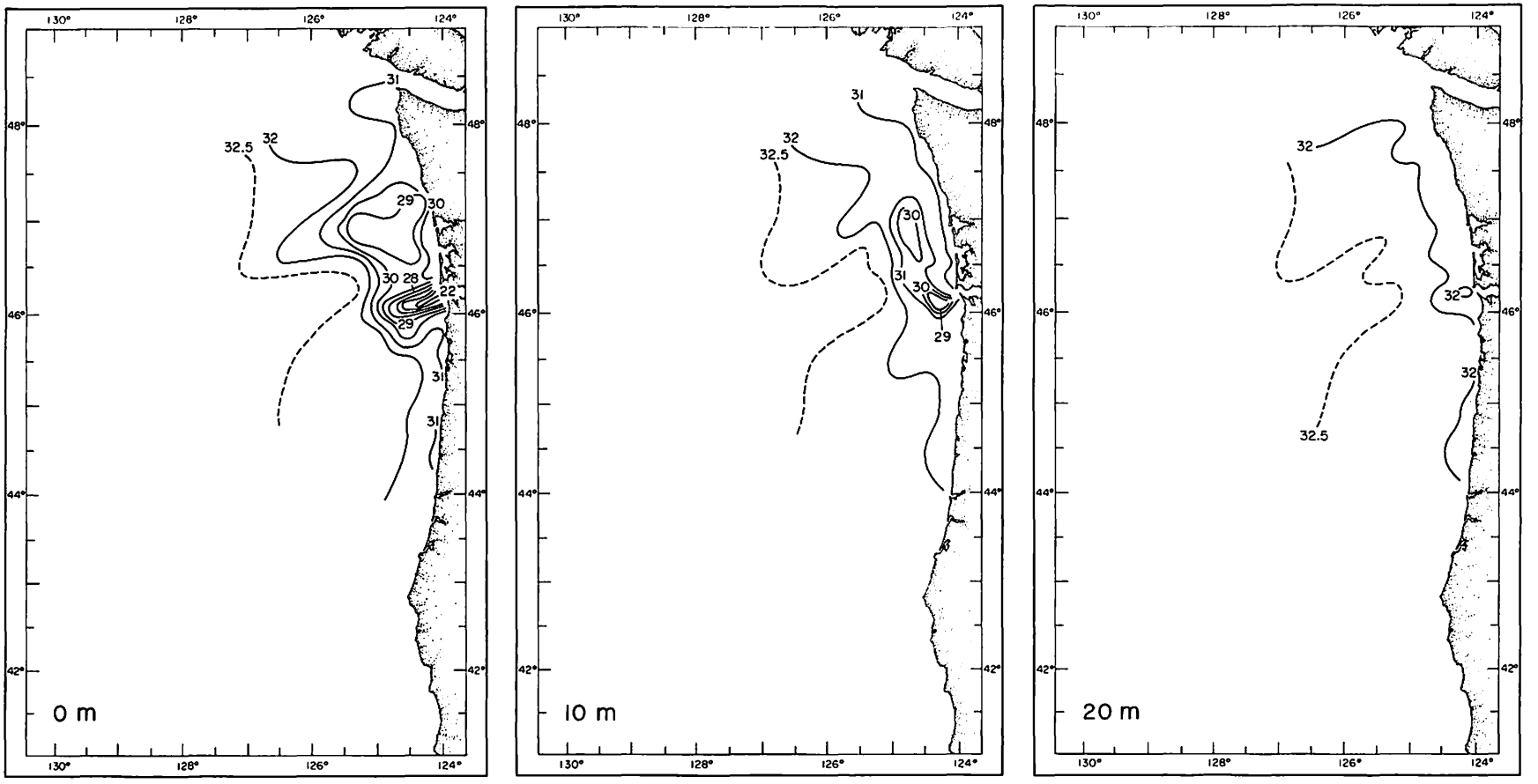

Fig. 23. Horizontal distributions of salinity (°/oo), Brown Bear Cruise 287.

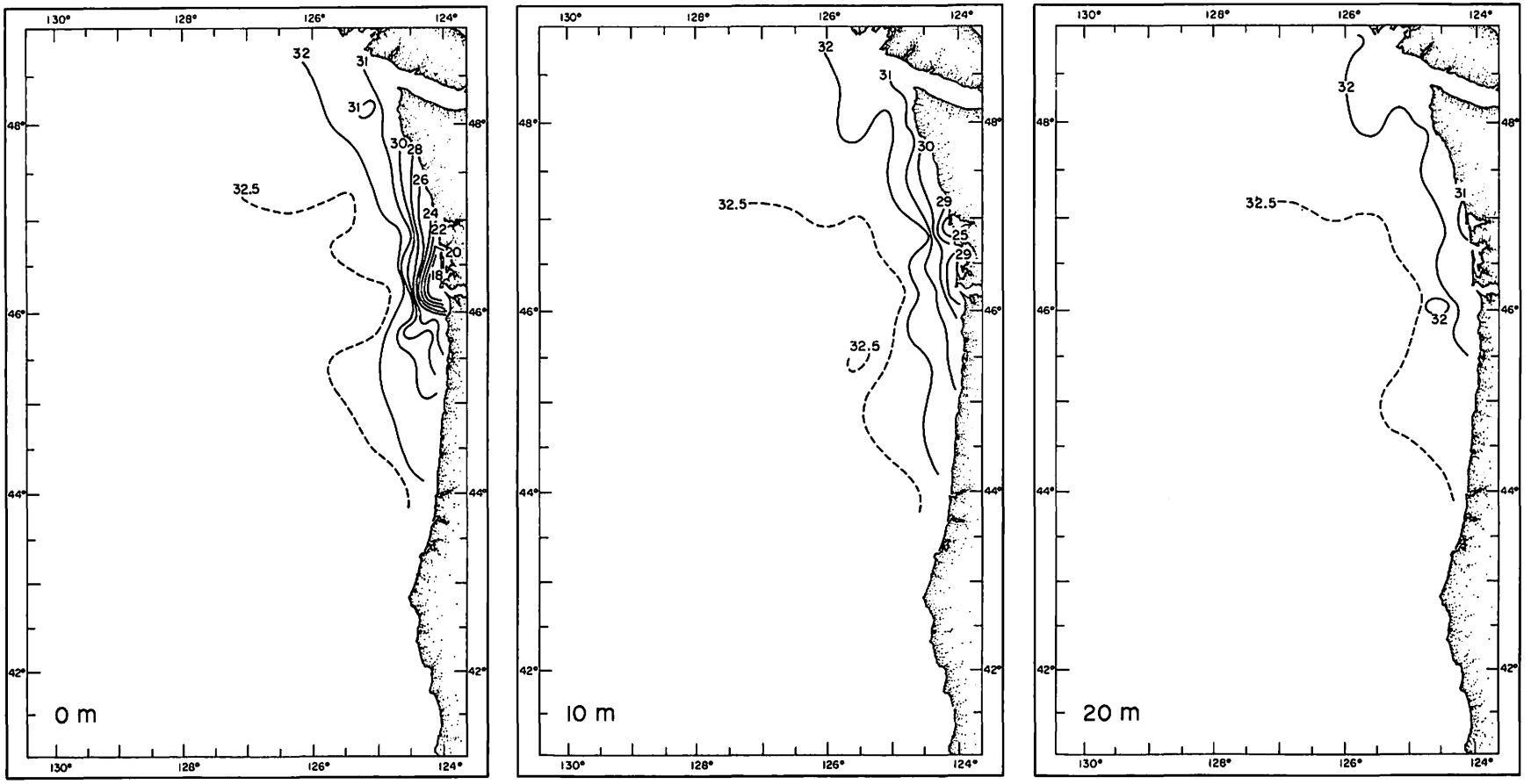

Fig. 24. Horizontal distributions of salinity (°/oo), Brown Bear Cruise 304.

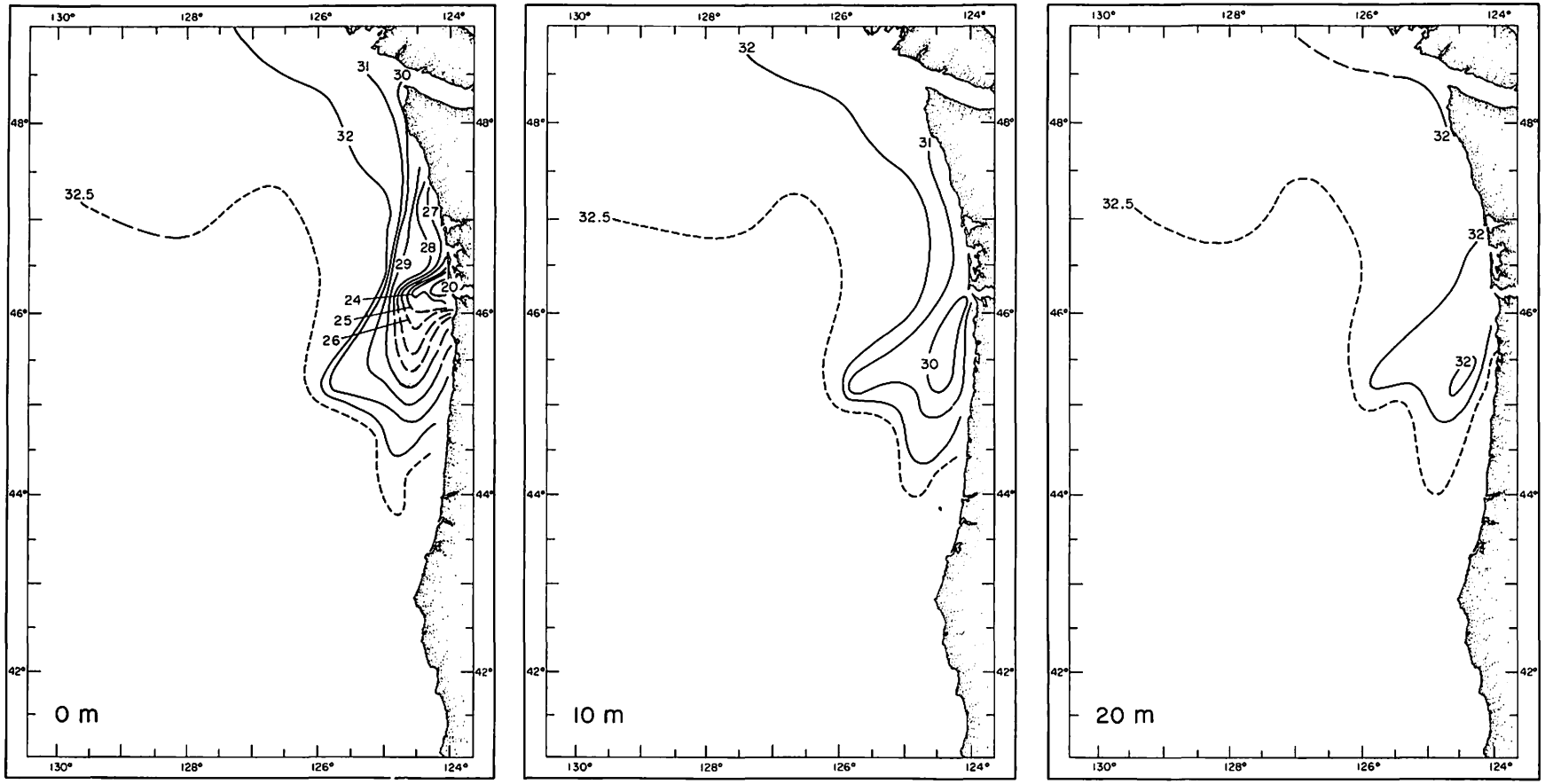

Fig. 25. Horizontal distributions of salinity (°/oo), Brown Bear Cruise 318 and Oshawa Cruise 001.

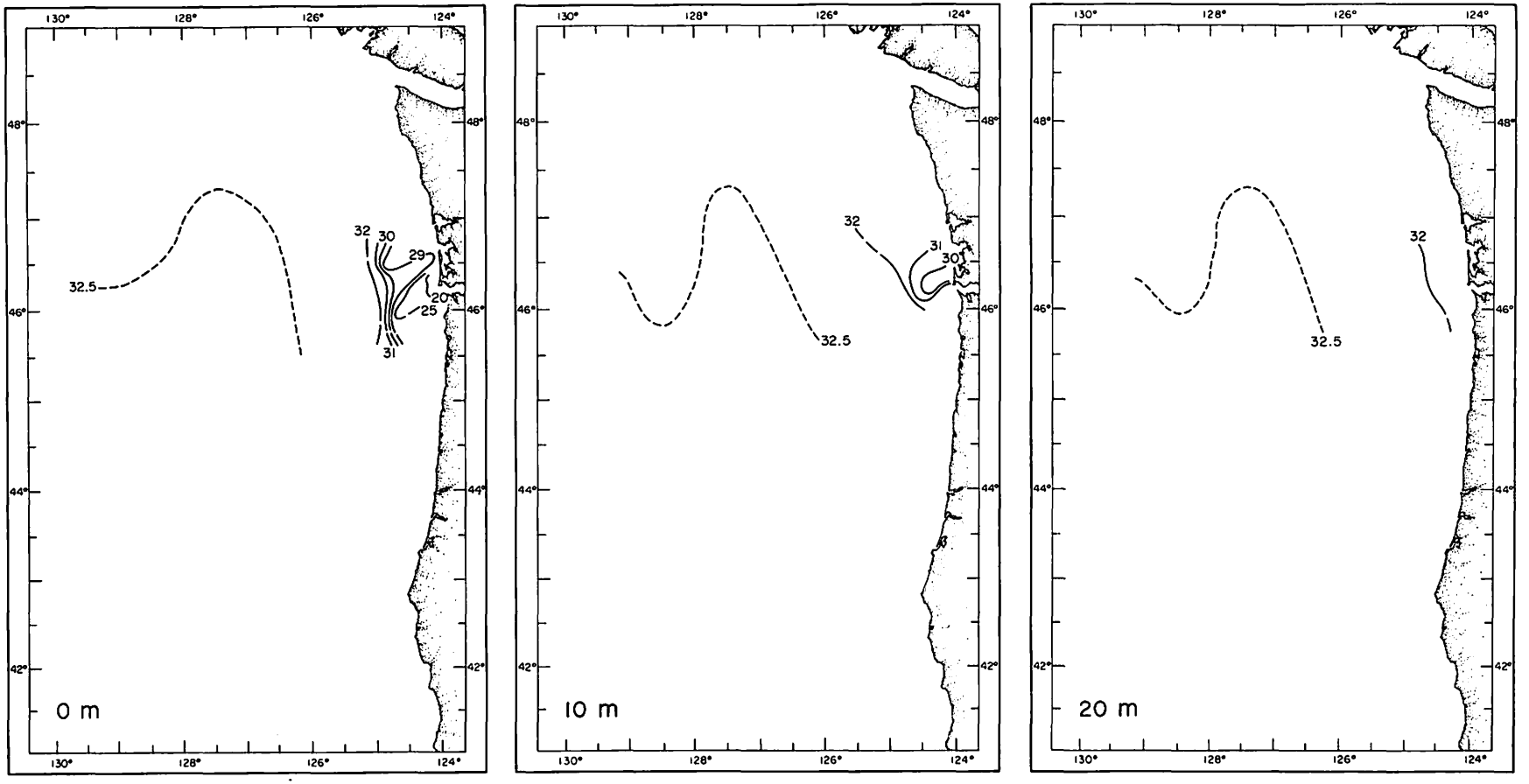

Fig. 28. Horizontal distributions of salinity (°/oo), Brown Bear Cruise 323.

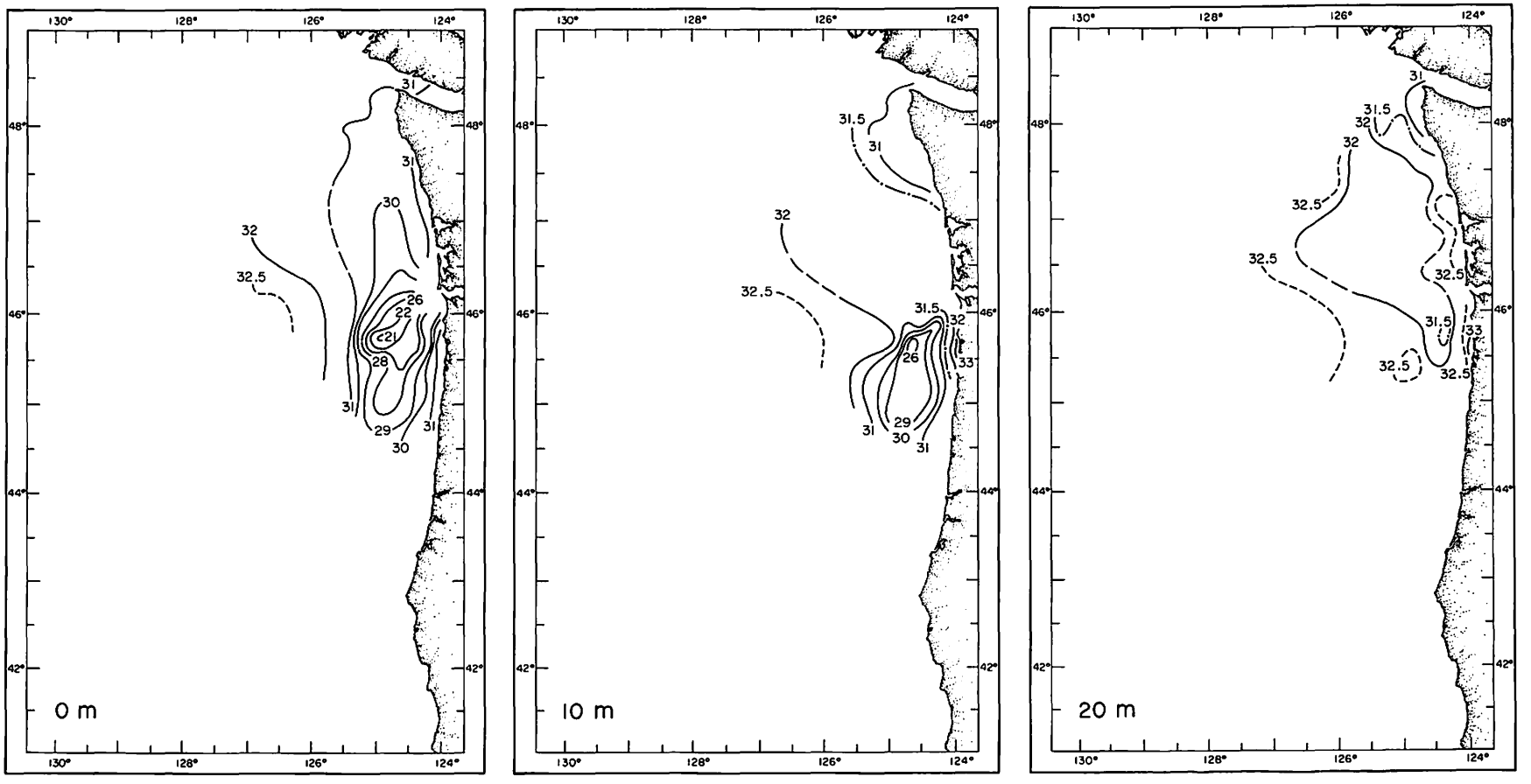

Fig. 29. Horizontal distributions of salinity (°/oo), Brown Bear Cruise 288.

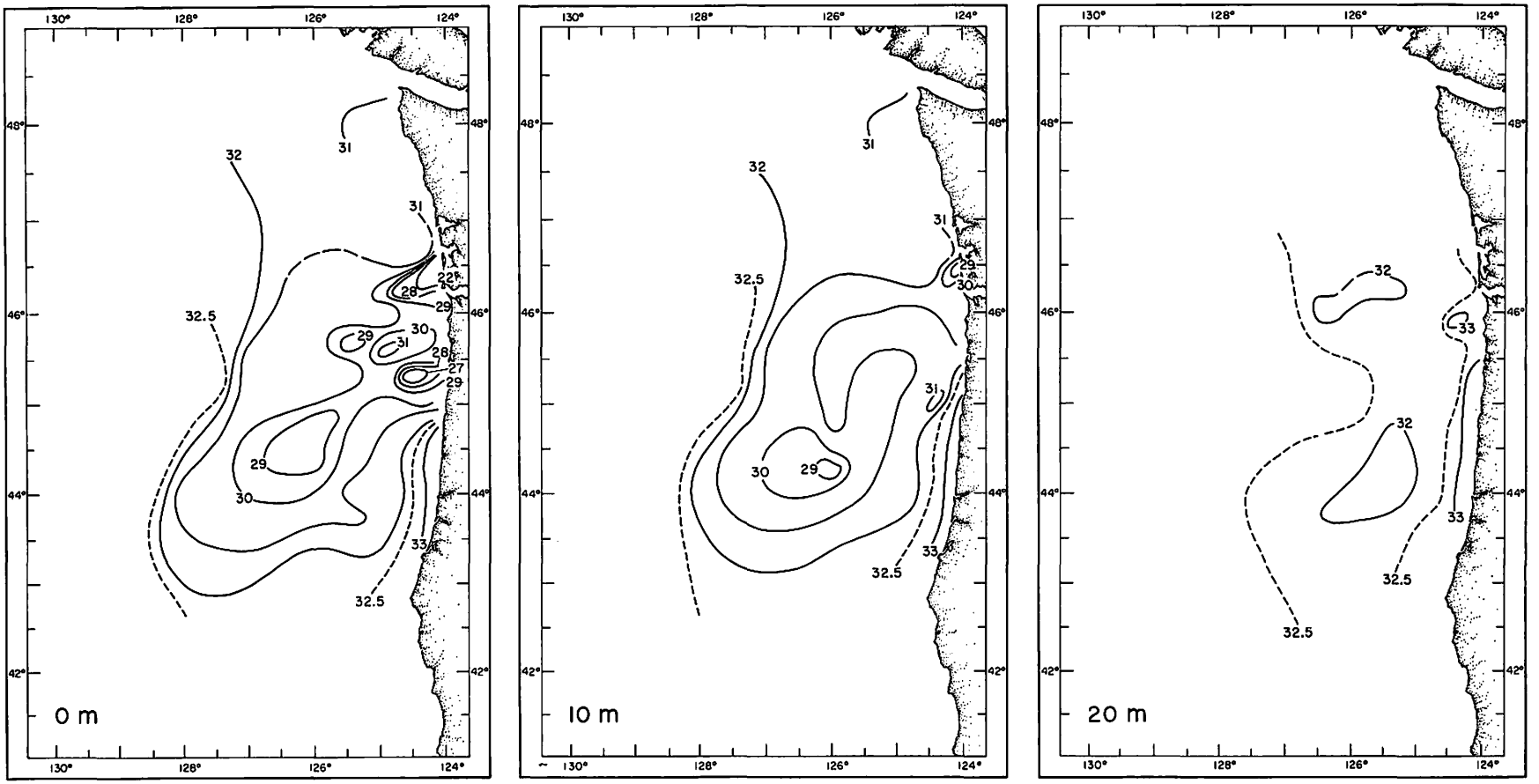

Fig. 30. Horizontal distributions of salinity (°/oo), Brown Bear Cruise 290.

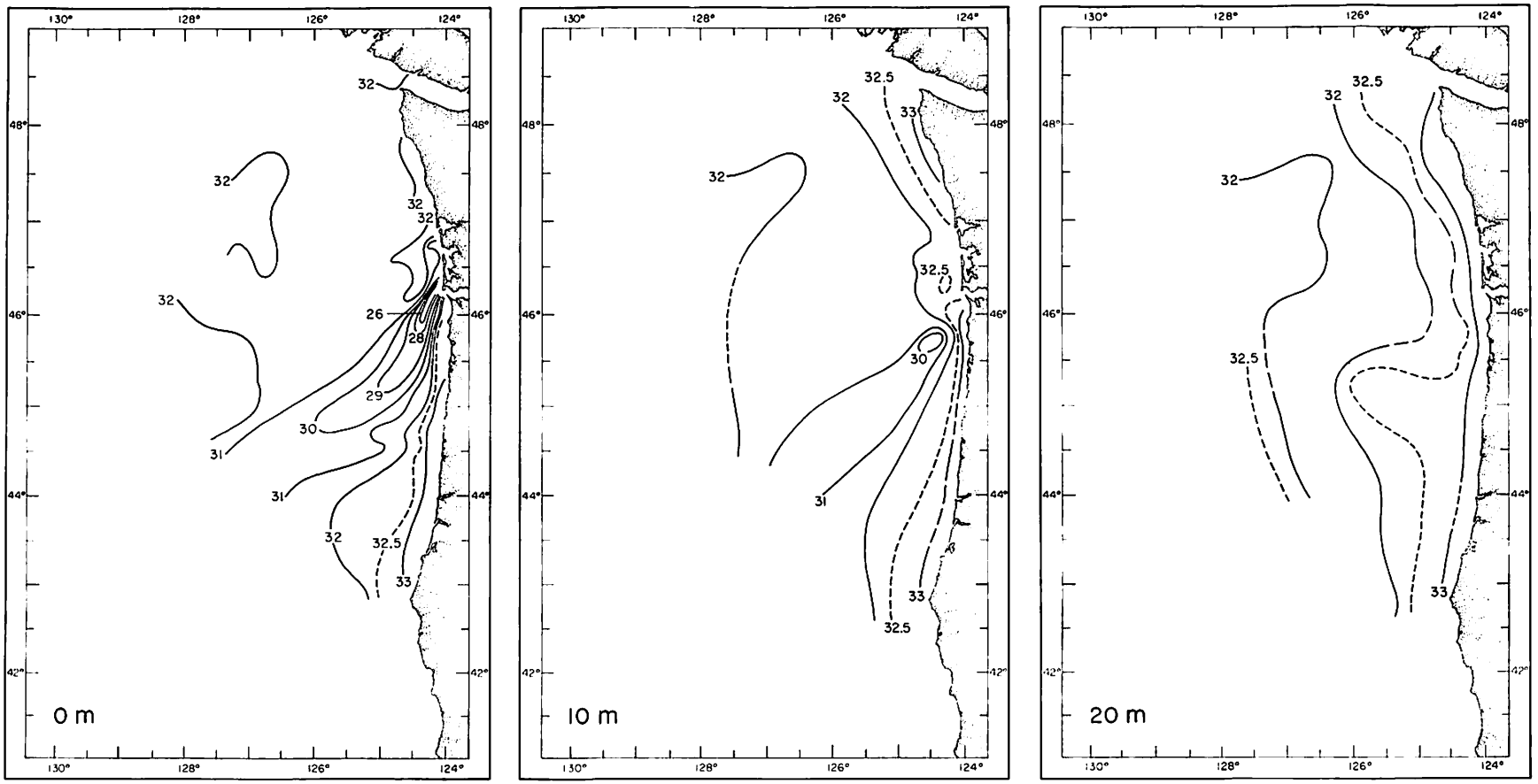

Fig. 31. Horizontal distributions of salinity (°/oo), Brown Bear Cruise 291.

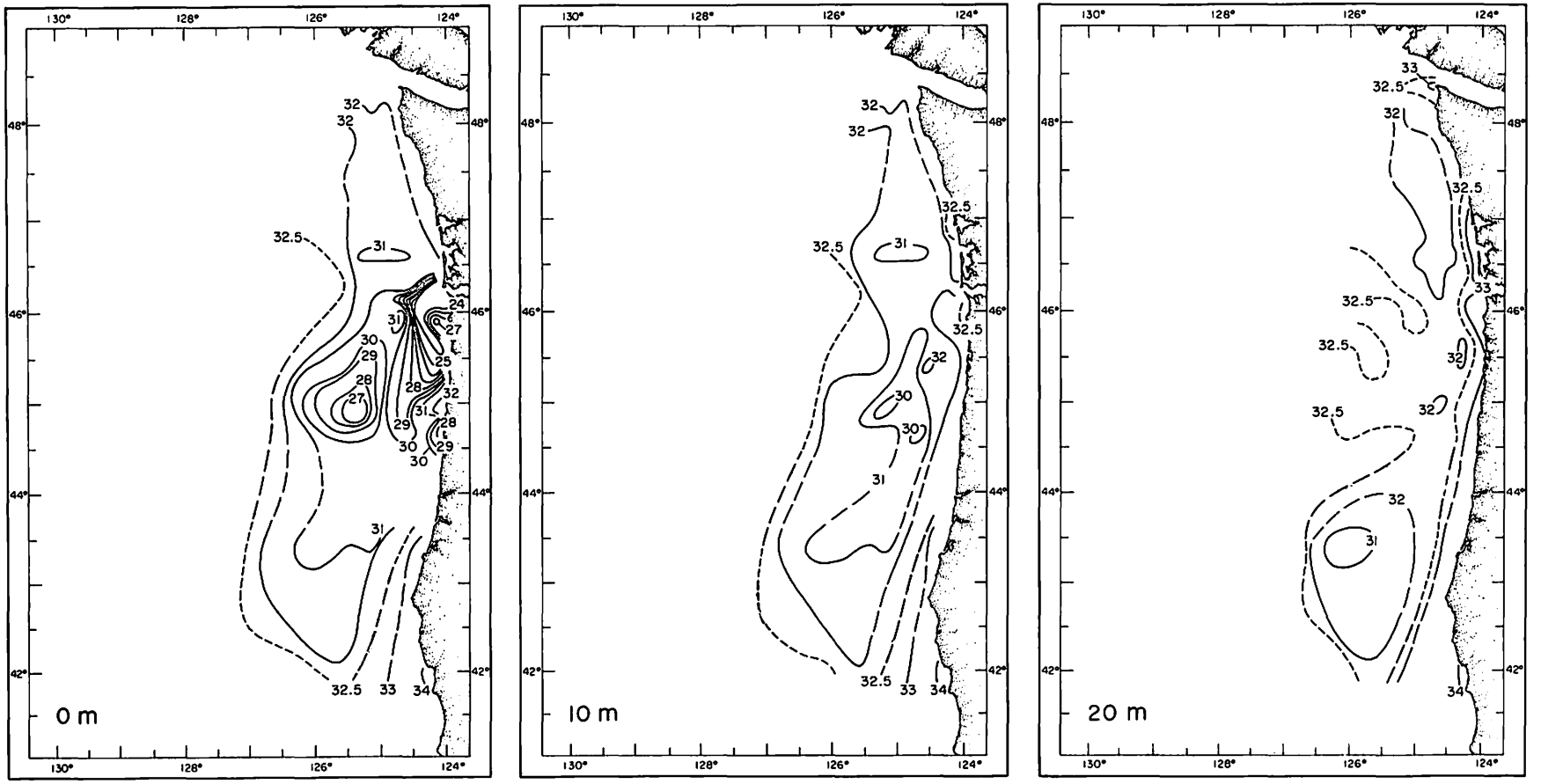

Fig. 32. Horizontal distributions of salinity (°/oo), Brown Bear Cruise 308 and Acona Cruise 6206

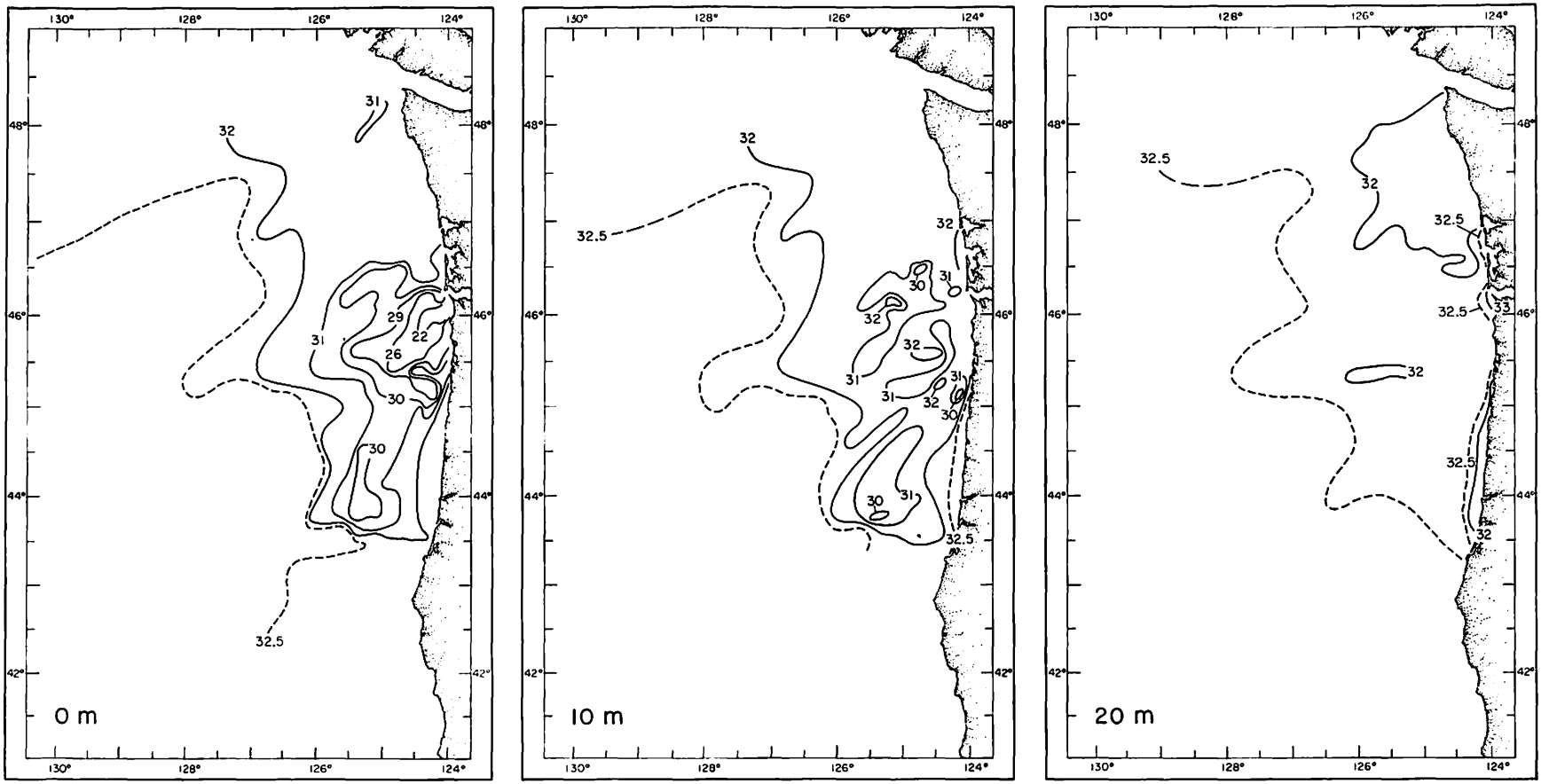

Fig. 33. Horizontal distributions of salinity (°/oo), Brown Bear Cruise 324 and Oshawa Cruise 002.

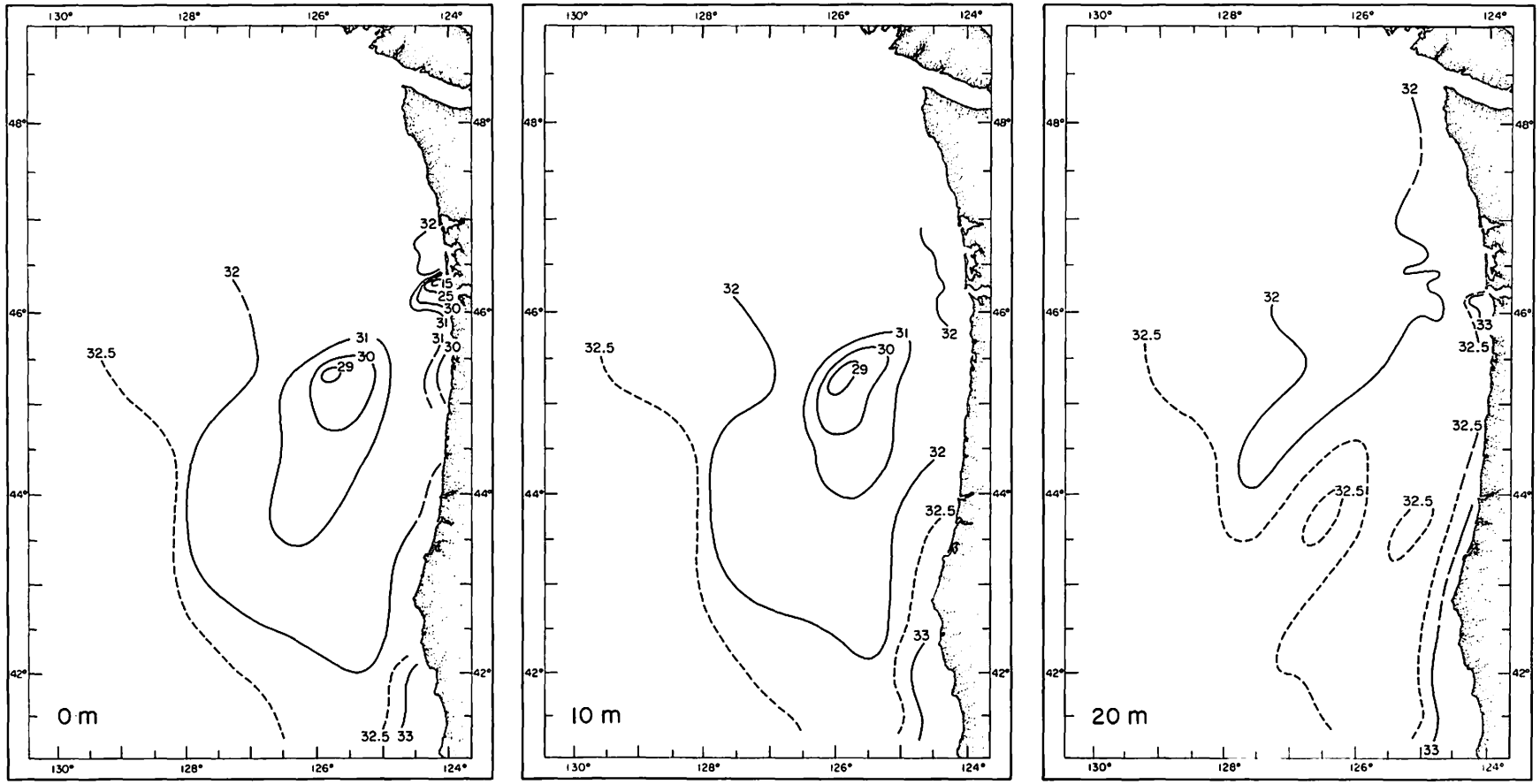

Fig. 34. Horizontal distributions of salinity (°/oo), Brown Bear Cruise 326 and Oshawa Cruise 003.

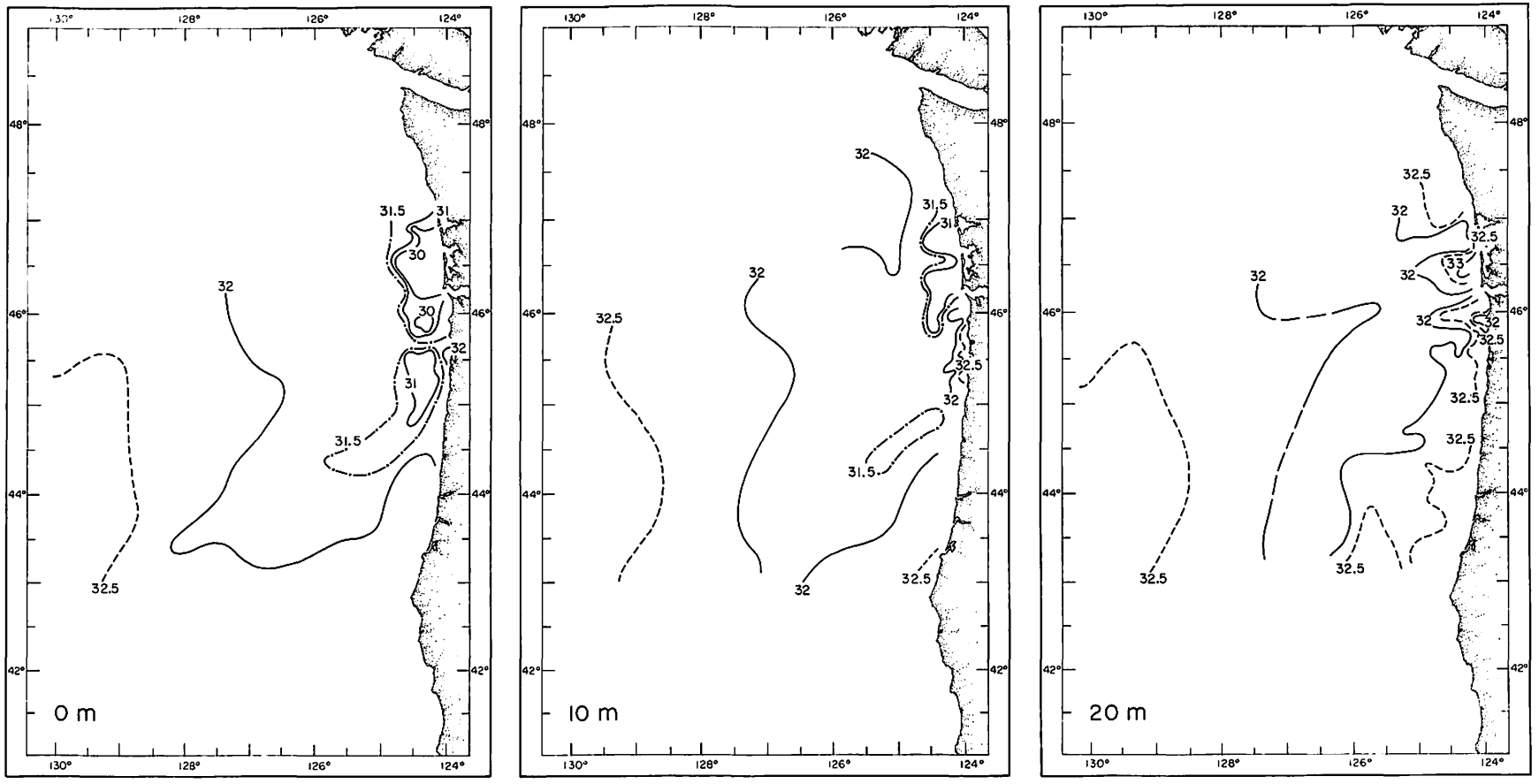

Fig. 35. Horizontal distributions of salinity (°/oo), Brown Bear Cruise 335 I.

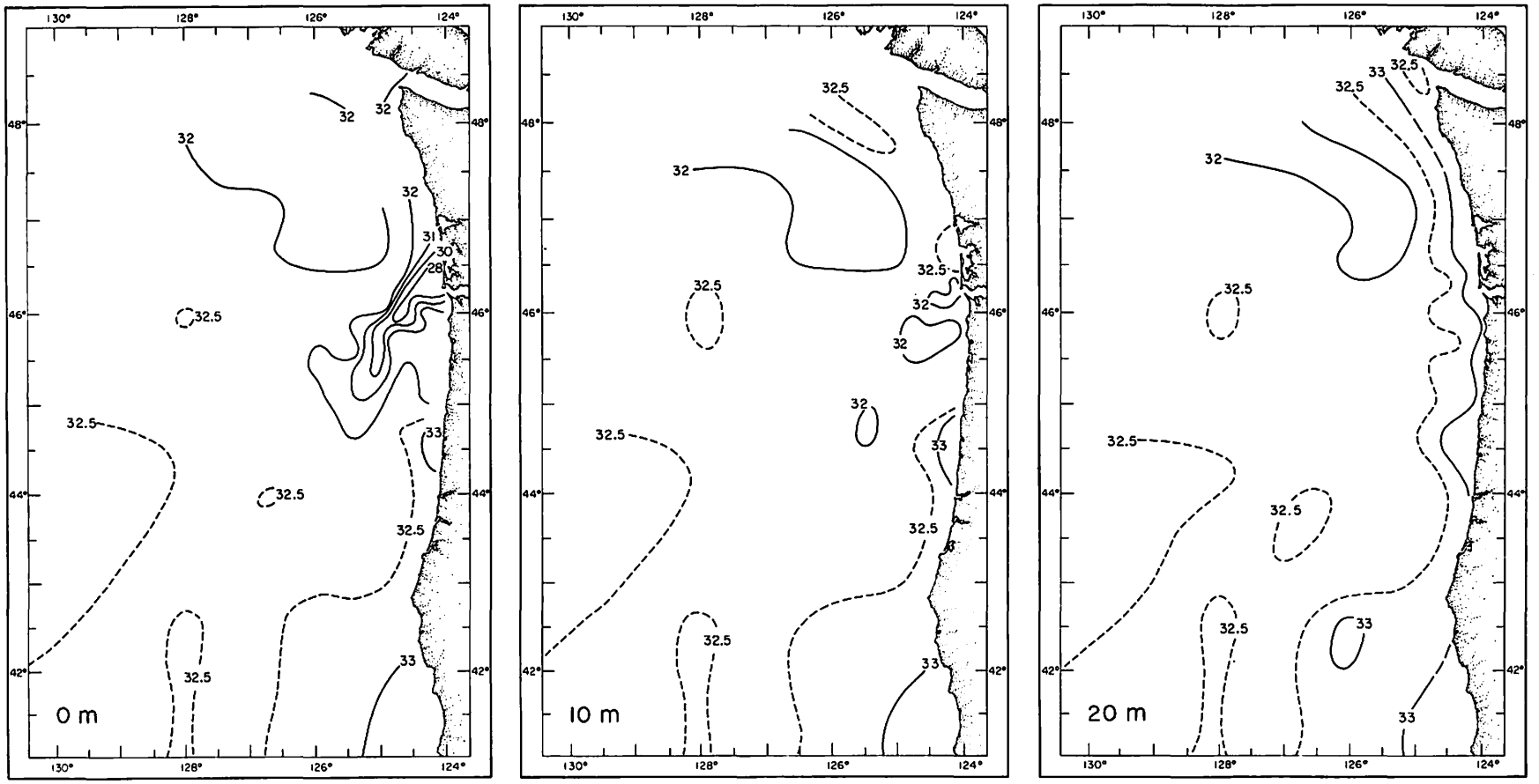

Fig. 36. Horizontal distributions of salinity (°/oo), Brown Bear Cruise 293

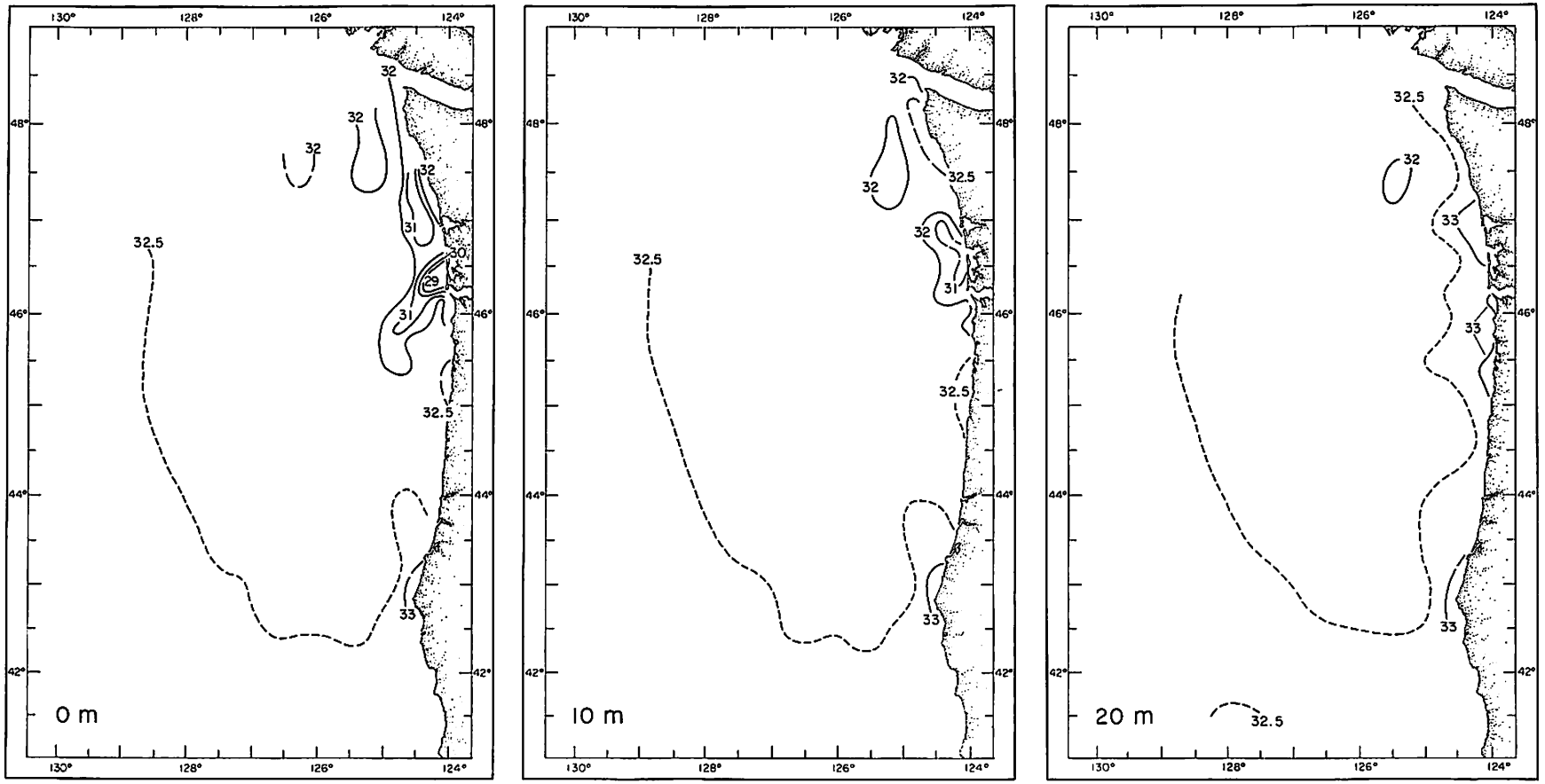

Fig. 37. Horizontal distributions of salinity (°/oo), Brown Bear Cruise 312.

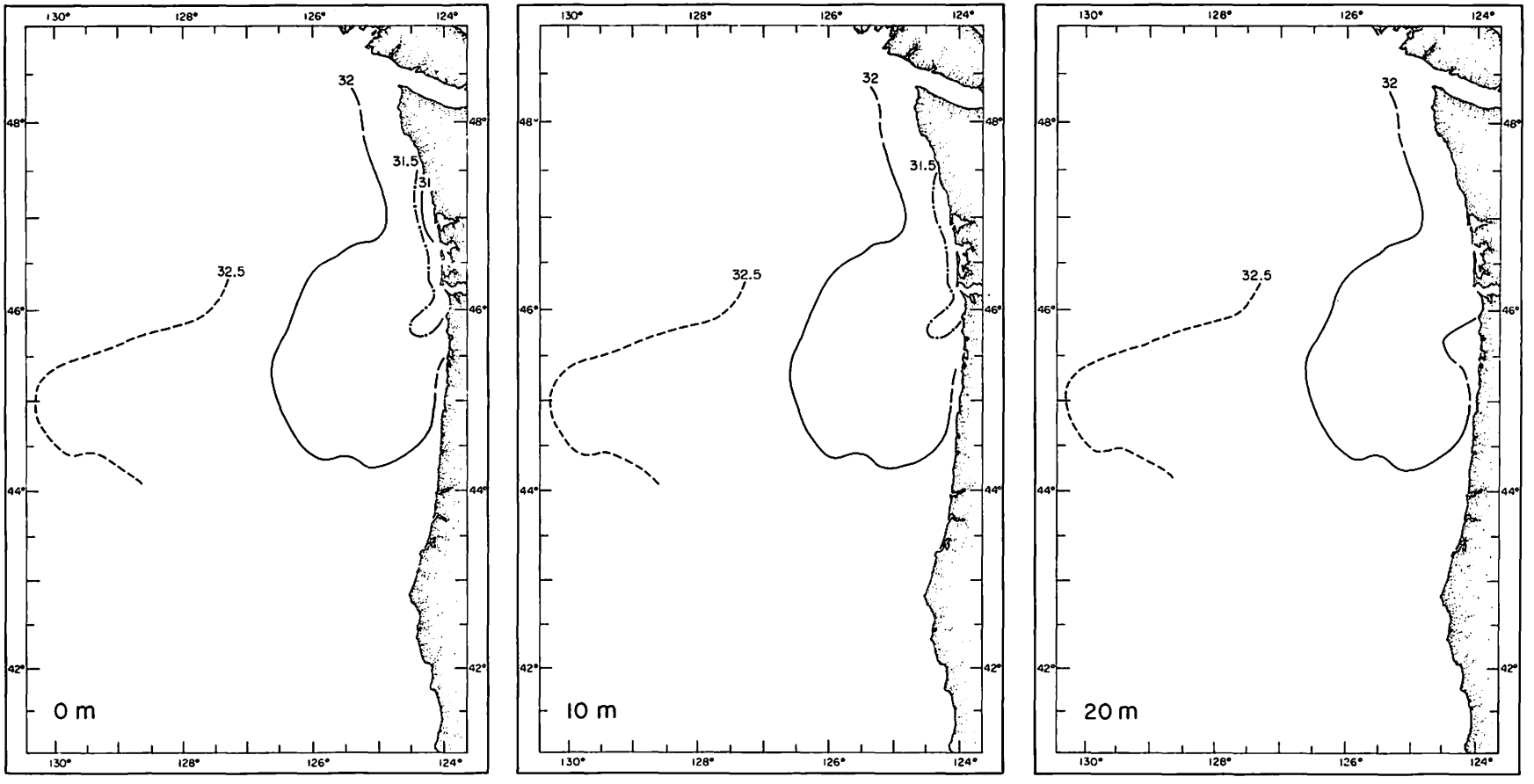

Fig. 38. Horizontal distributions of salinity (°/oo), Brown Bear Cruise 335 II.

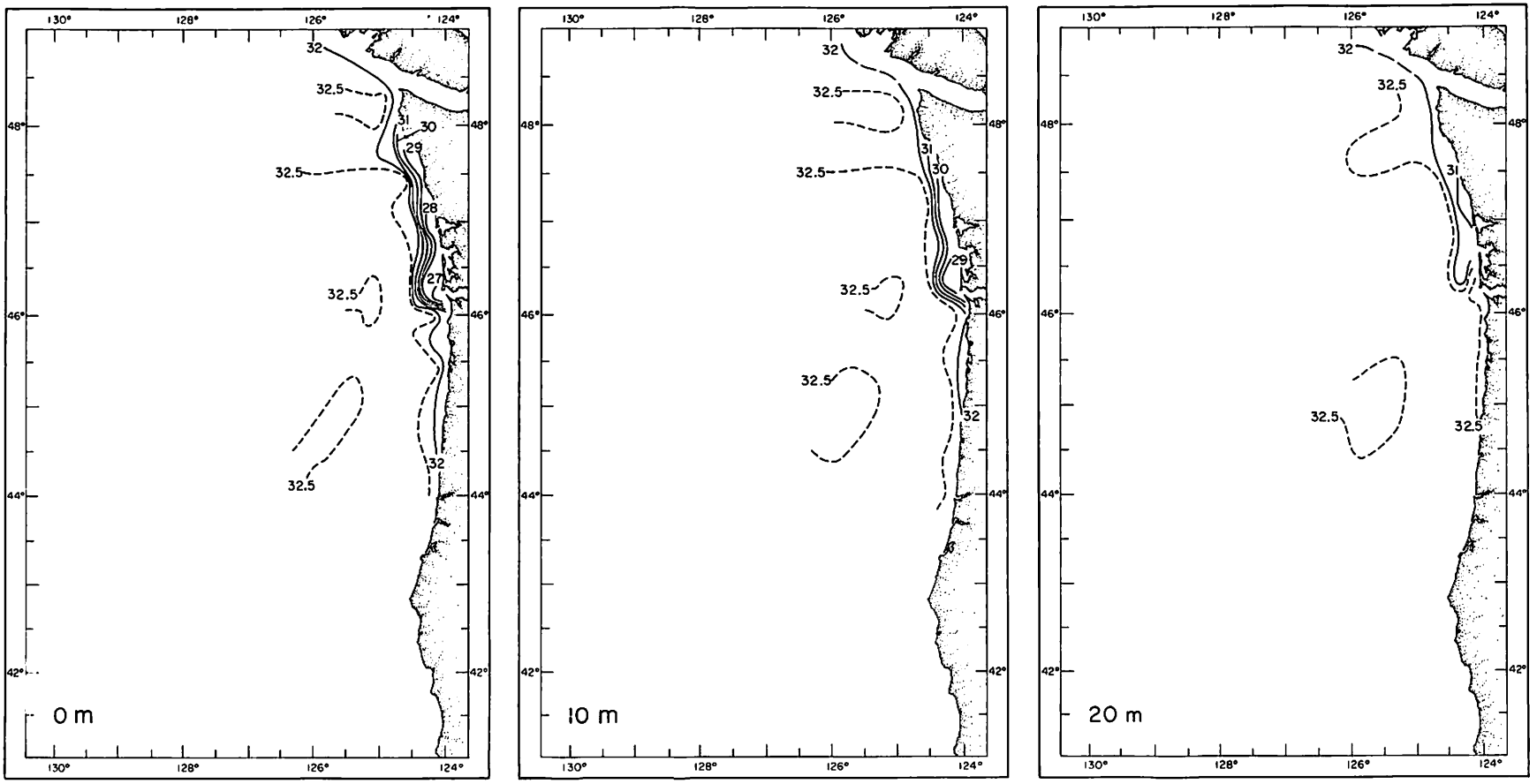

Fig. 39. Horizontal distributions of salinity (°/oo), Brown Bear Cruise 275.

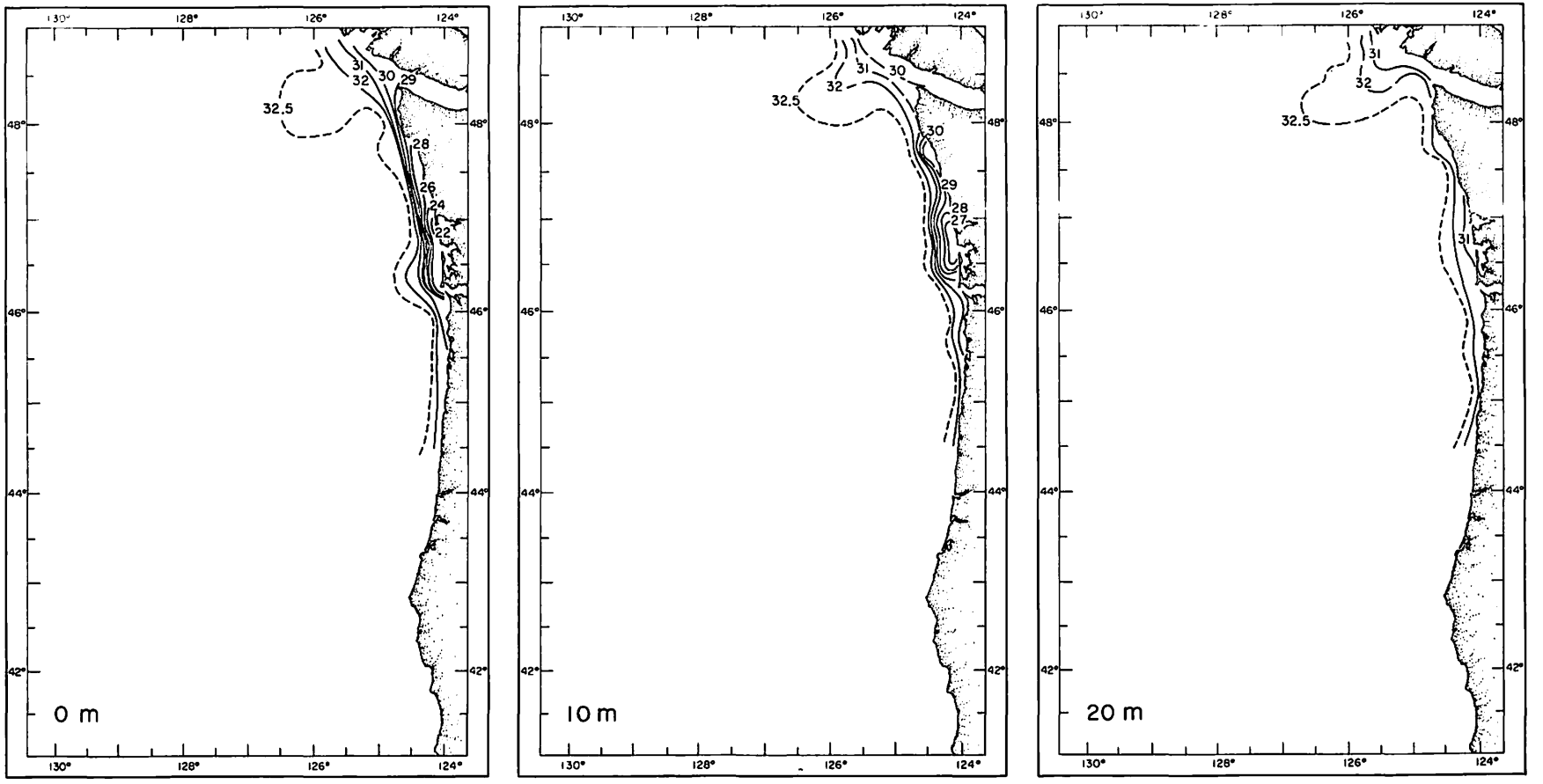

Fig. 40. Horizontal distributions of salinity (°/oo), Brown Bear Cruise 280.

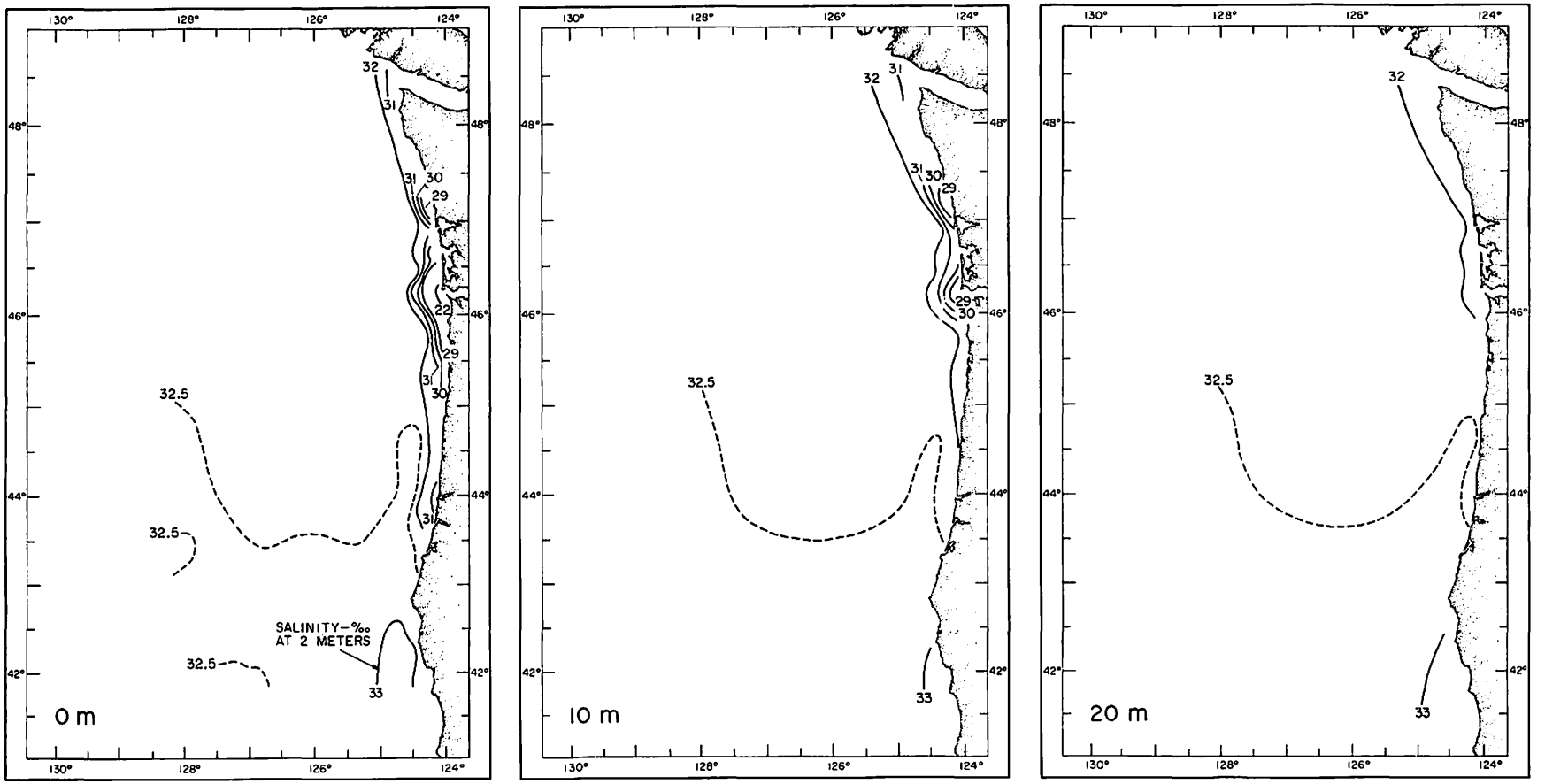

Fig. 41. Horizontal distributions of salinity (°/oo), Brown Bear Cruise 297.

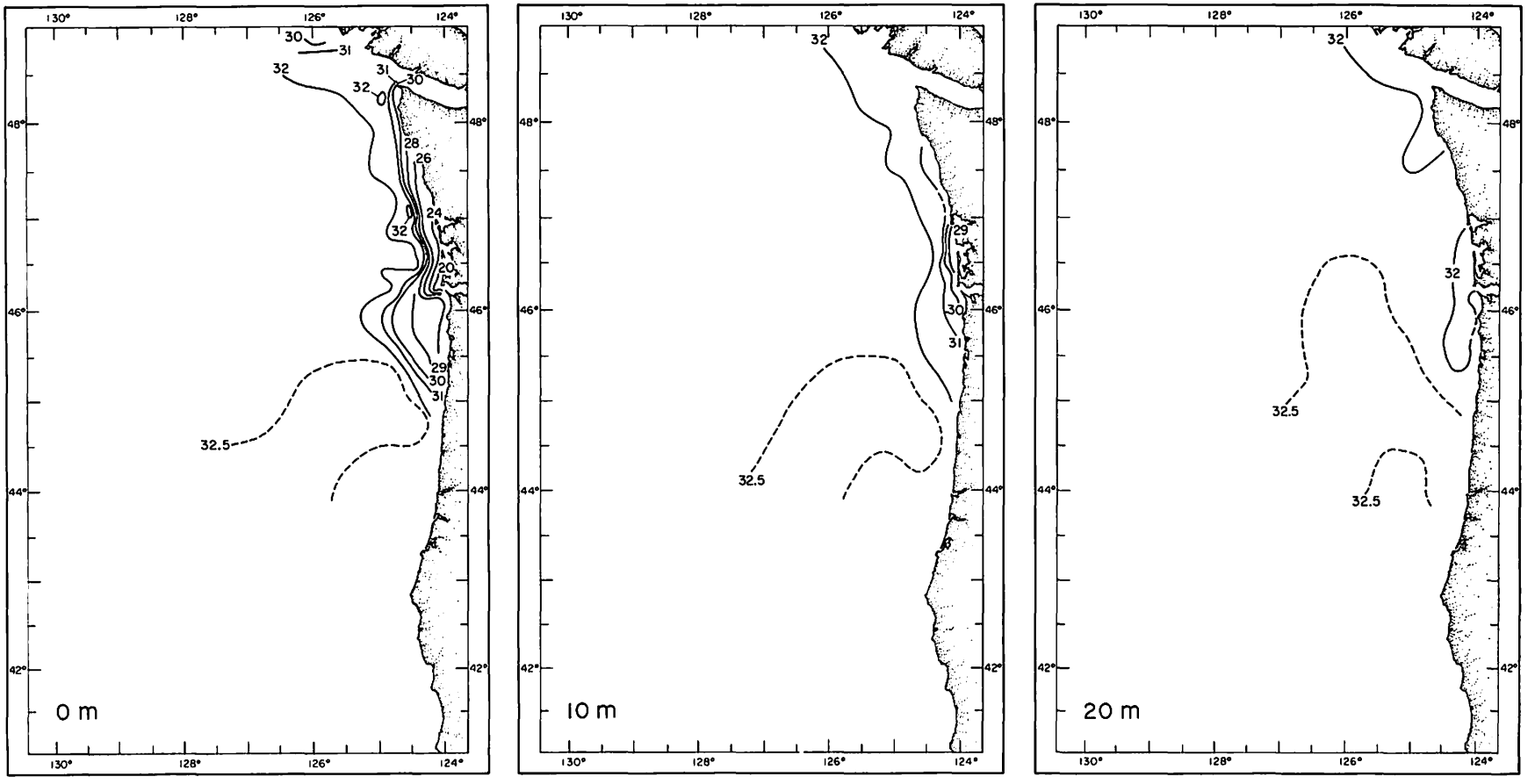

Fig. 42. Horizontal distributions of salinity (°/oo), Brown Bear Cruise 299.

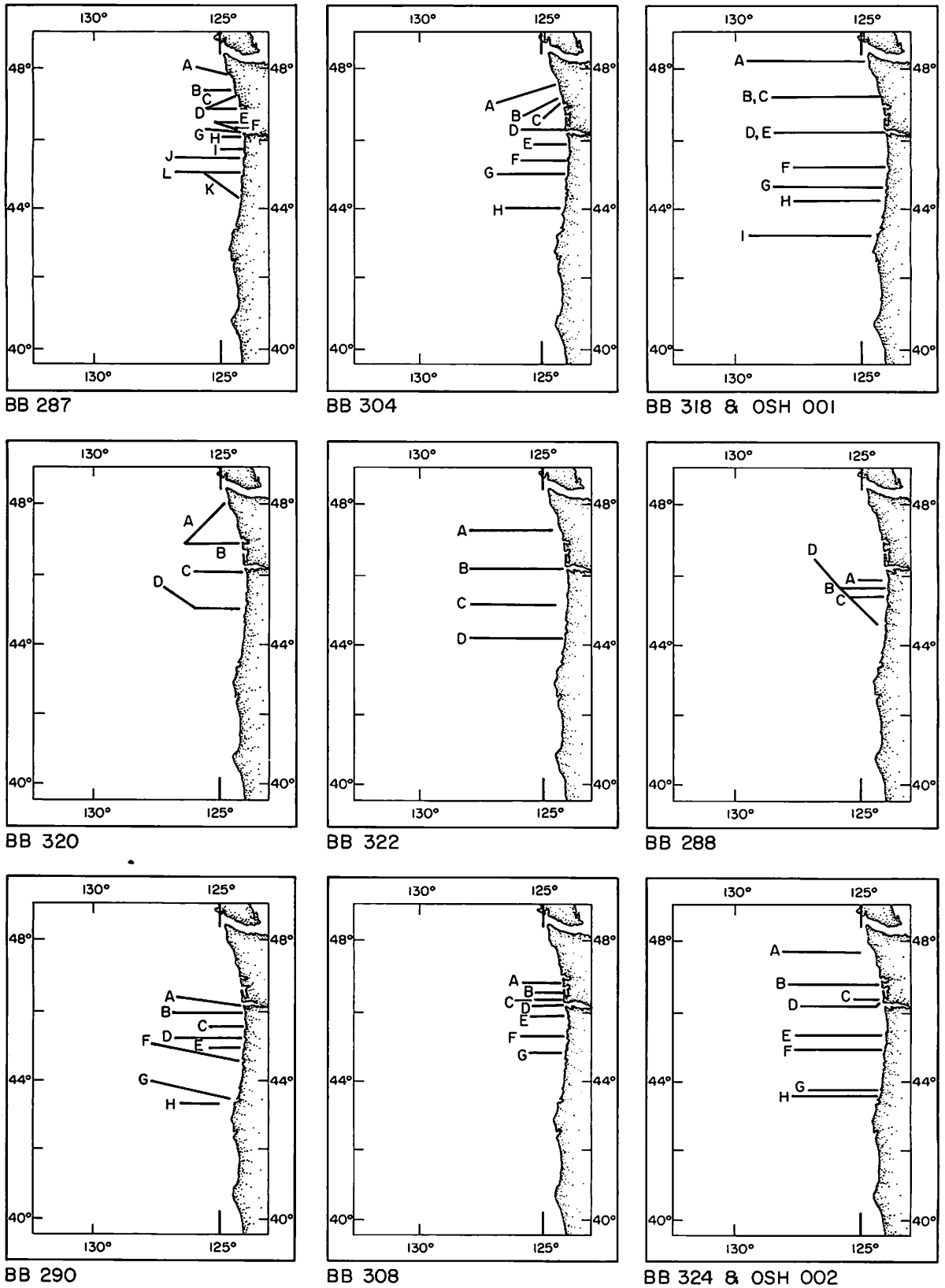

Fig. 43. Location charts I for vertical salinity distributions.

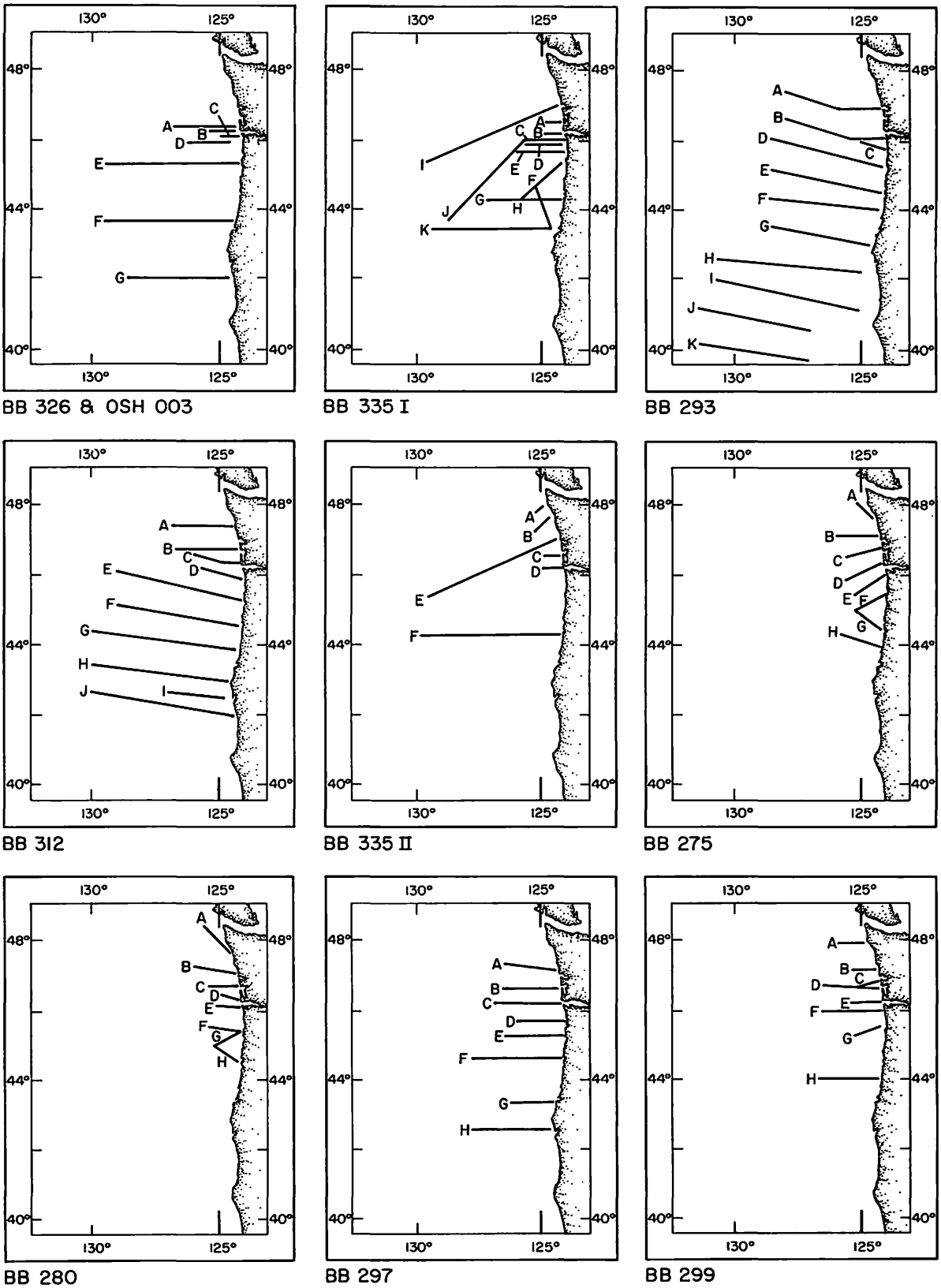

Fig. 44. Location charts II for vertical salinity distributions.

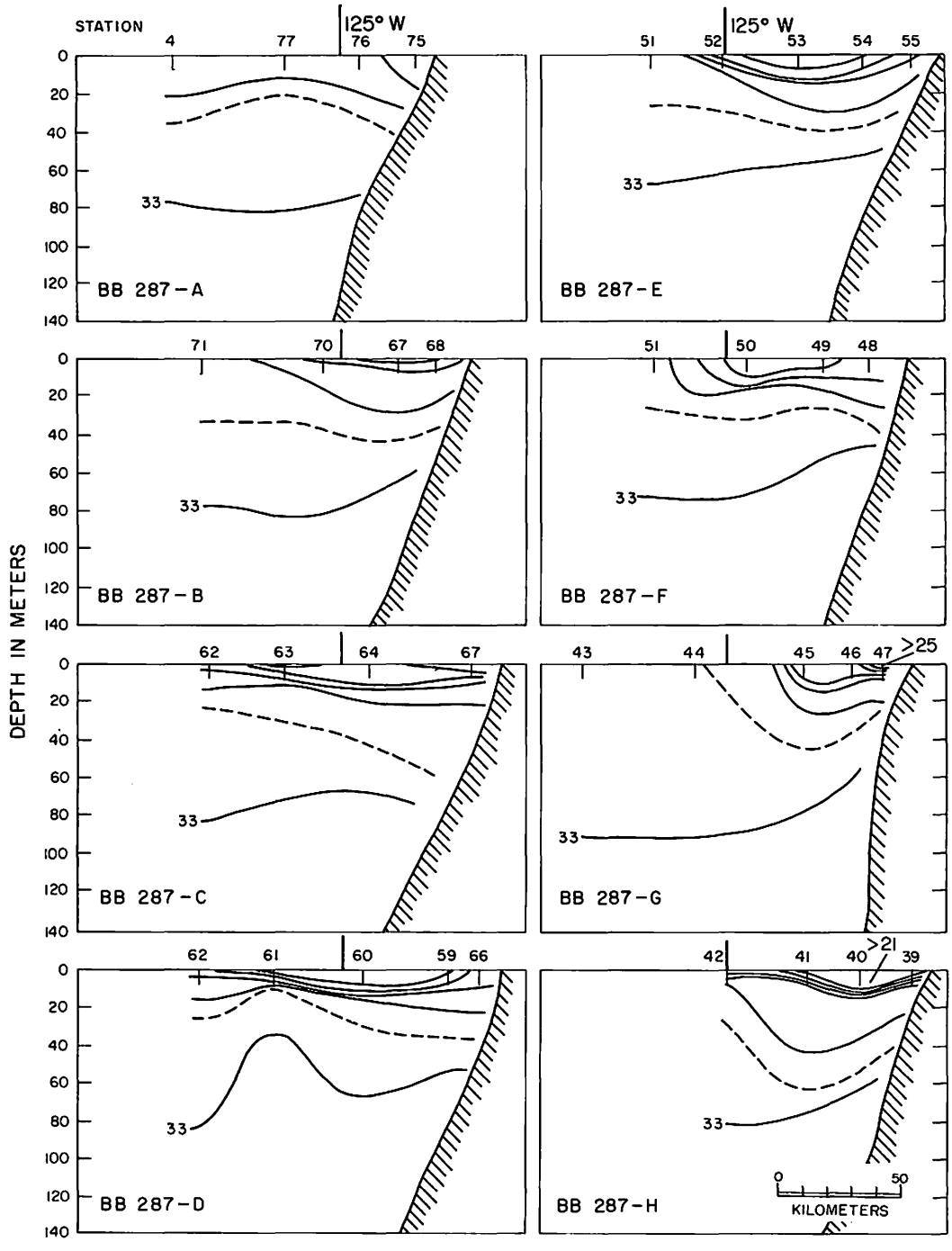

Fig. 45. Vertical distributions of salinity (—— ..., 31, 32, 33°/oo; --- 32.5°/oo) for Brown Bear Cruise 287, sections A-H.

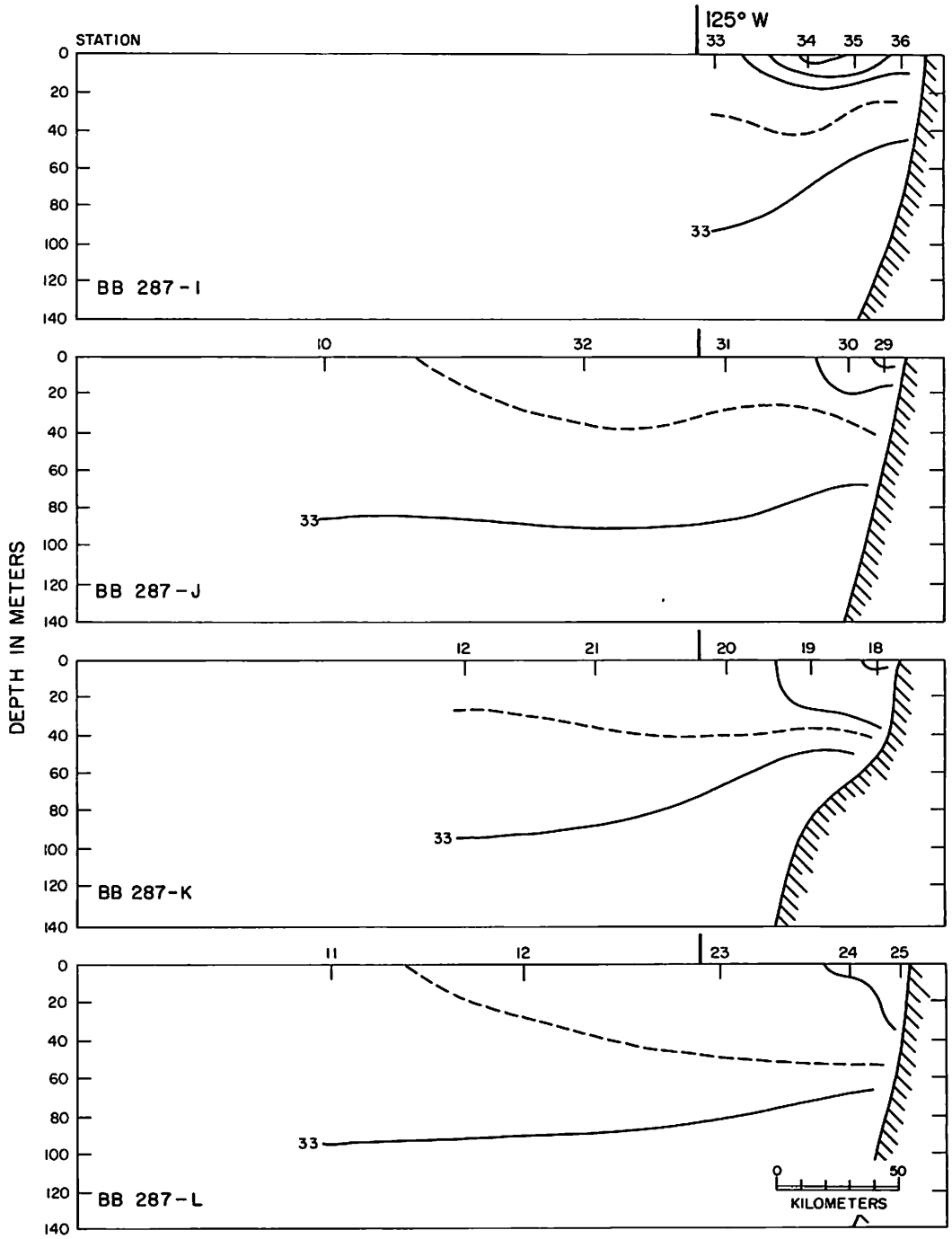

Fig. 46. Vertical distributions of salinity (—— ..., 31, 32, 33°/oo; --- 32.5°/oo) for Brown Bear Cruise 287, sections I-L.

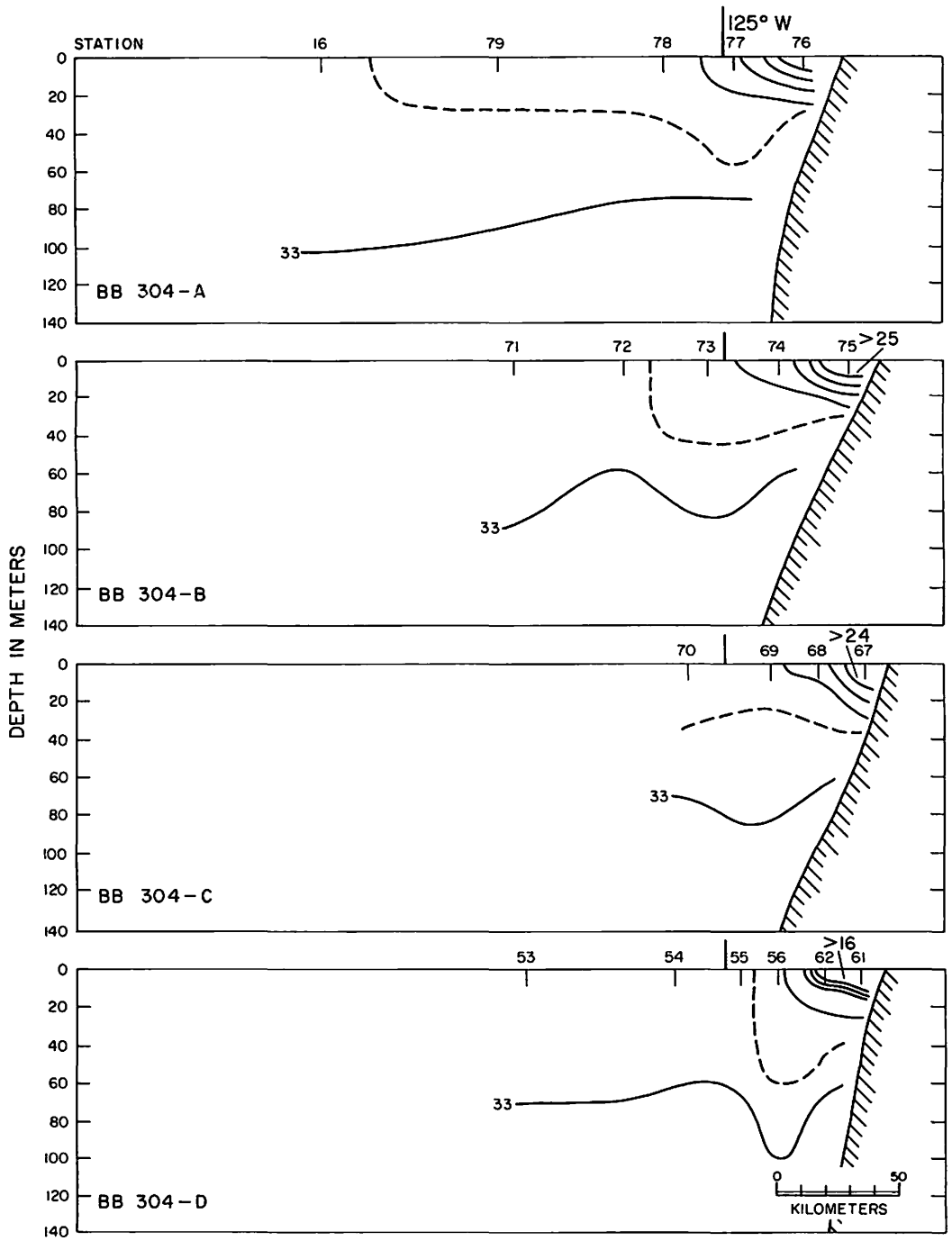

Fig. 47. Vertical distributions of salinity (—— ..., 31, 32, 33°/oo; --- 32.5°/oo) for Brown Bear Cruise 304, sections A-D.

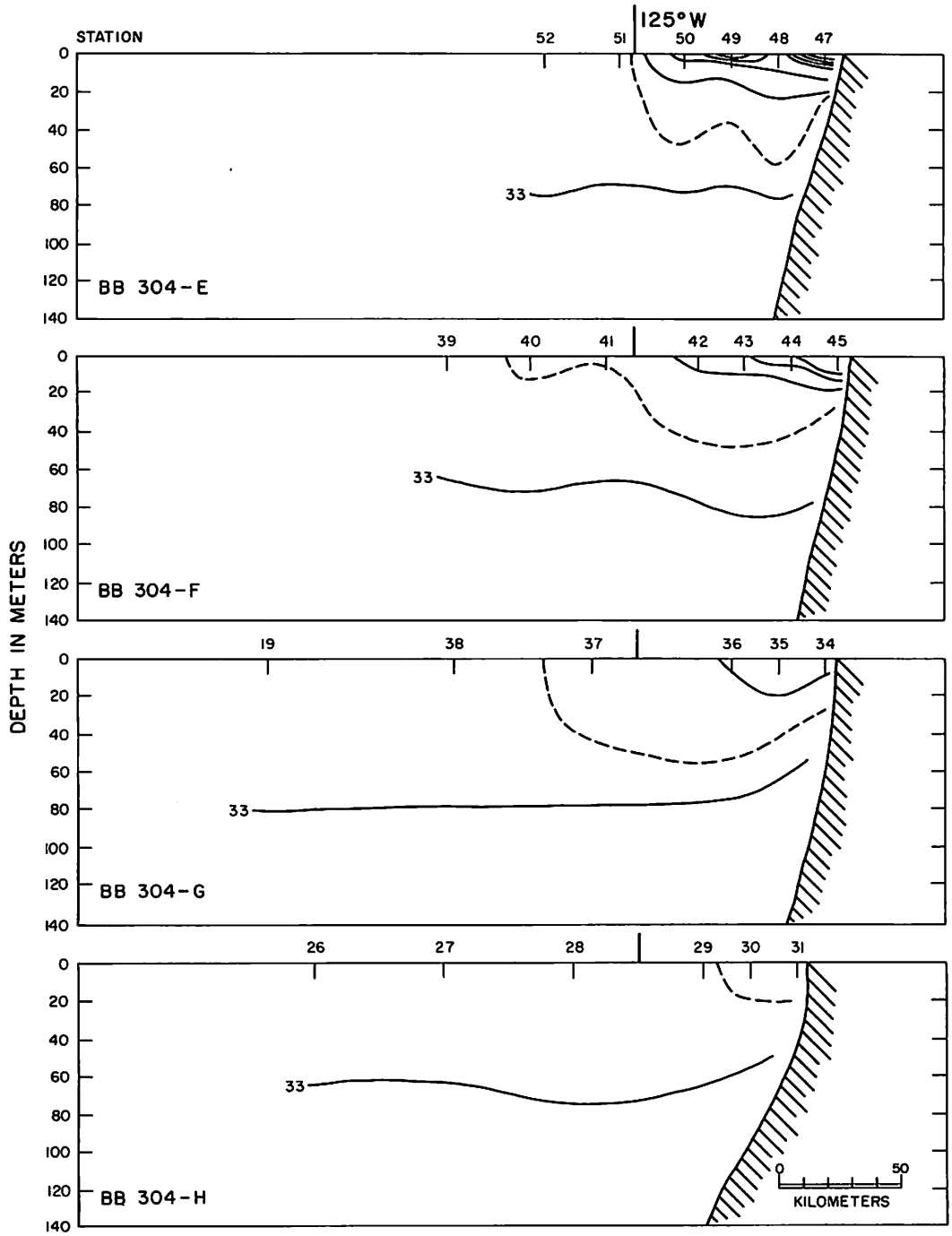

Fig. 48. Vertical distributions of salinity (—— ..., 31, 32, 33°/oo; --- 32.5°/oo) for Brown Bear Cruise 304, sections E-H.

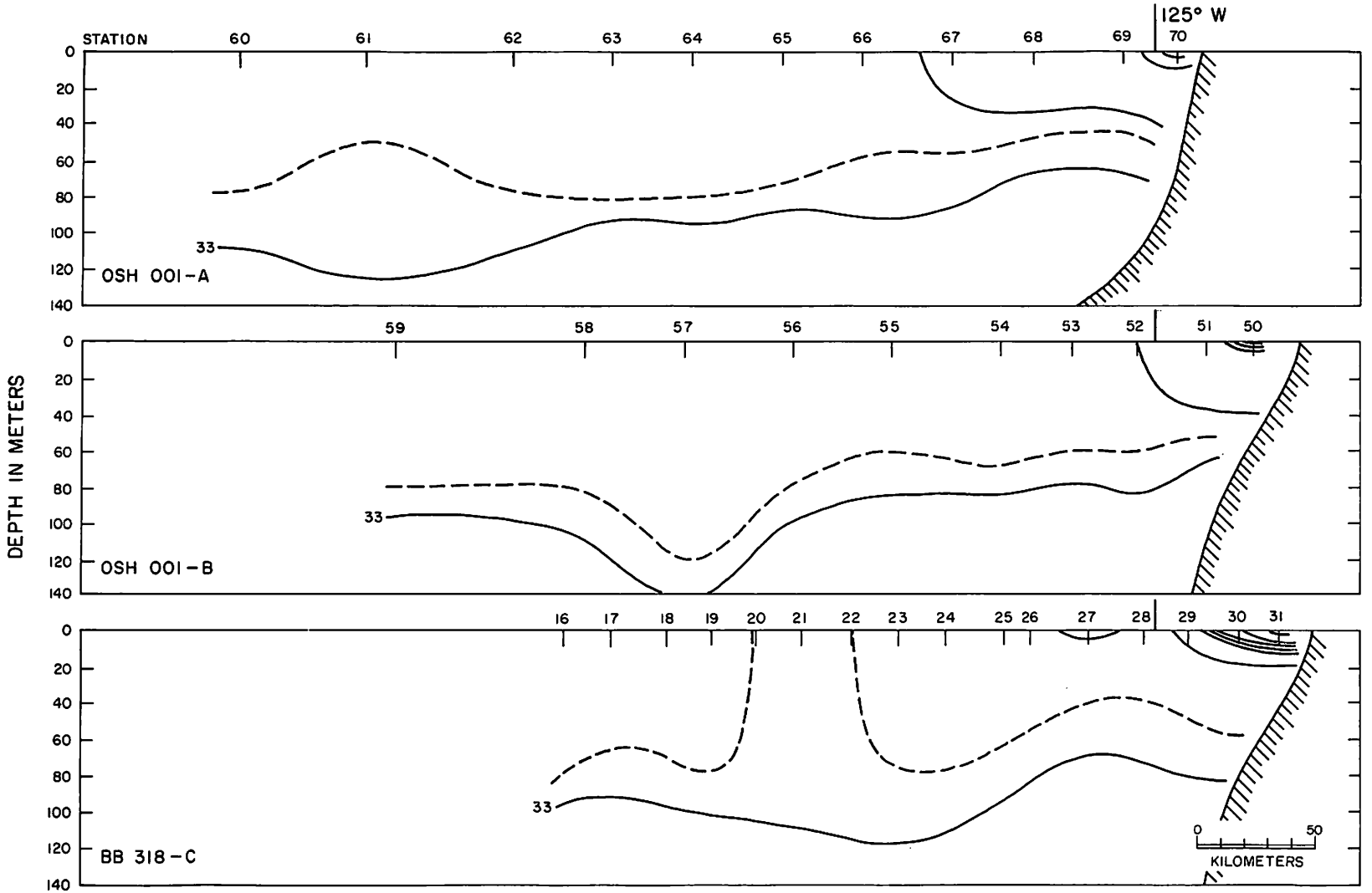

Fig. 49. Vertical distributions of salinity (—— ..., 31, 32, 33°/oo; --- 32.5°/oo) for Brown Bear Cruise 318, section C, and Oshawa Cruise 001, sections A and B.

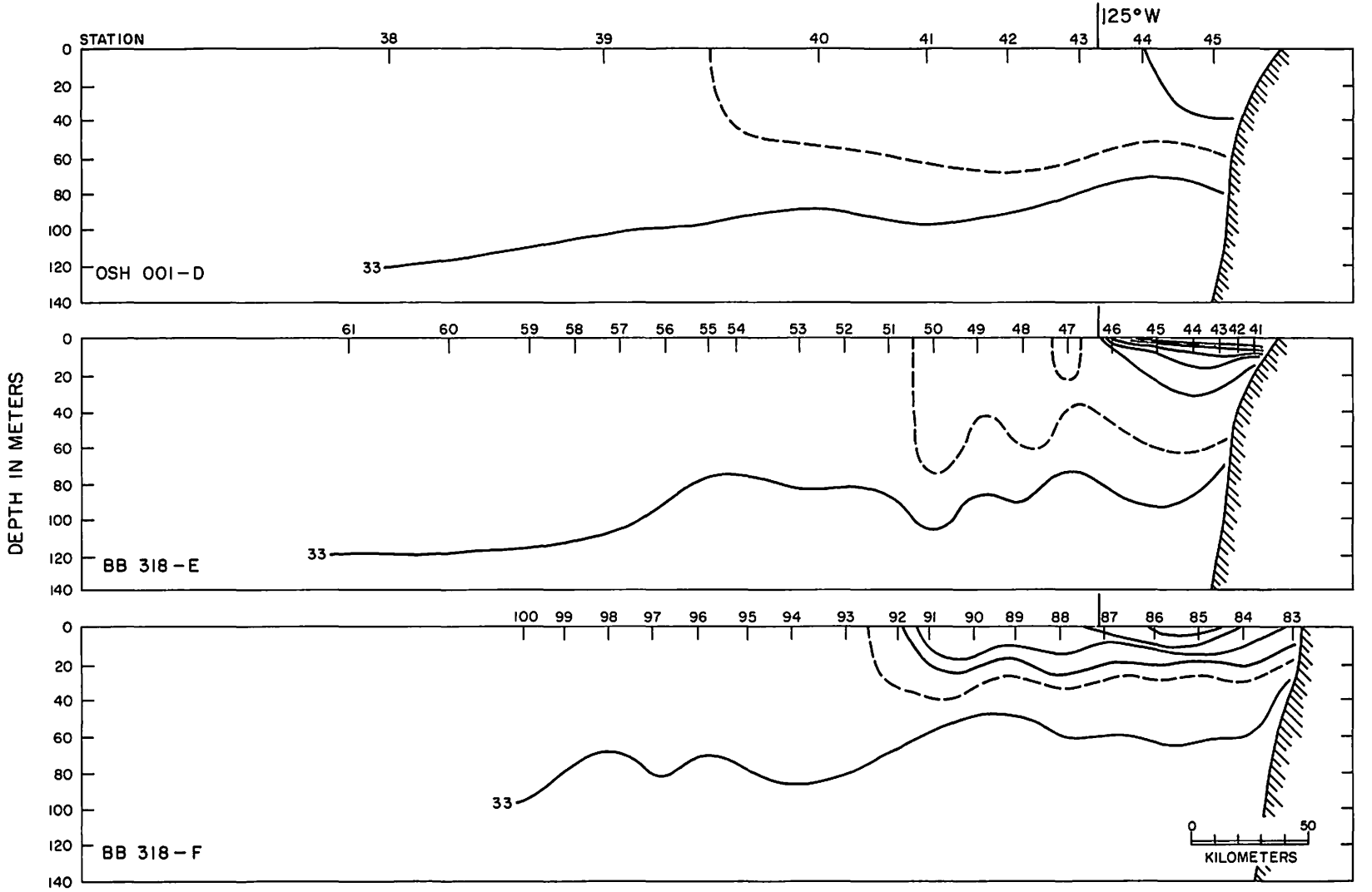

Fig. 50. Vertical distributions of salinity (—— ..., 31, 32, 33°/oo; --- 32.5°/oo) for Brown Bear Cruise 318, sections E and F, and Oshawa Cruise 001, section D.

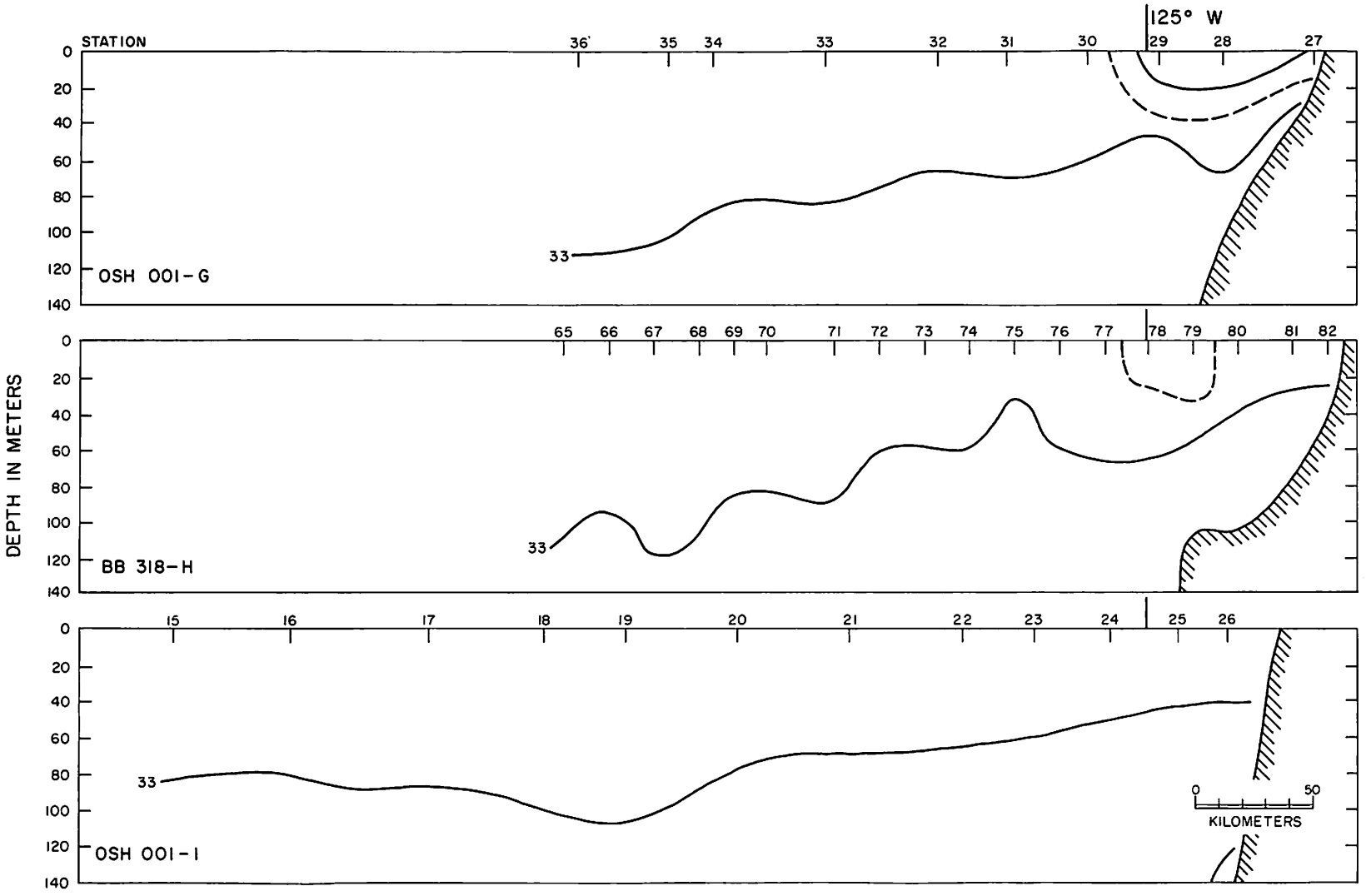

Fig. 51. Vertical distributions of salinity (—— ..., 31, 32, 33°/oo; --- 32.5°/oo) for Brown Bear Cruise 318, section H, and Oshawa Cruise 001, sections G and I.

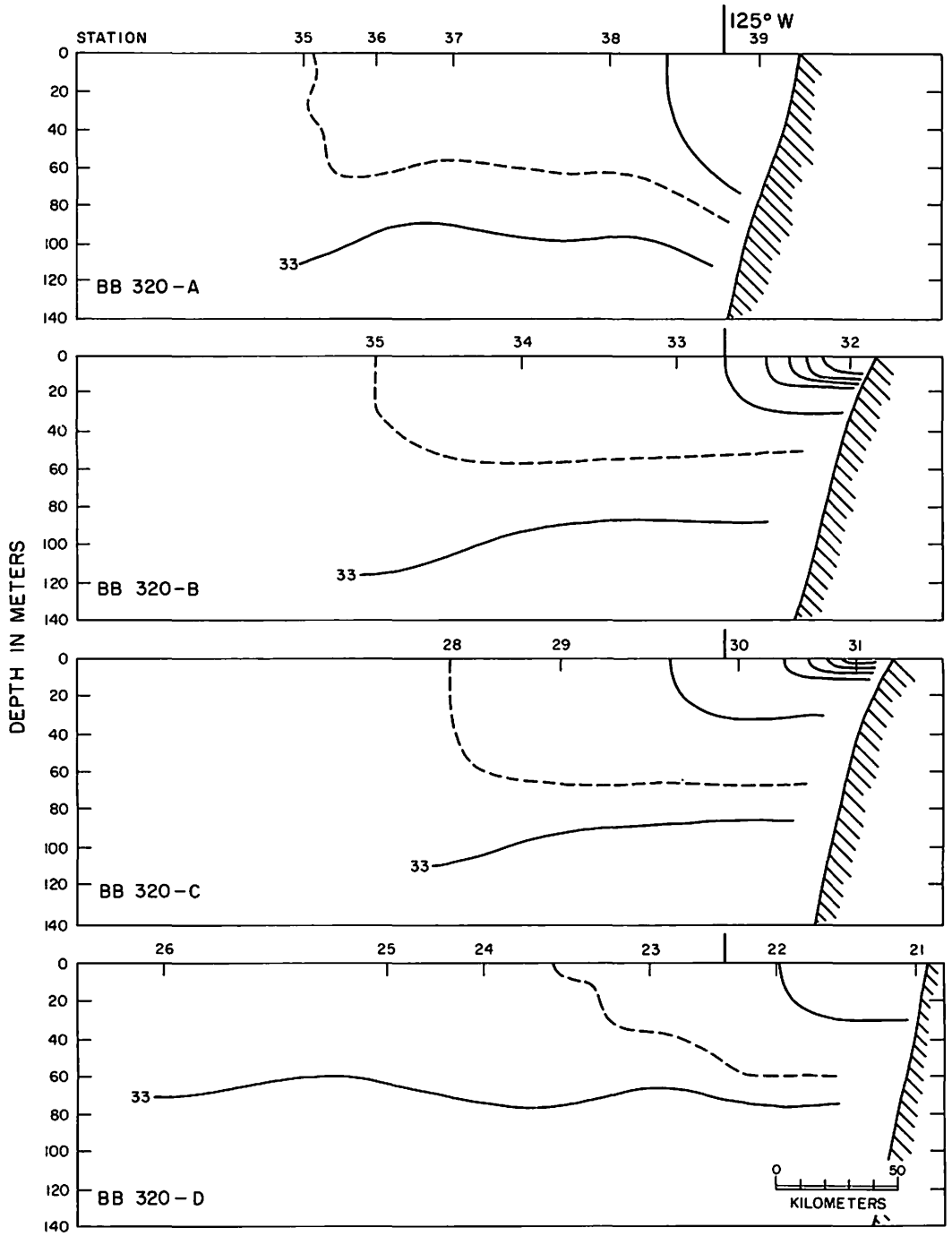

Fig. 52. Vertical distributions of salinity (—— ..., 31, 32, 33°/oo; --- 32.5°/oo) for Brown Bear Cruise 320, sections A-D.

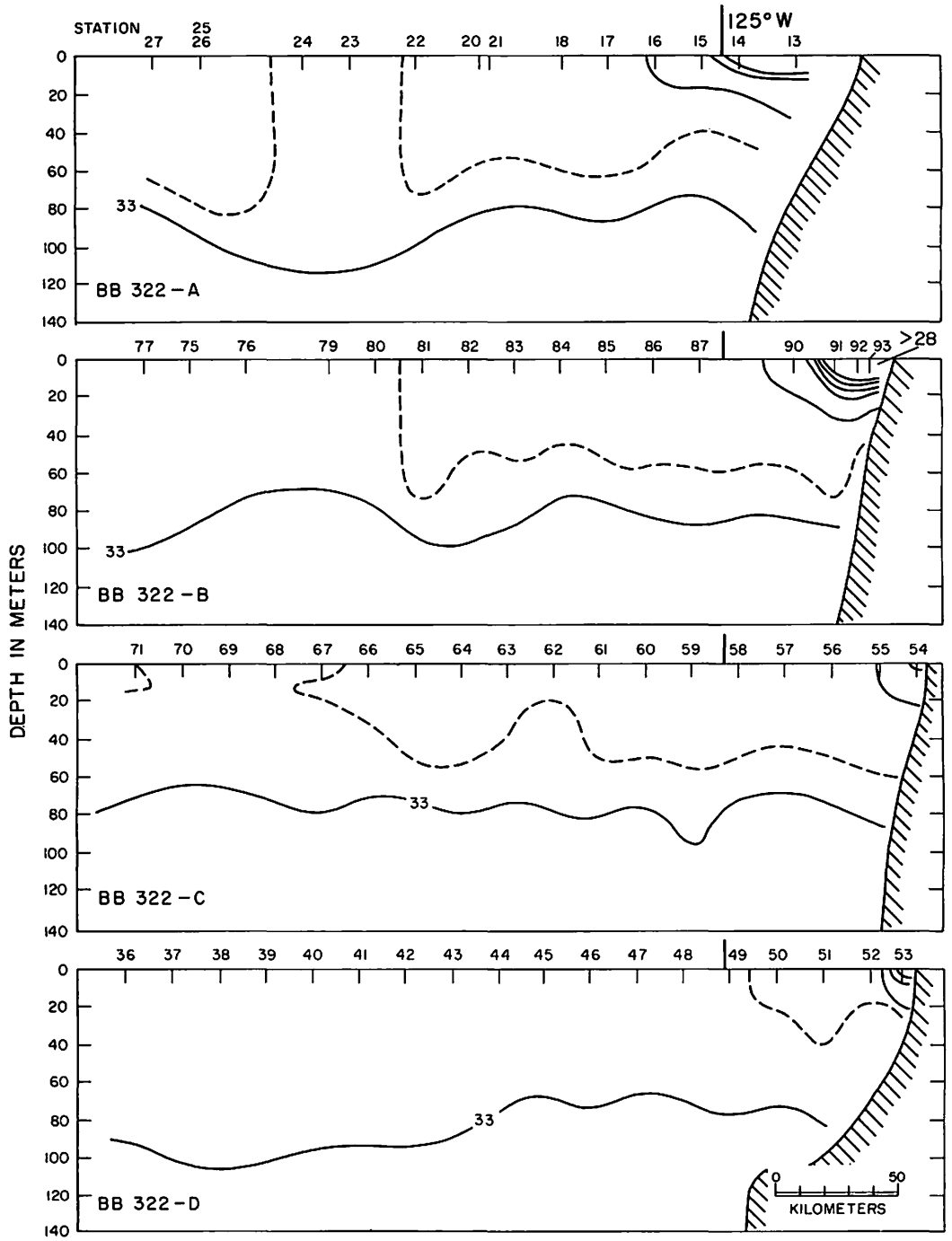

Fig. 53. Vertical distributions of salinity (—— ..., 31, 32, 33°/oo; --- 32.5°/oo) for Brown Bear Cruise 322, sections A-D.

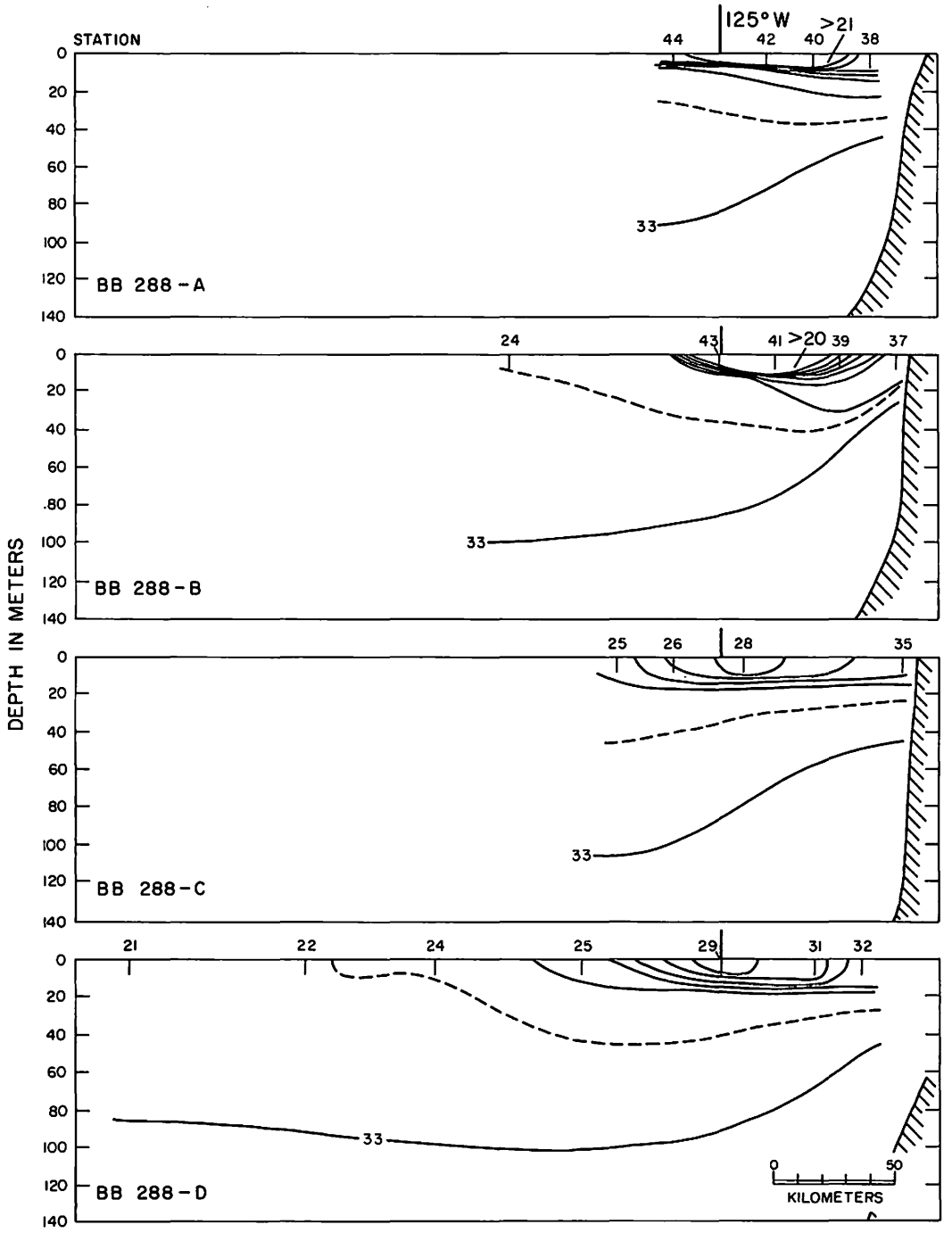

Fig. 54. Vertical distributions of salinity (—— ..., 31, 32, 33°/oo; --- 32.5°/oo) for Brown Bear Cruise 288, sections A-D.

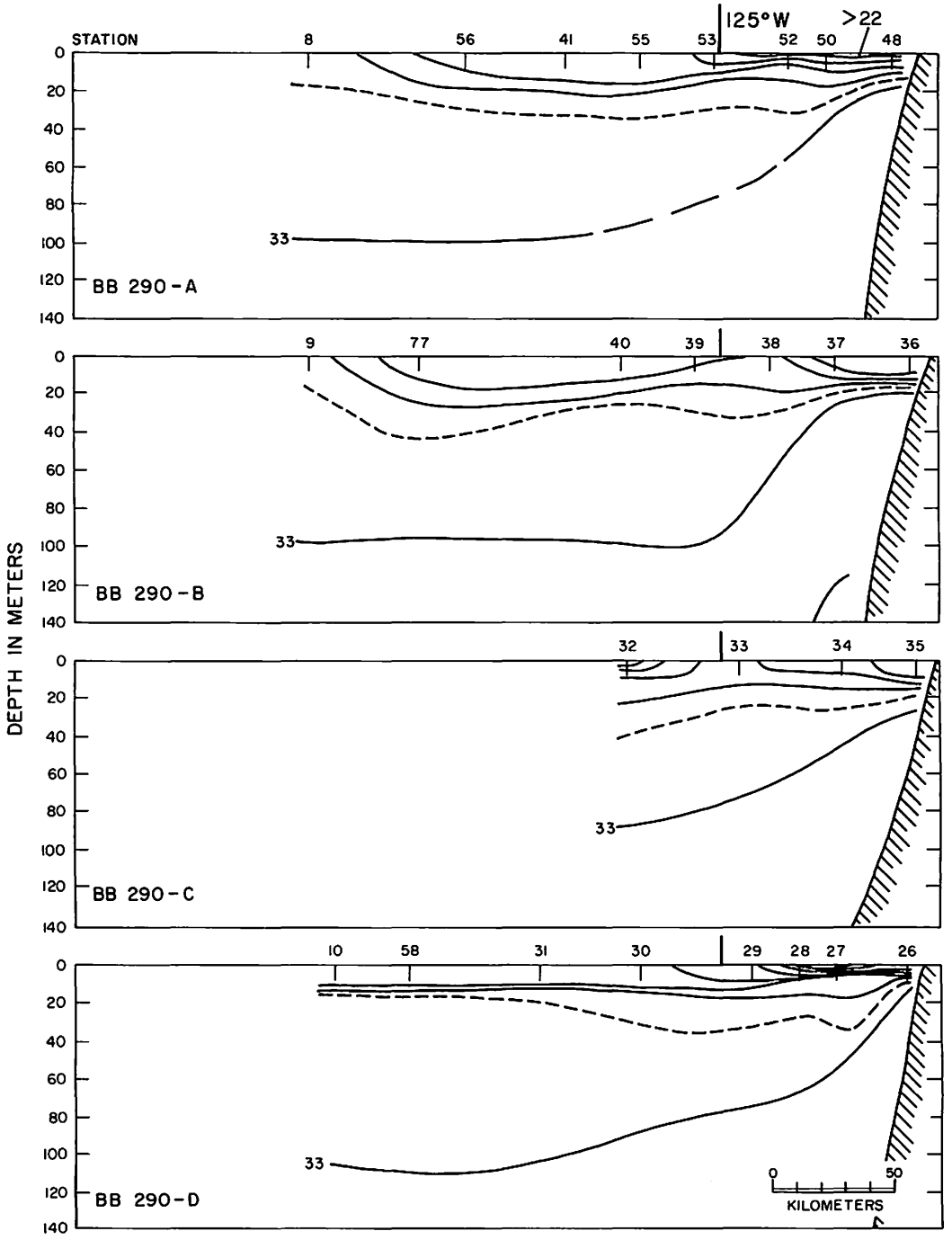

Fig. 55. Vertical distributions of salinity (—— ..., 31, 32, 33°/oo; --- 32.5°/oo for Brown Bear Cruise 290, sections A-D.

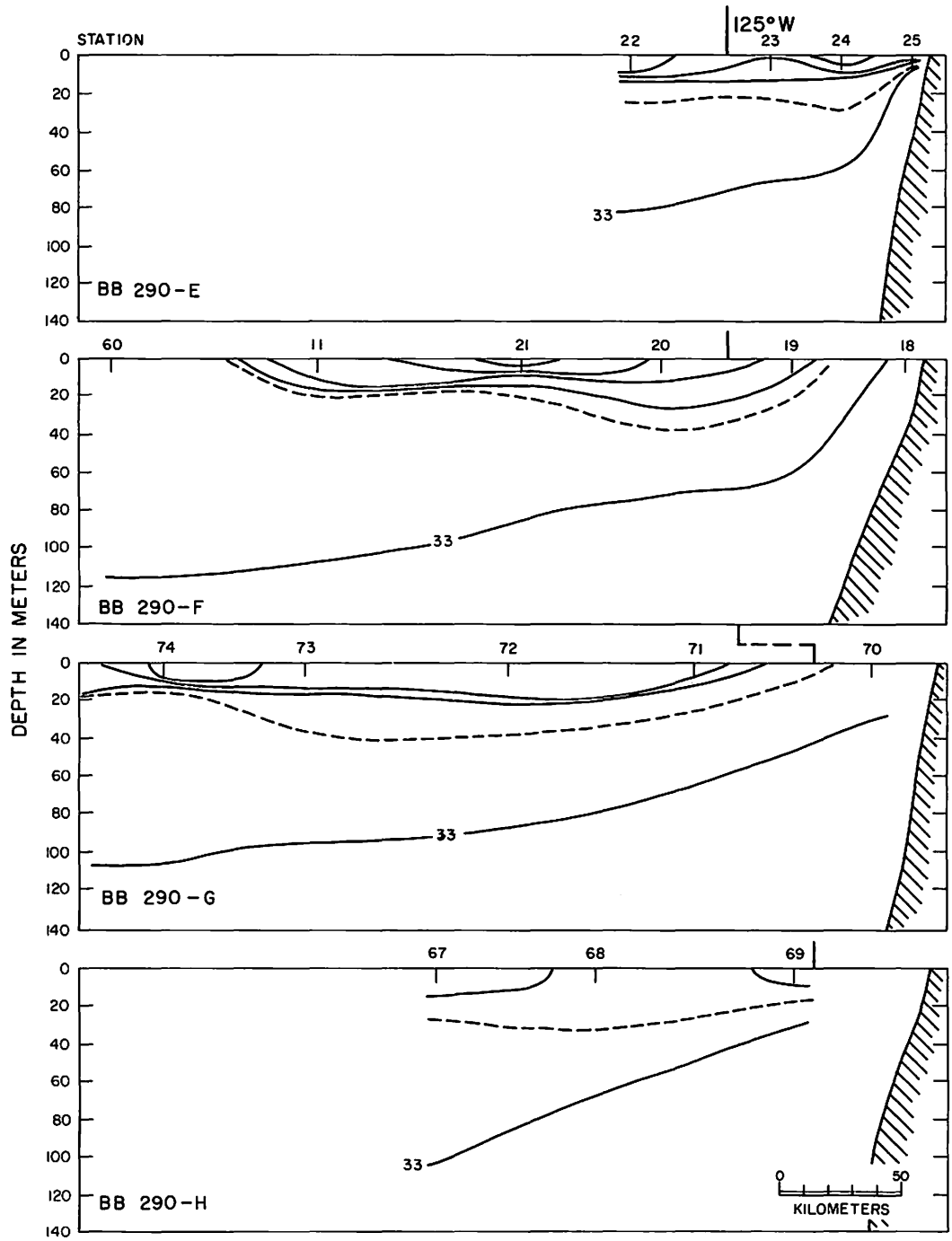

Fig. 56. Vertical distributions of salinity (—— ..., 31, 32, 33°/oo; --- 32.5°/oo) for Brown Bear Cruise 290, sections E-H.

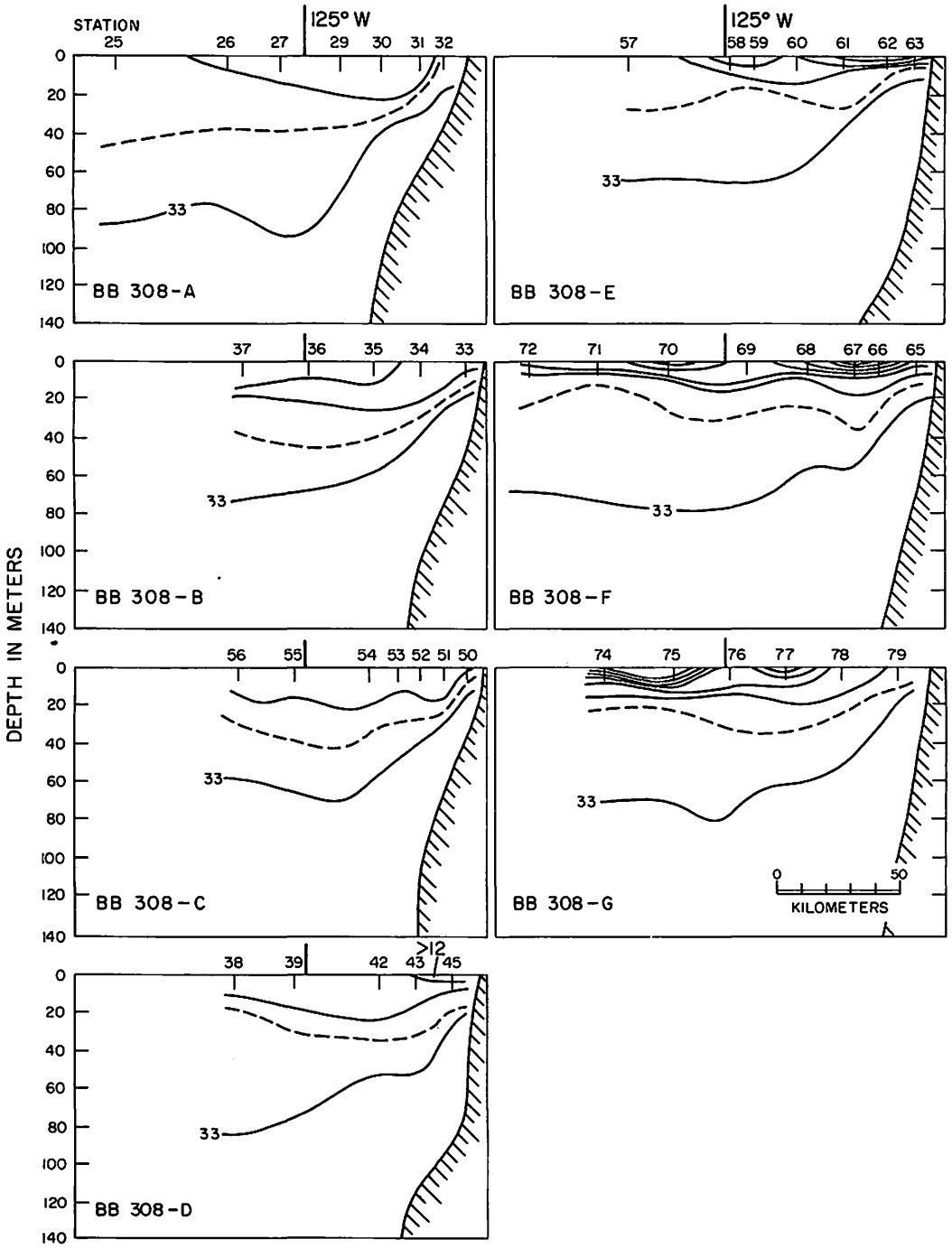

Fig. 57. Vertical distributions of salinity (—— ..., 31, 32, 33°/oo; --- 32.5°/oo) for Brown Bear Cruise 308, sections A-G.

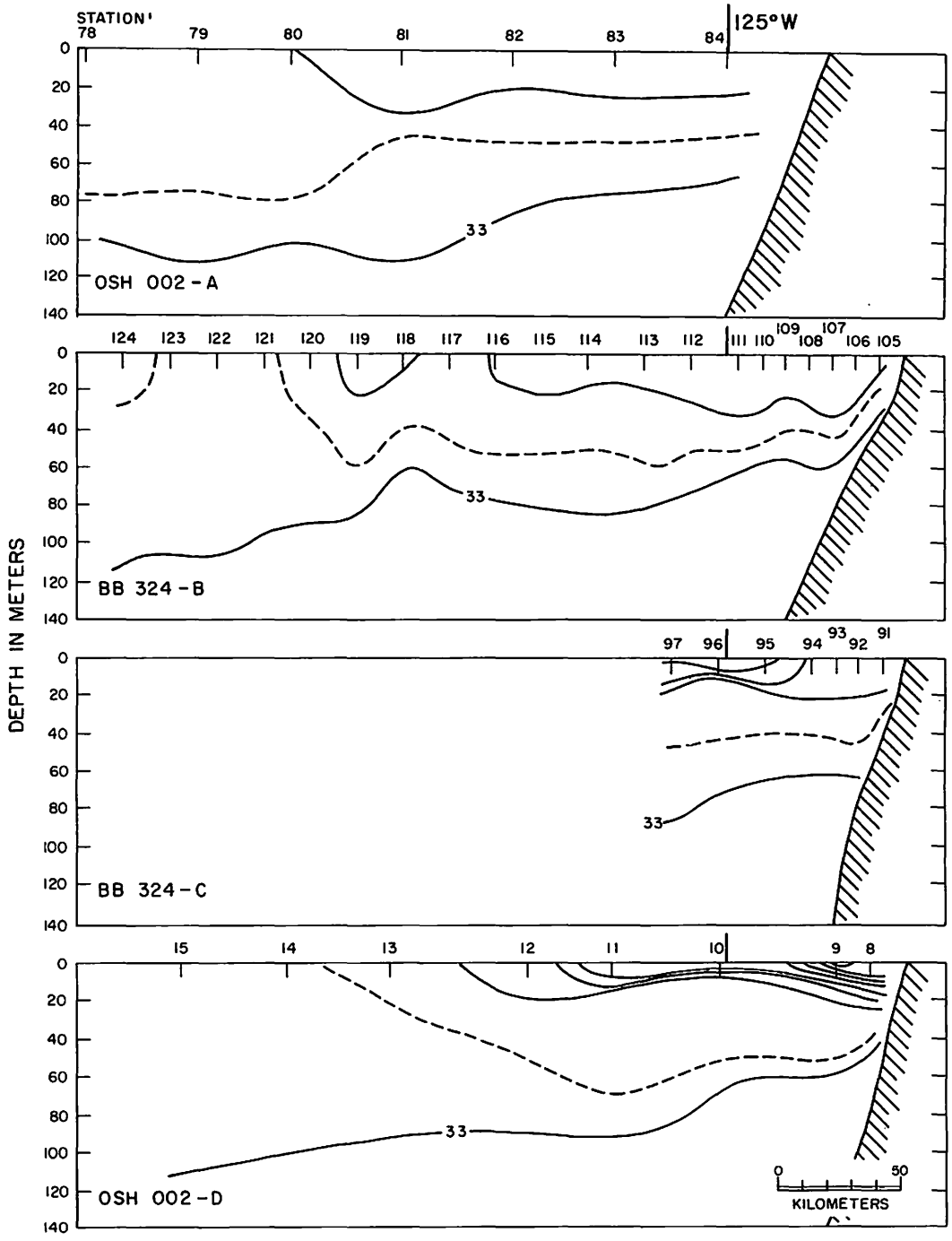

Fig. 58. Vertical distributions of salinity (—— ..., 31, 32, 33°/oo; --- 32.5°/oo) for Brown Bear Cruise 324, sections B and C, and Oshawa Cruise 002, sections A and D.

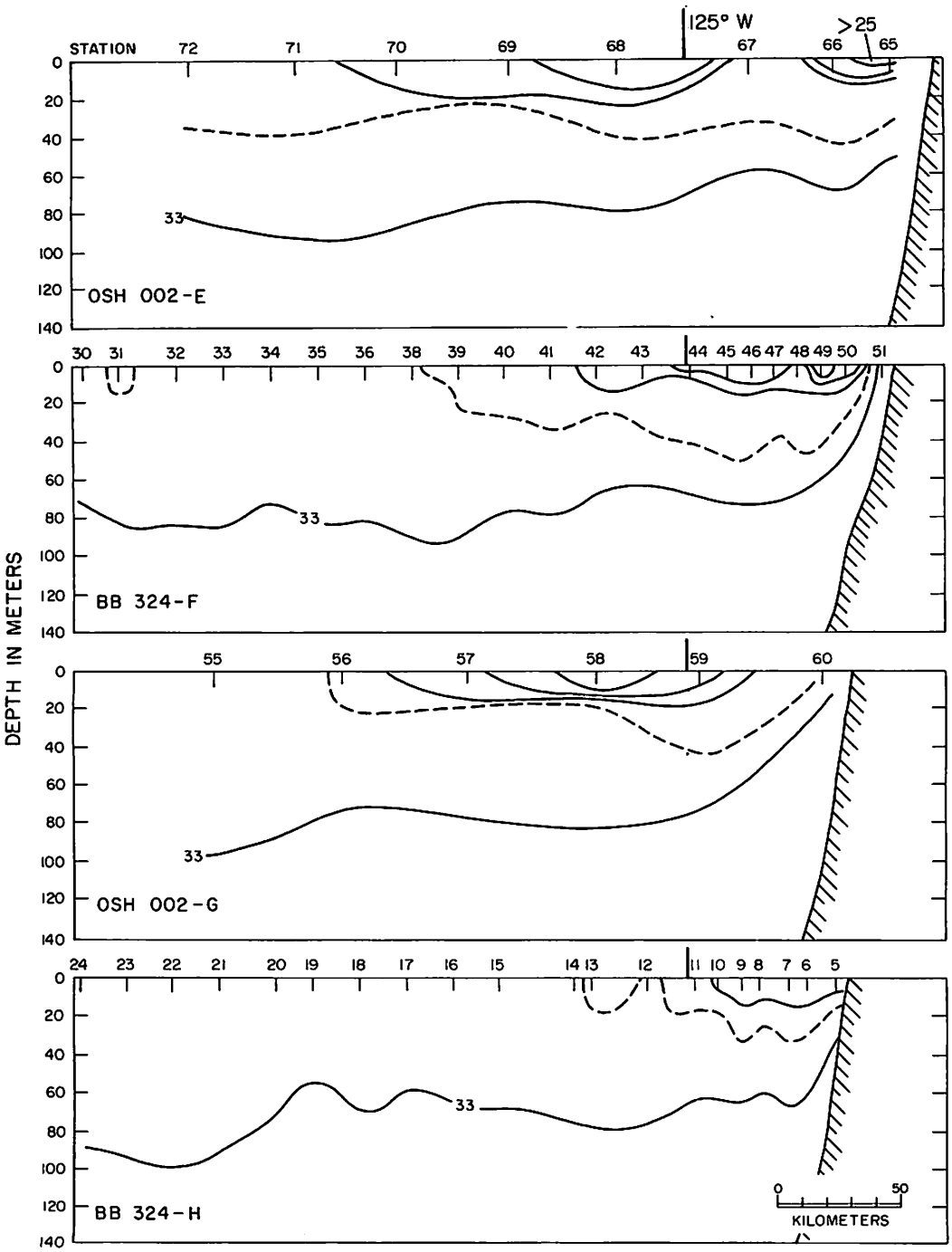

Fig. 59. Vertical distributions of salinity (—— ..., 31, 32, 33°/oo; --- 32.5°/oo) for Brown Bear Cruise 324, sections F and H, and Oshawa Cruise 002, sections E and G.

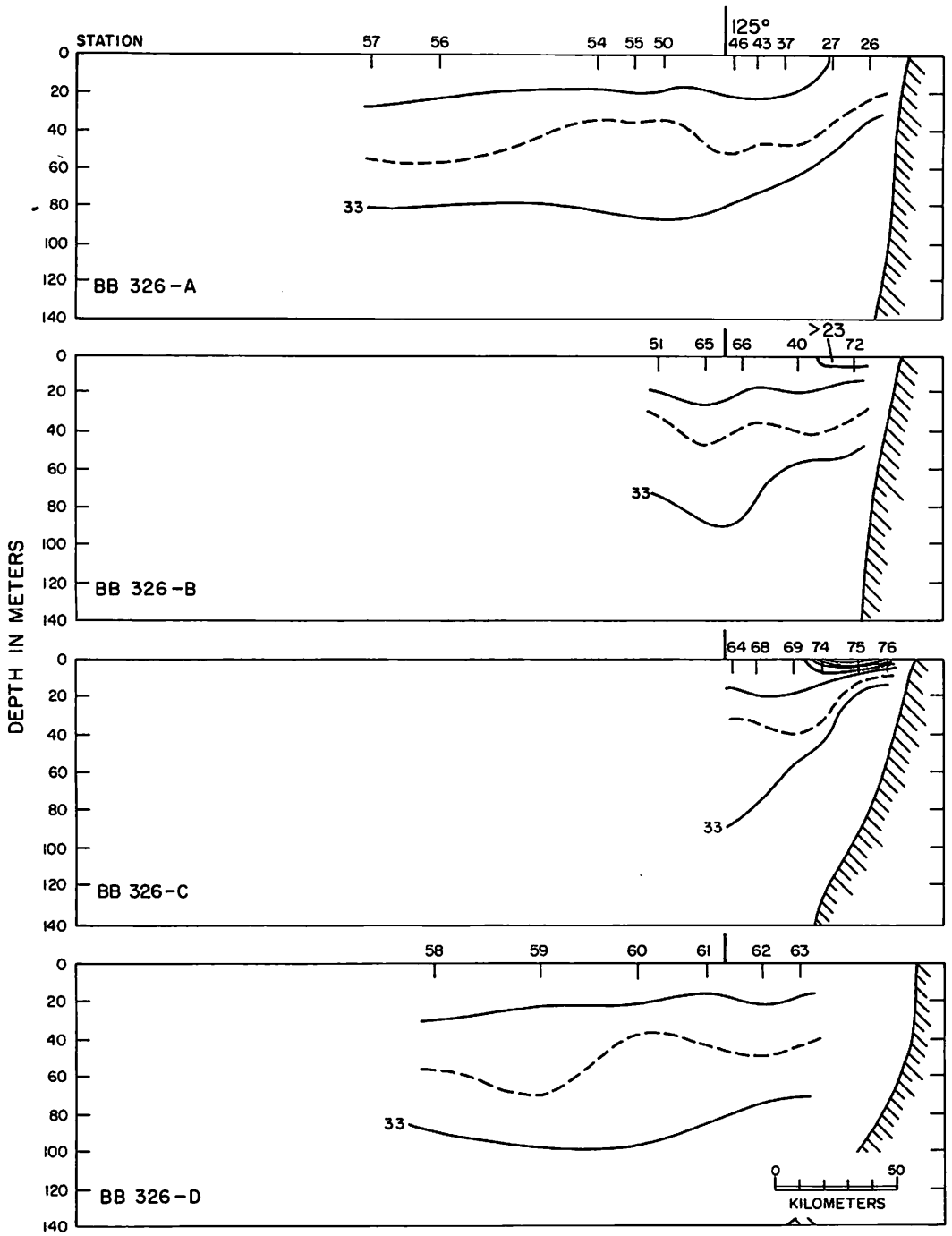

Fig. 60. Vertical distributions of salinity (—— ..., 31, 32, 33°/oo; --- 32.5°/oo) for Brown Bear Cruise 326, sections A-D.

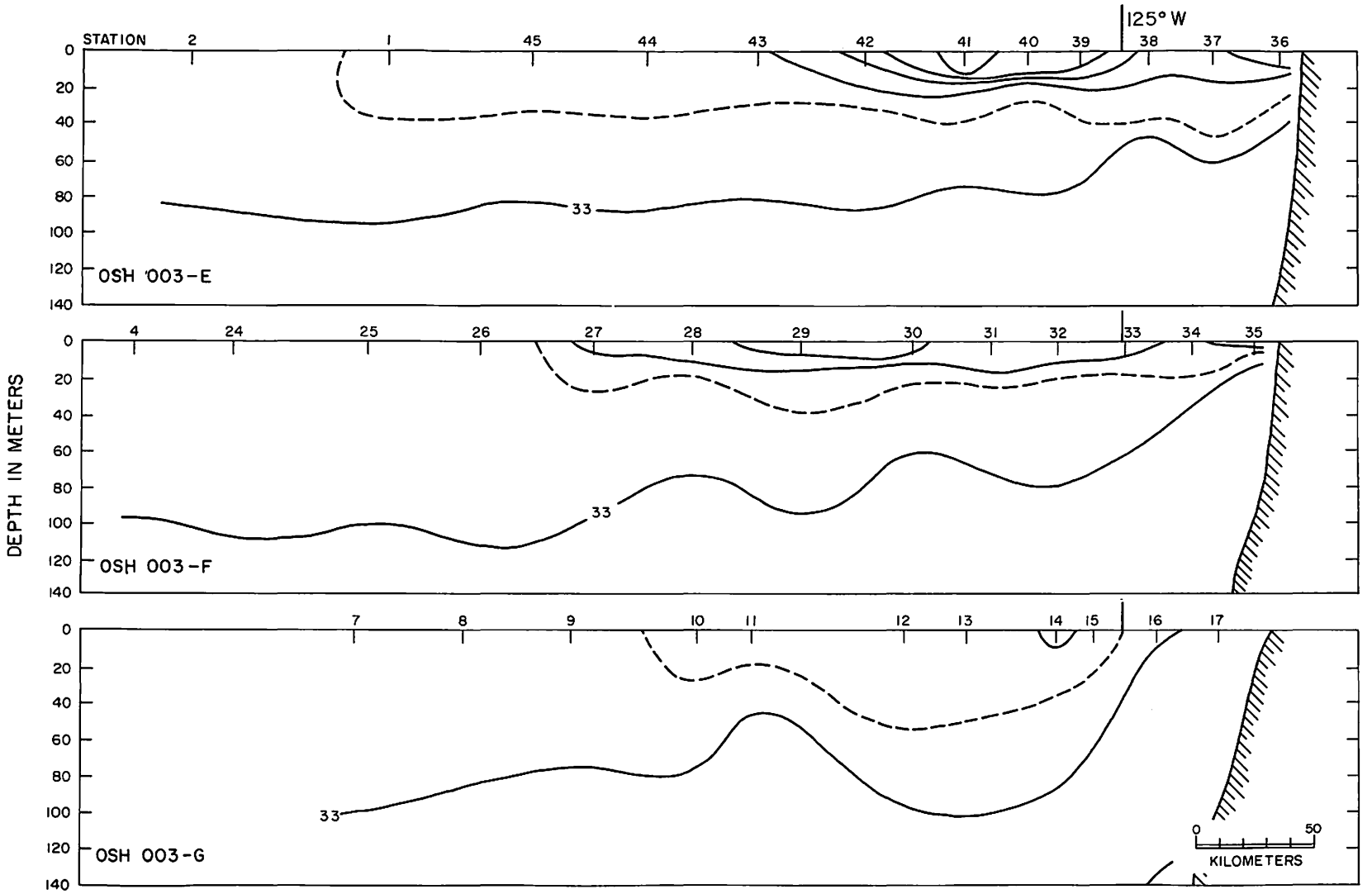

Fig. 61. Vertical distributions of salinity (—— ..., 31, 32, 33°/oo; --- 32.5°/oo) for Oshawa Cruise 003, sections E-G.

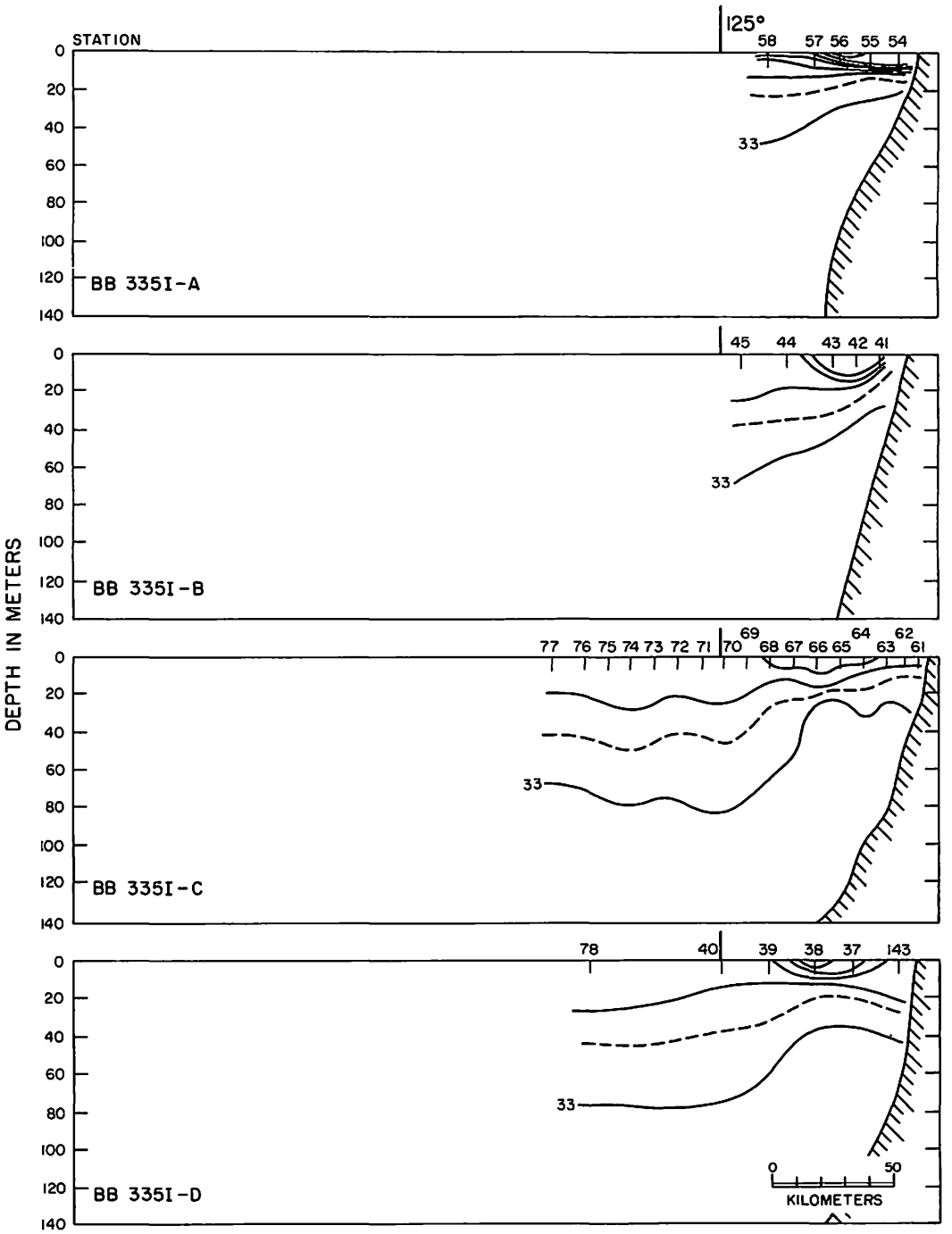

Fig. 62. Vertical distributions of salinity (—— ..., 31, 32, 33°/oo; --- 32.5°/oo) for Brown Bear Cruise 335 I, sections A-D.

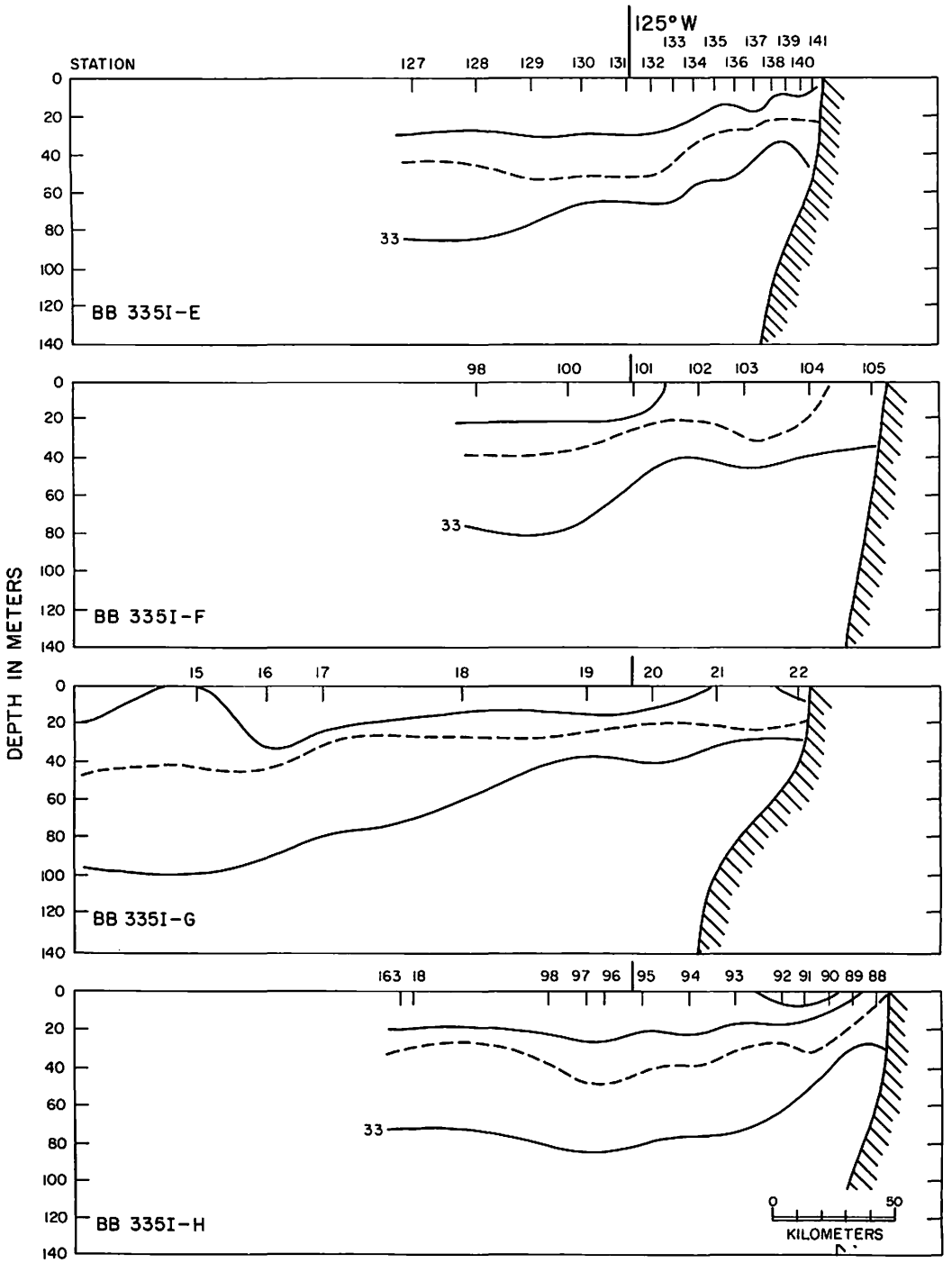

Fig. 63. Vertical distributions of salinity (—— ..., 31, 32, 33°/oo; --- 32.5°/oo) for Brown Bear Cruise 335 I, sections E-H.

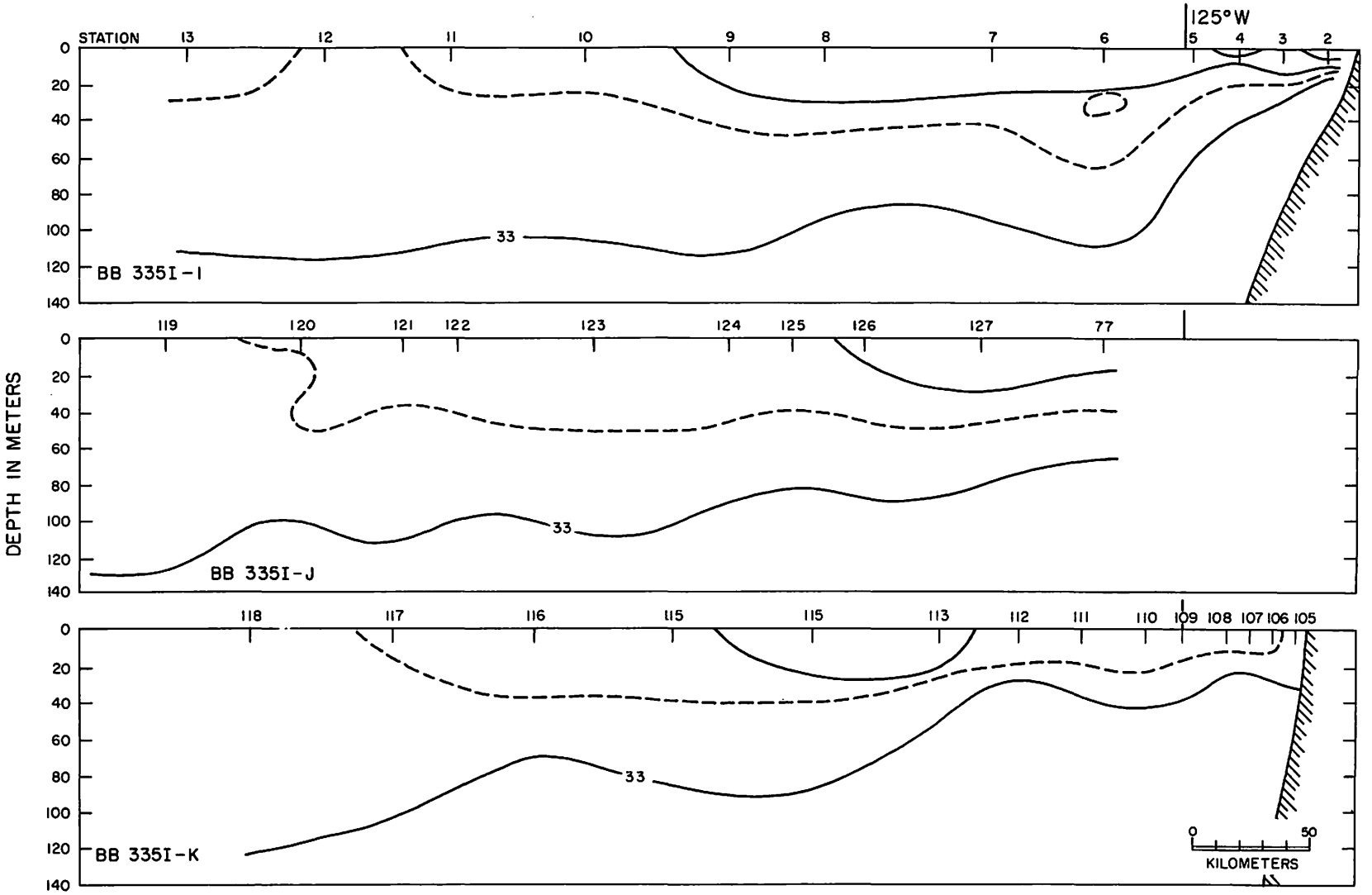

Fig. 64 Vertical distributions of salinity (—— ..., 31, 32, 33°/oo; --- 32.5°/oo) for Brown Bear Cruise 335 I, sections I-K.

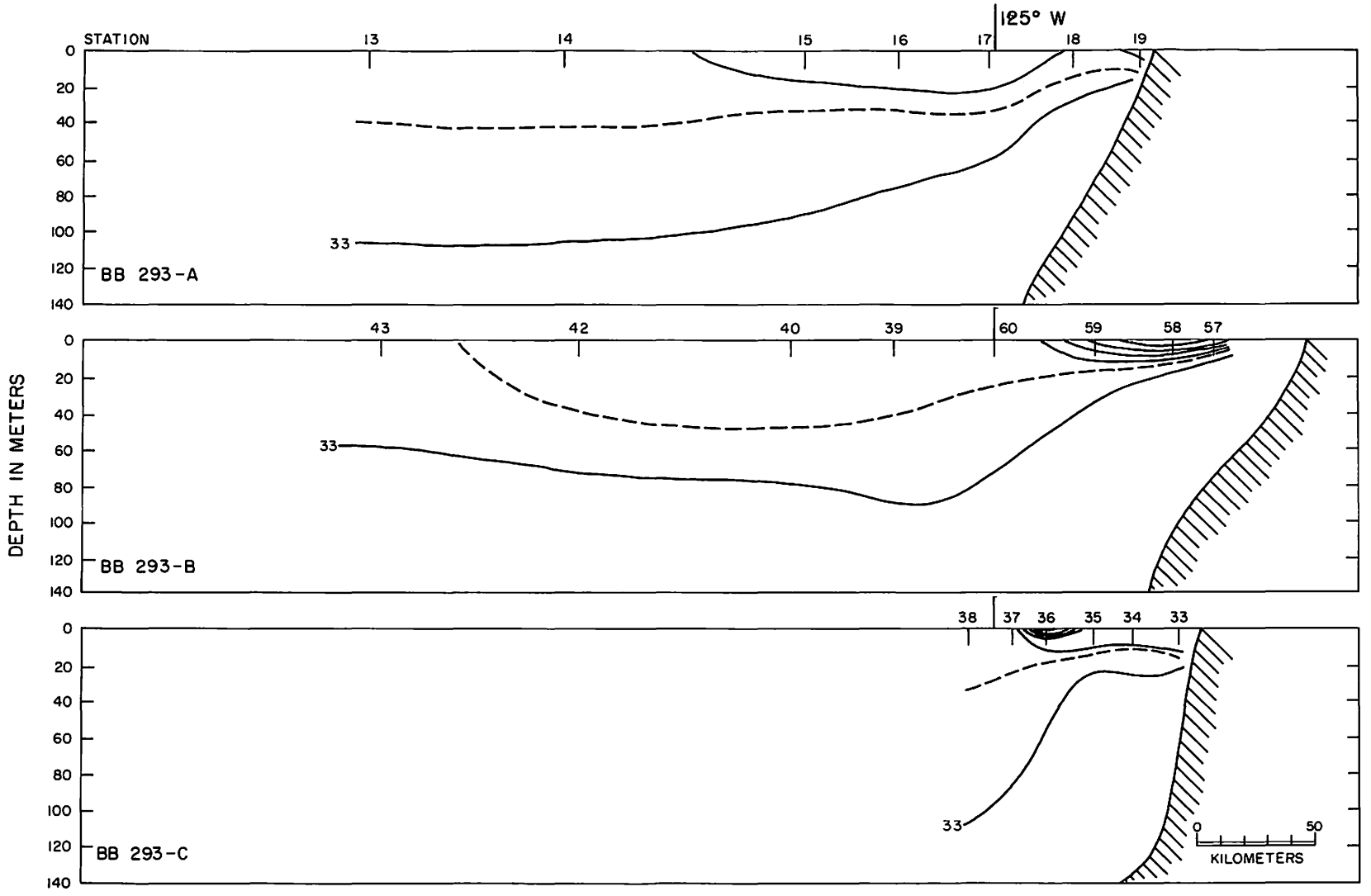

Fig. 65. Vertical distributions of salinity (—— ..., 31, 32, 33°/oo; --- 32.5°/oo) for Brown Bear Cruise 293, sections A-C.

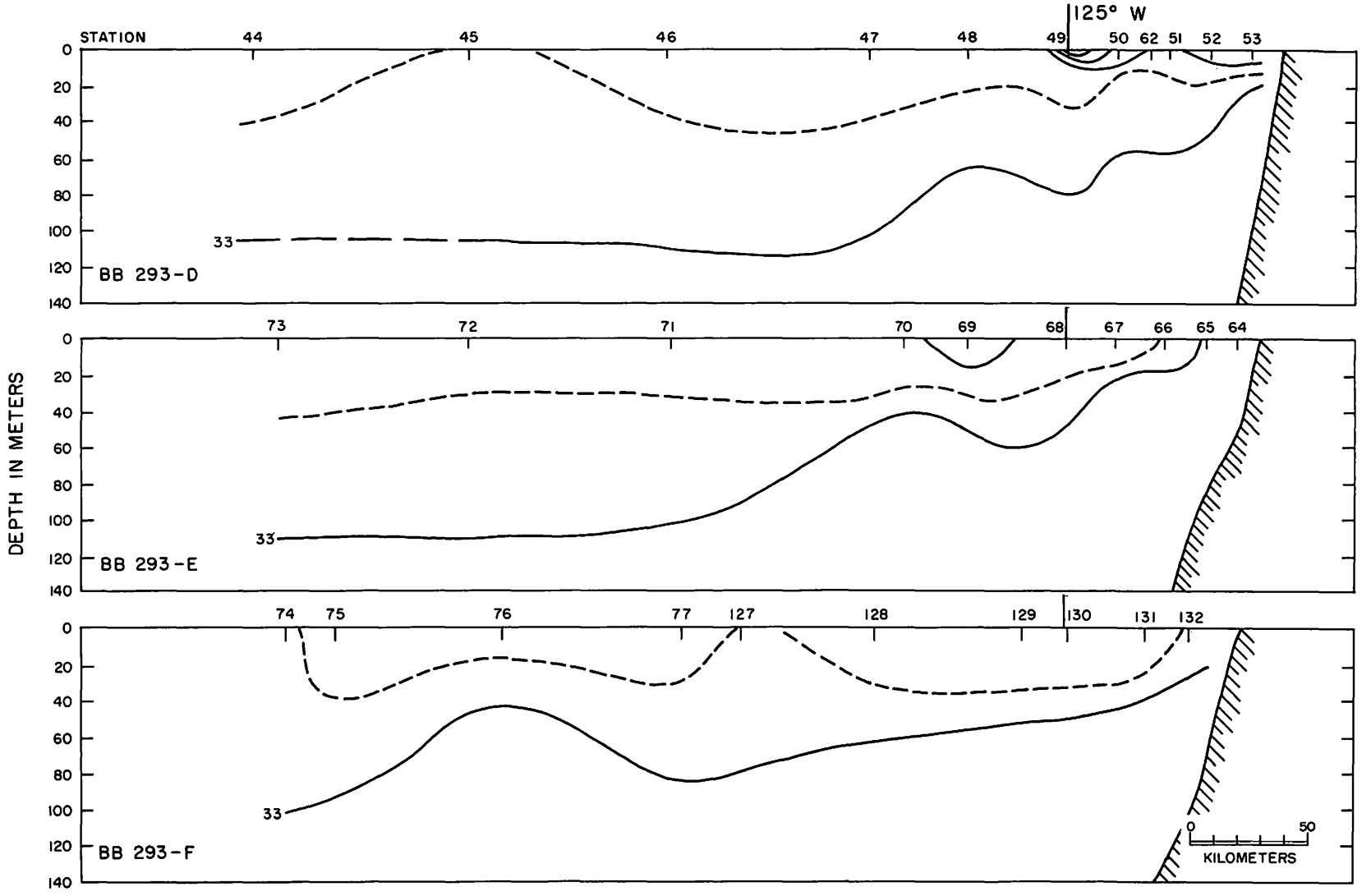

Fig. 66. Vertical distributions of salinity (—— ..., 31, 32, 33°/oo; --- 32.5°/oo) for Brown Bear Cruise 293, sections D-F.

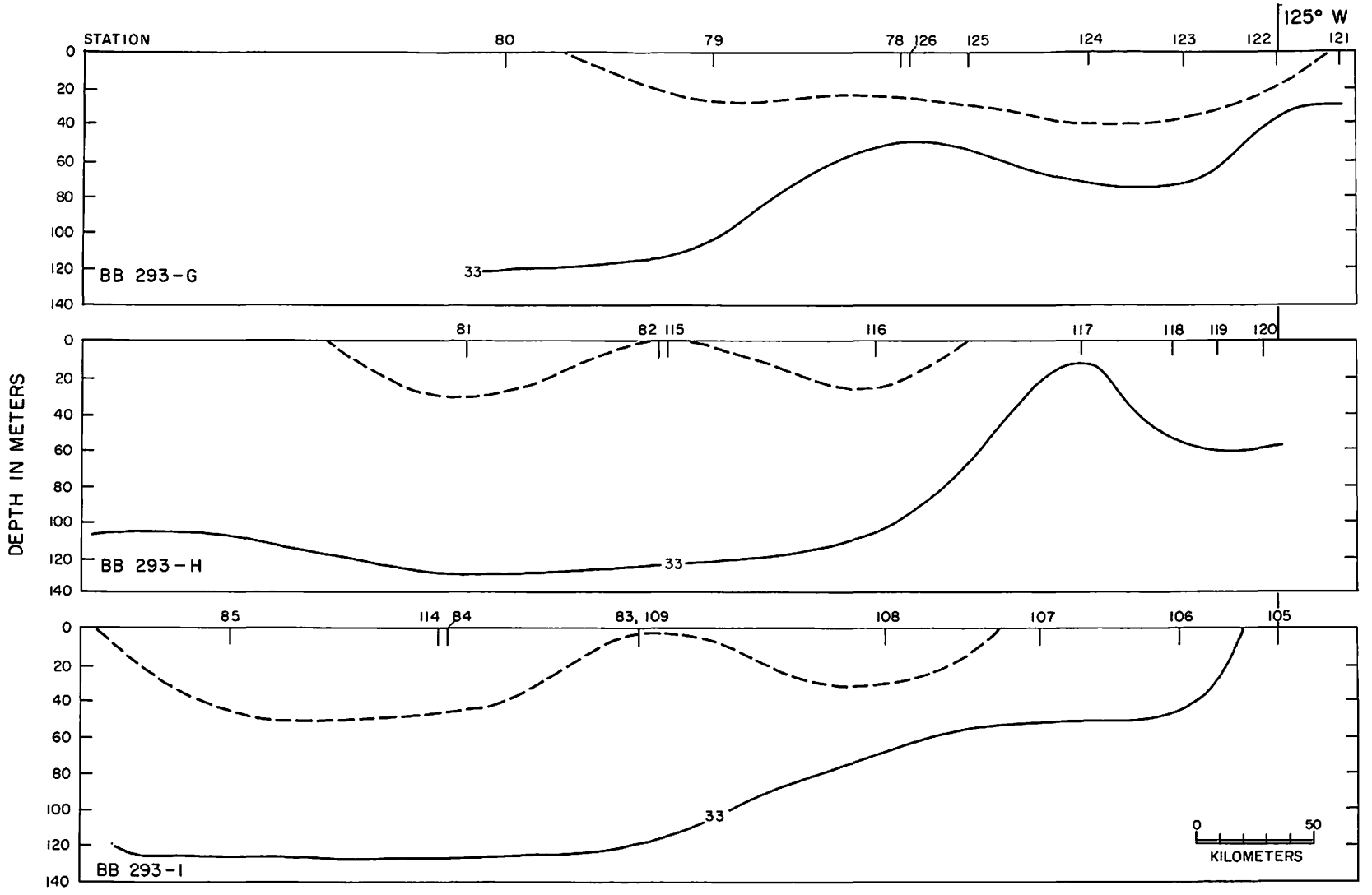

Fig. 67. Vertical distributions of salinity (—— ..., 31, 32, 33°/oo; --- 32.5°/oo) for Brown Bear Cruise 293, sections G-I.

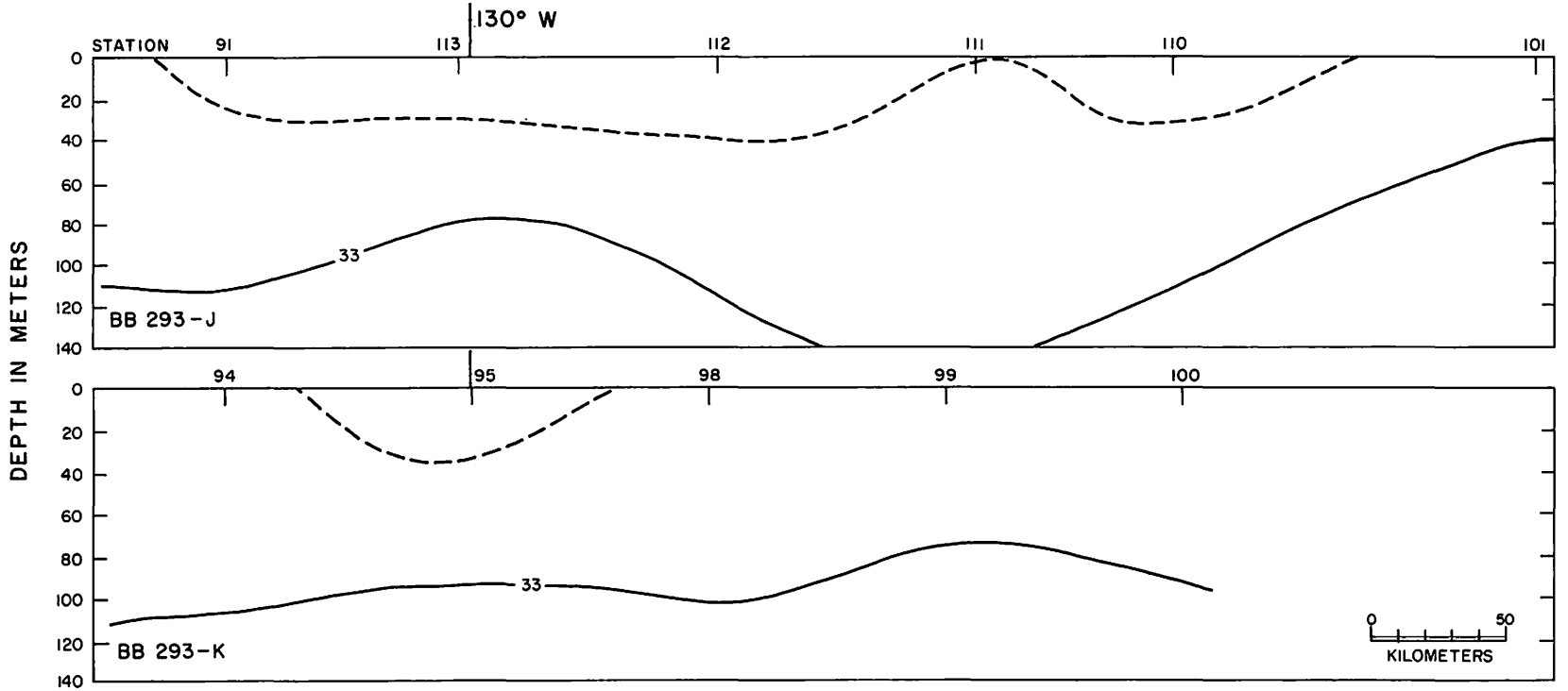

Fig. 68. Vertical distributions of salinity (—— ..., 31, 32, 33°/oo; --- 32.5°/oo) for Brown Bear Cruise 293, sections J and K.

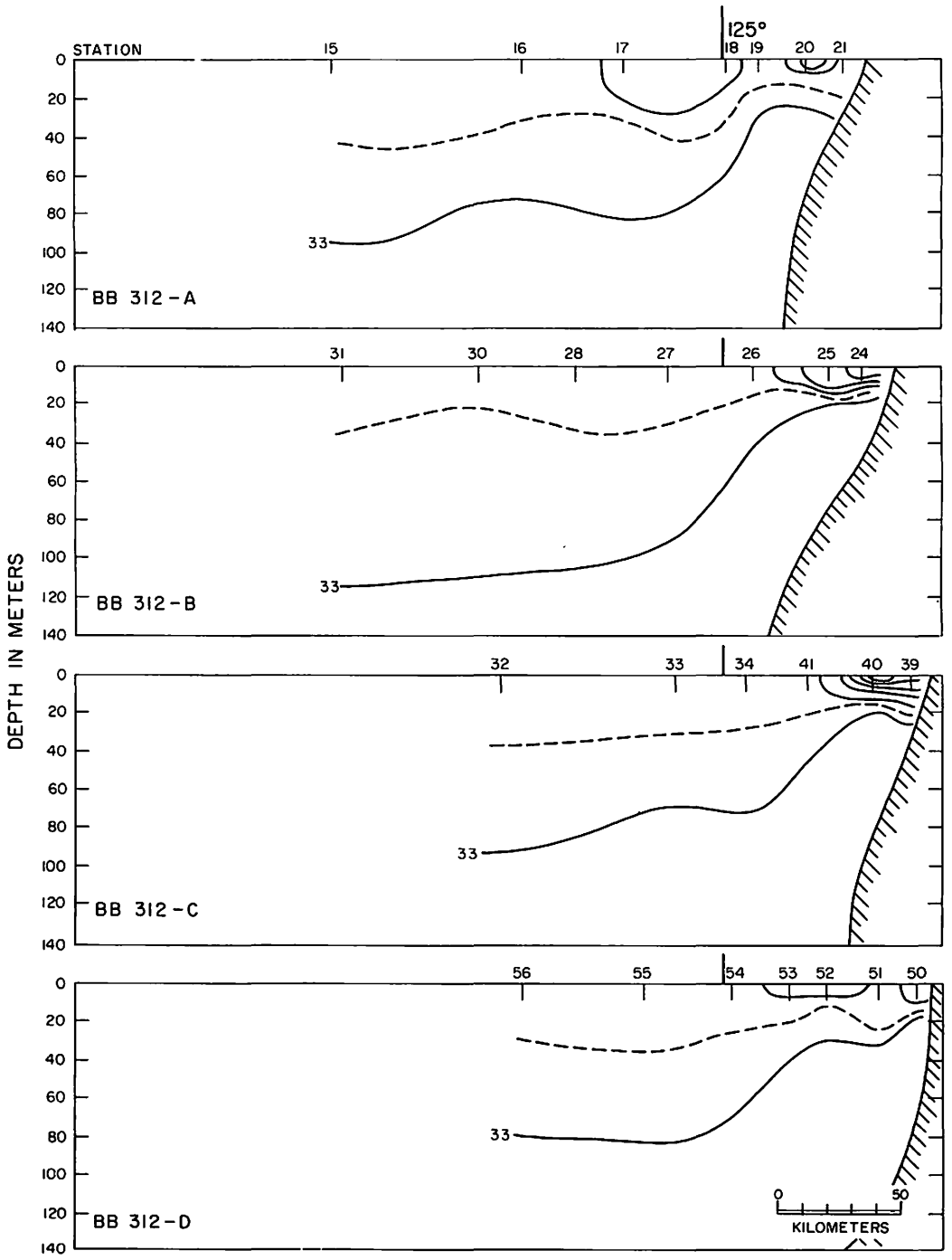

Fig. 69. Vertical distributions of salinity (—— ..., 31, 32, 33°/oo; --- 32.5°/oo) for Brown Bear Cruise 312, sections A-D.

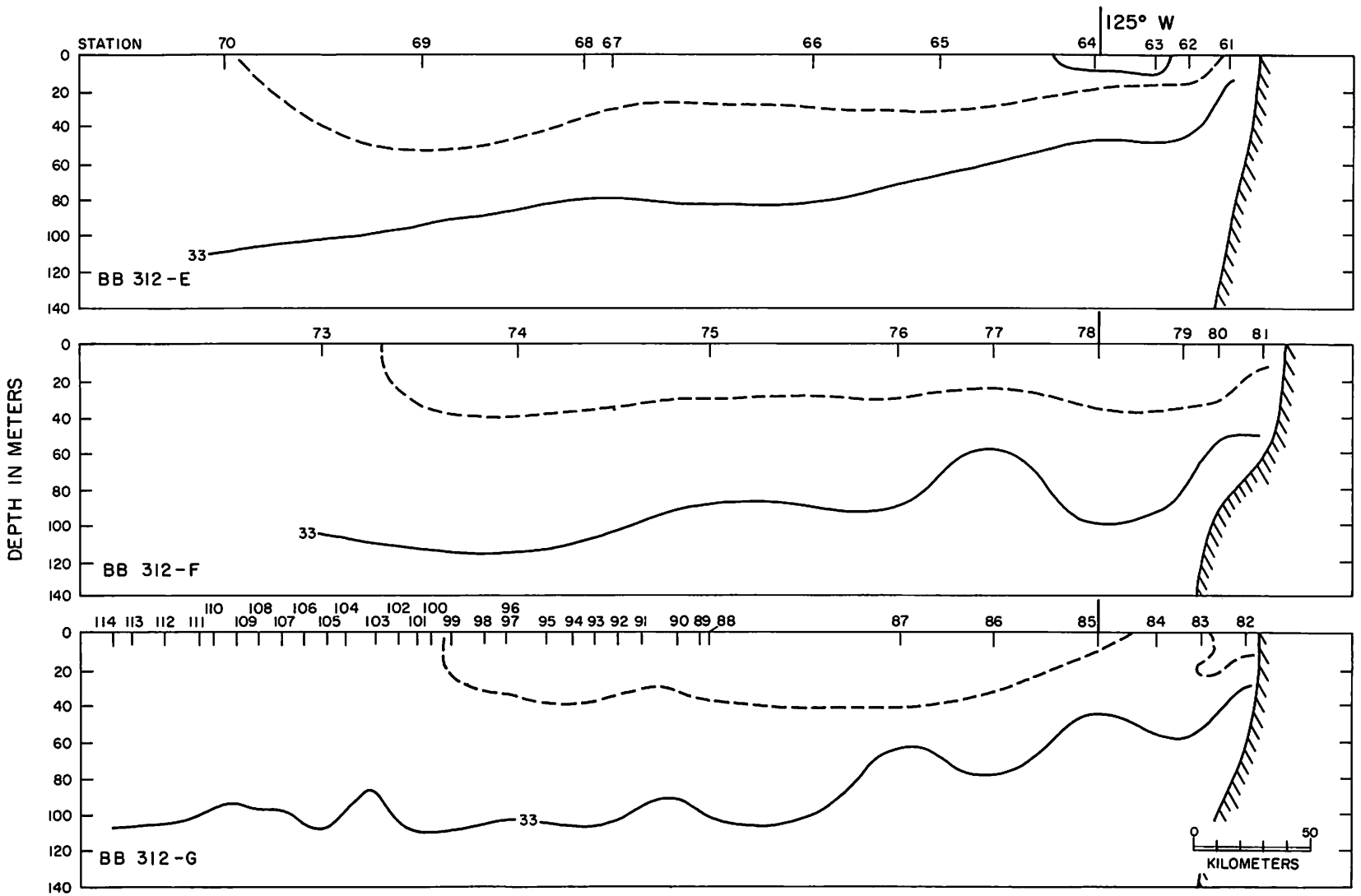

Fig. 70. Vertical distributions of salinity (—— ..., 31, 32, 33°/oo; --- 32.5°/oo) for Brown Bear Cruise 312, sections E-G.

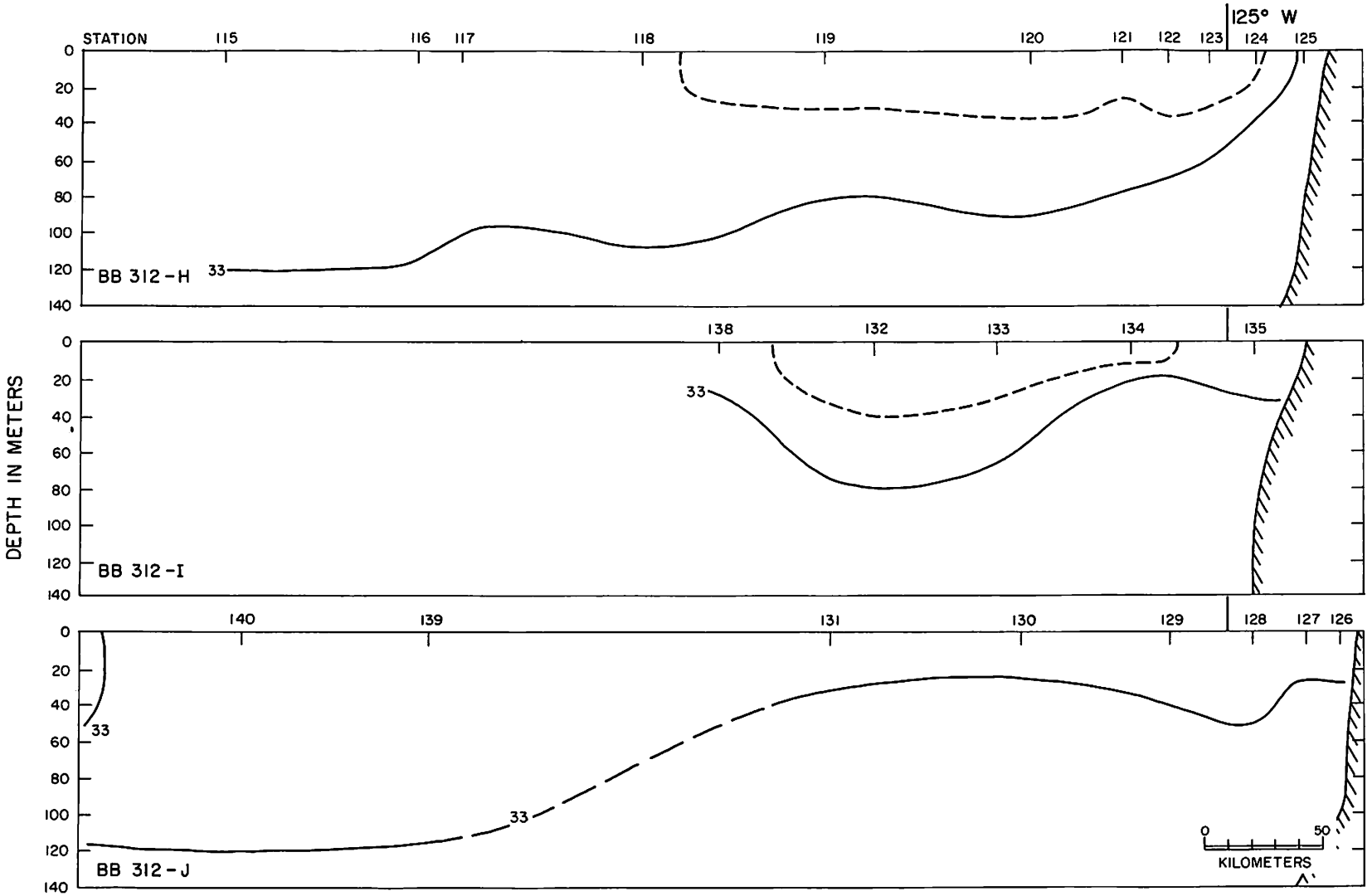

Fig. 71. Vertical distributions of salinity (—— ..., 31, 32, 33°/oo; --- 32.5°/oo) for Brown Bear Cruise 312, sections H-J.

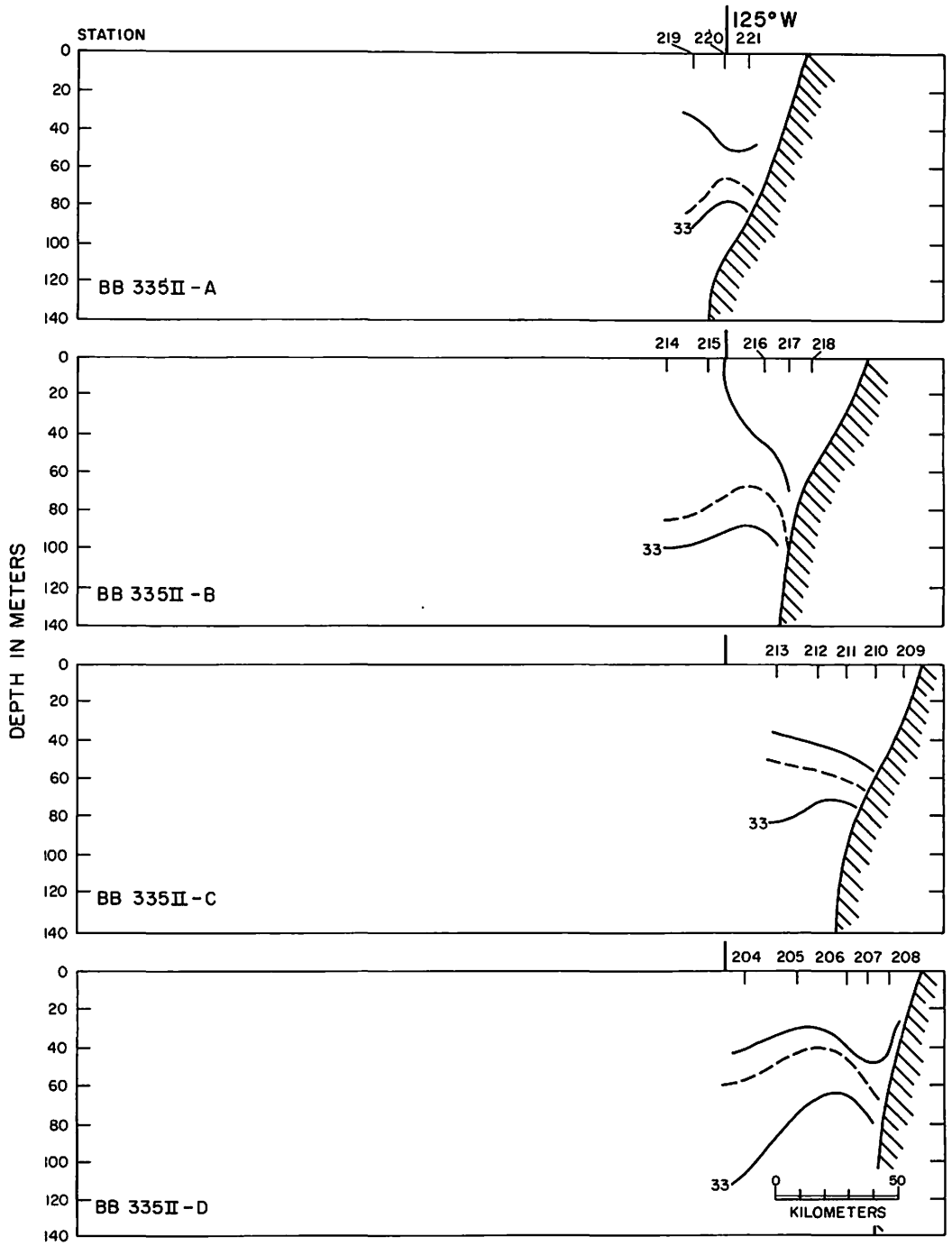

Fig. 72. Vertical distributions of salinity (—— ..., 31, 32, 33°/oo; --- 32.5°/oo) for Brown Bear Cruise 335 II, sections A-D.

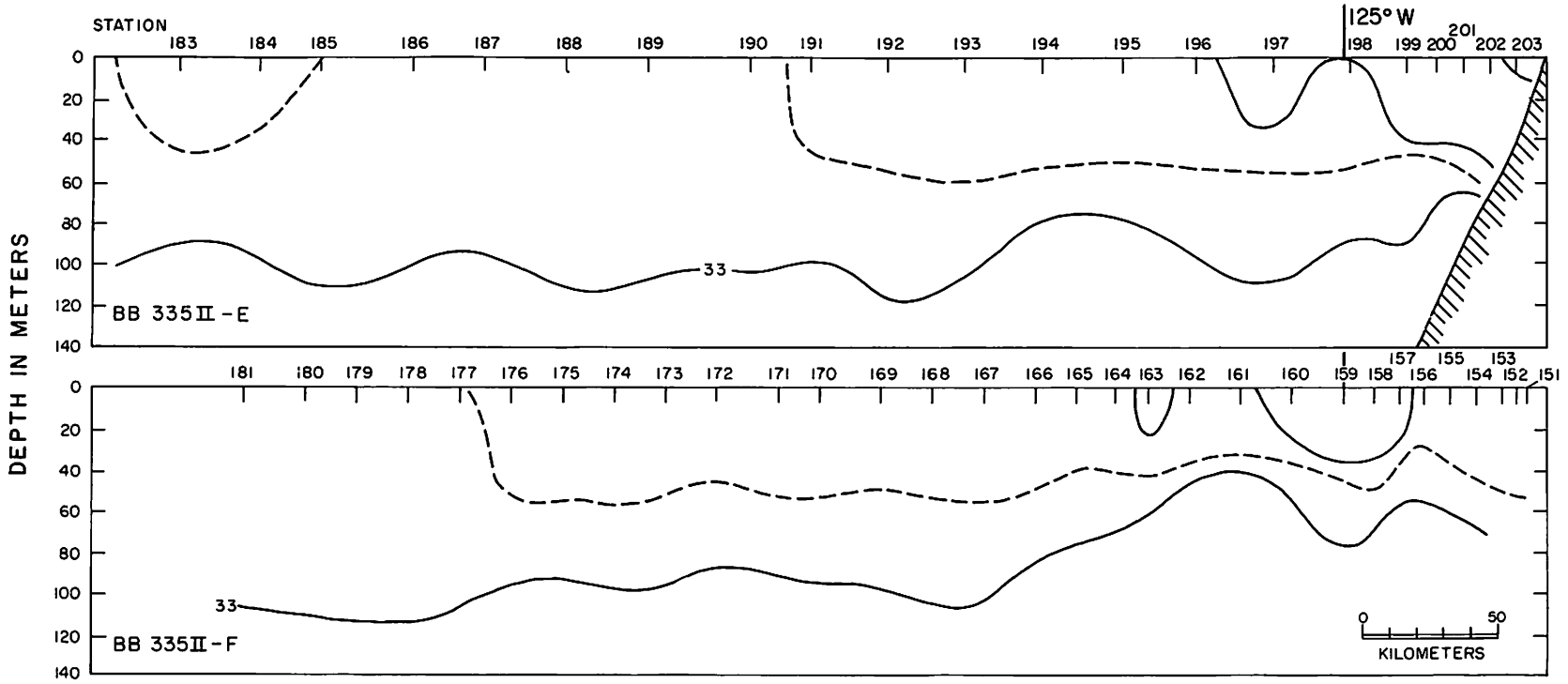

Fig. 73. Vertical distributions of salinity (—— ..., 31, 32, 33°/oo; --- 32.5°/oo) for Brown Bear Cruise 335 II, sections E and F.

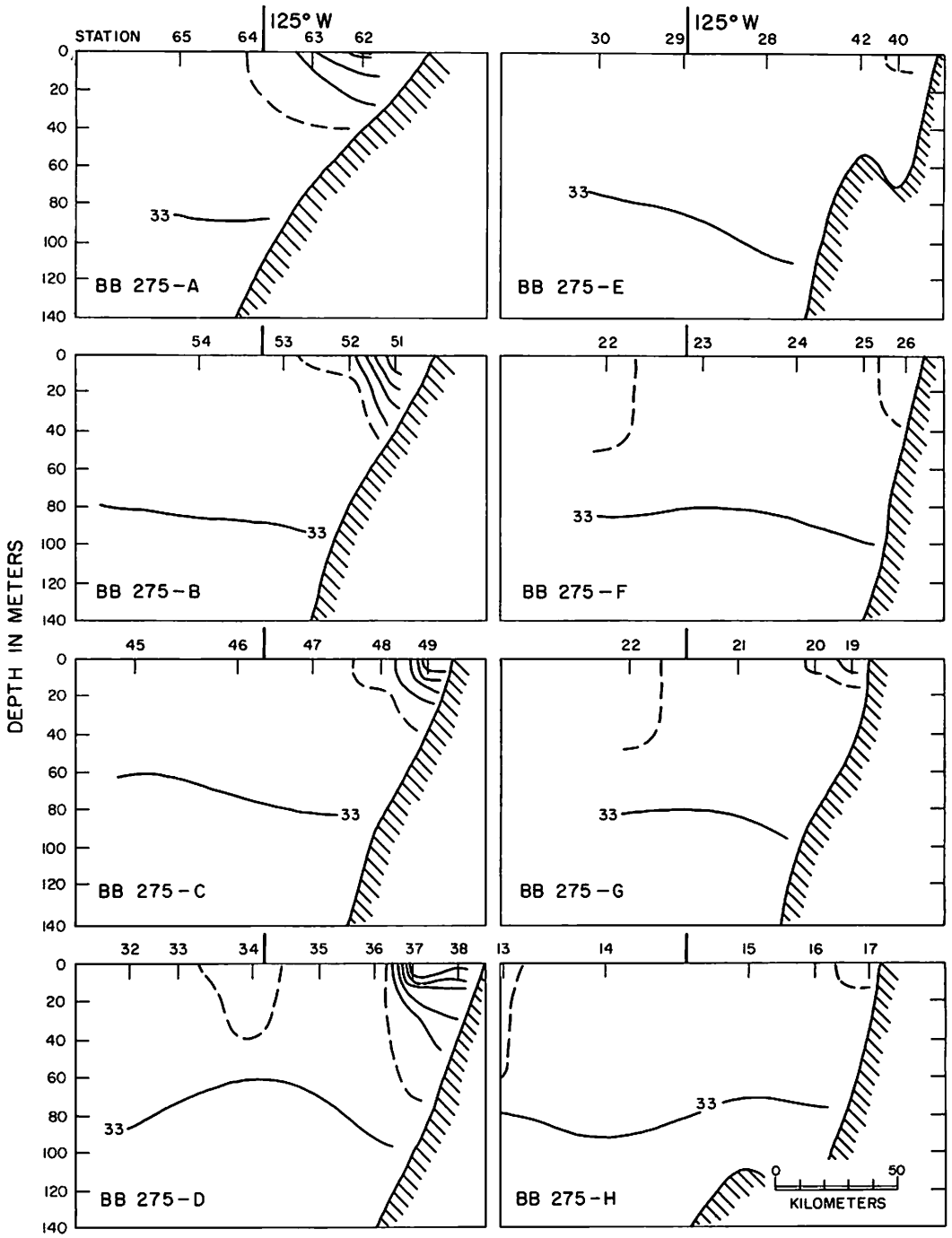

Fig. 74. Vertical distributions of salinity (—— ..., 31, 32, 33°/oo; --- 32.5°/oo) for Brown Bear Cruise 275, sections A-H.

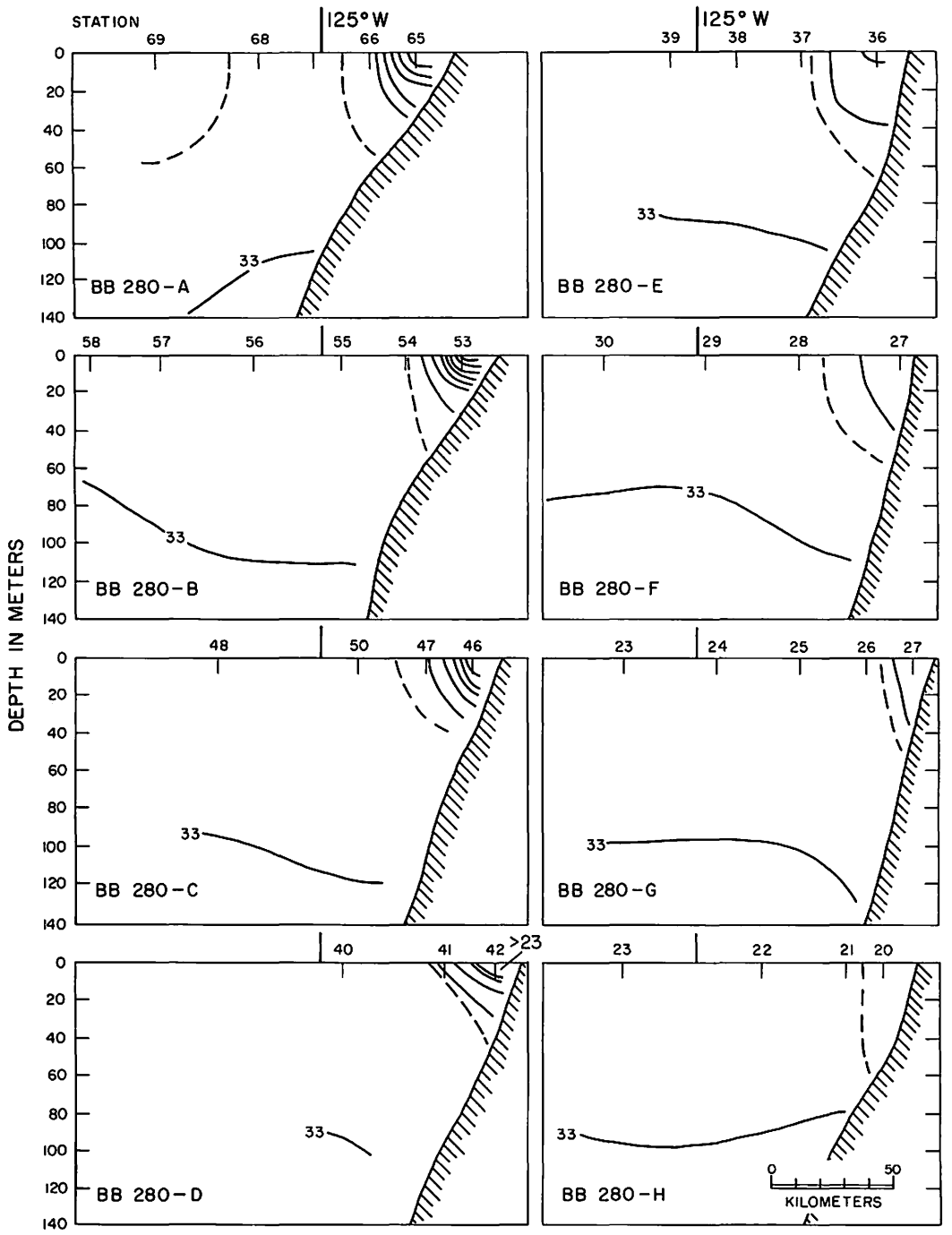

Fig. 75. Vertical distributions of salinity (—— ..., 31, 32, 33°/oo; --- 32.5°/oo) for Brown Bear Cruise 280, sections A-H.

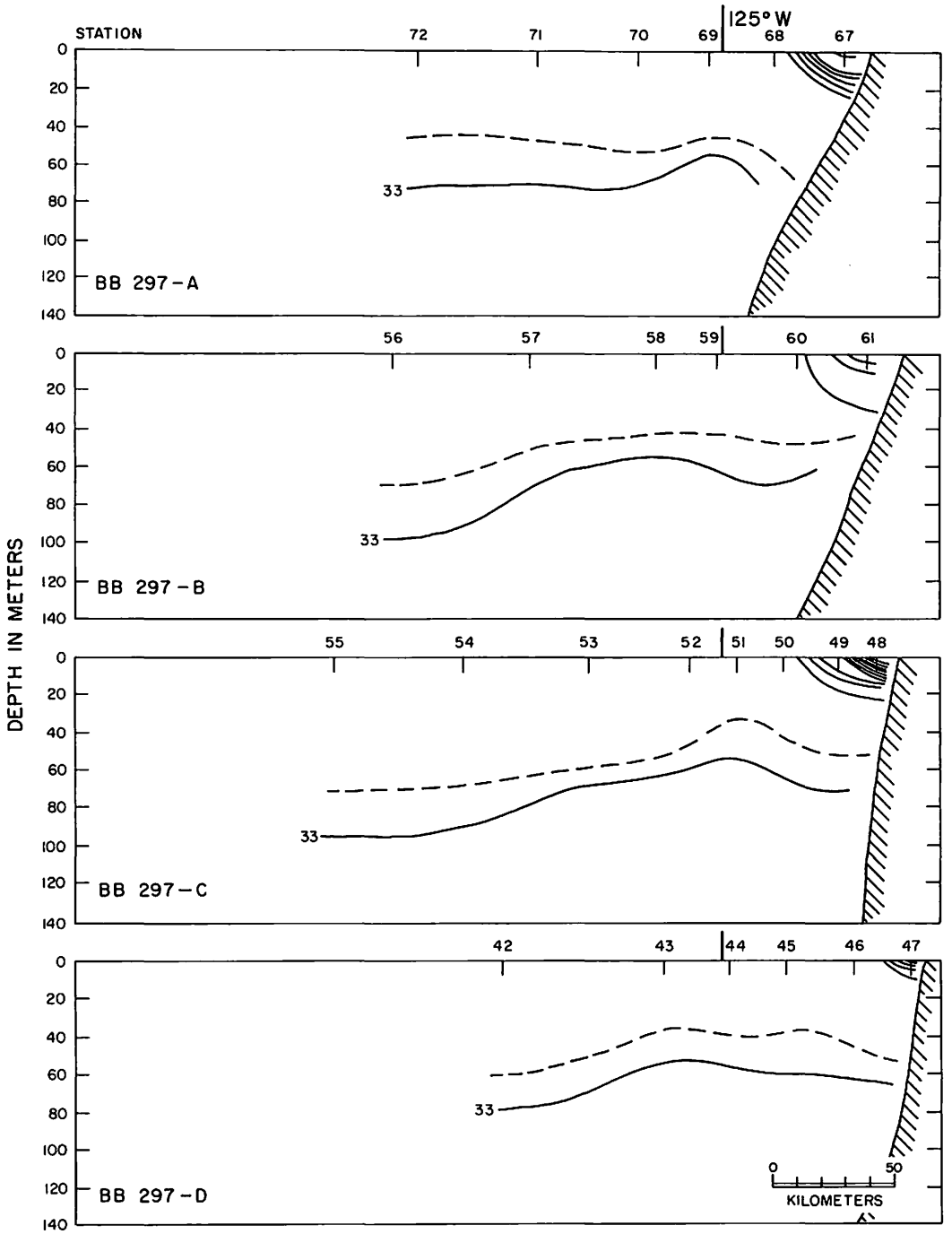

Fig. 76. Vertical distributions of salinity (—— ..., 31, 32, 33°/oo; --- 32.5°/oo) for Brown Bear Cruise 297, sections A-D.

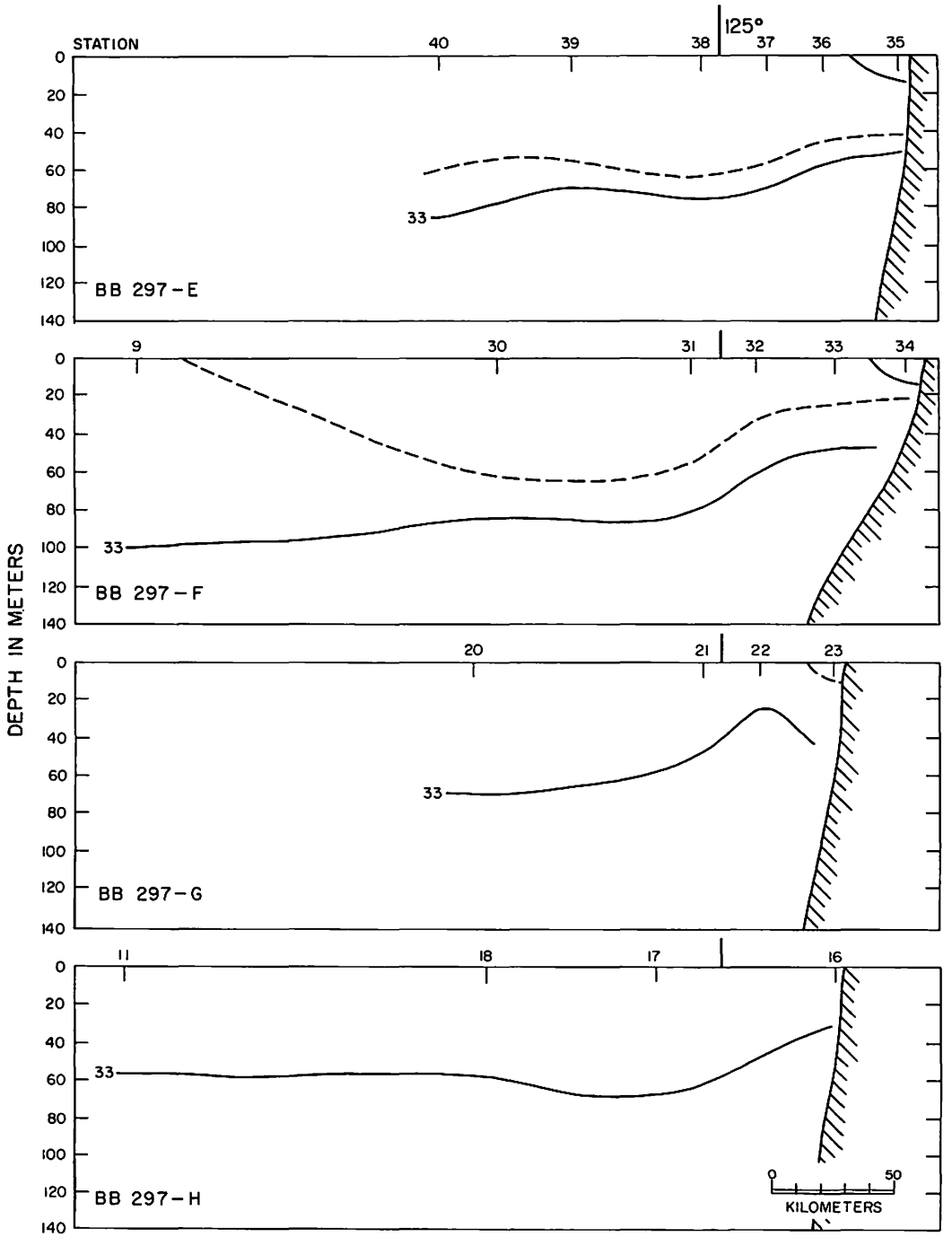

Fig. 77. Vertical distributions of salinity (—— ..., 31, 32, 33°/oo; --- 32.5°/oo) for Brown Bear Cruise 297, sections E-H.

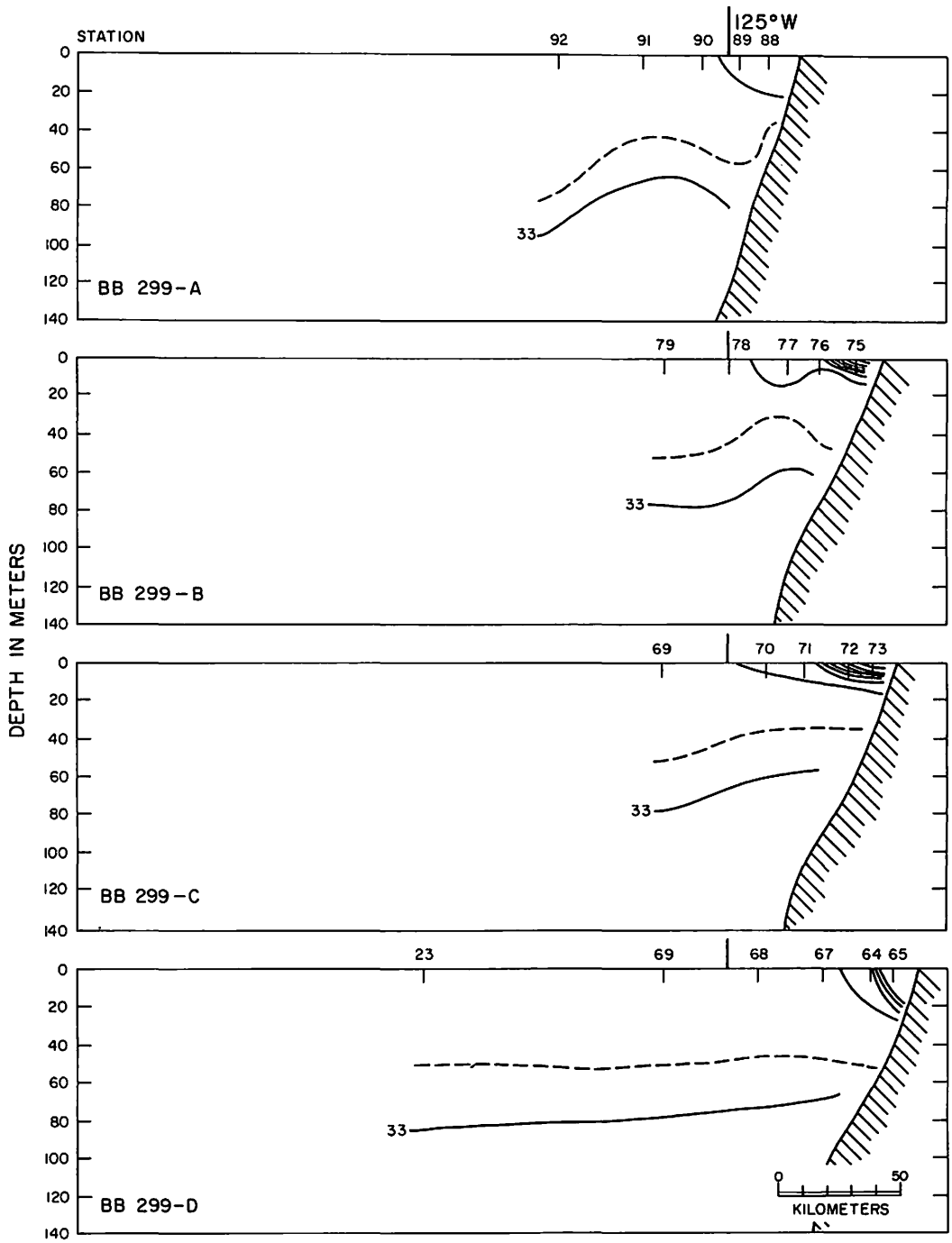

Fig. 78. Vertical distributions of salinity (—— ..., 31, 32, 33°/oo; --- 32.5°/oo) for Brown Bear Cruise 299, sections A-D.

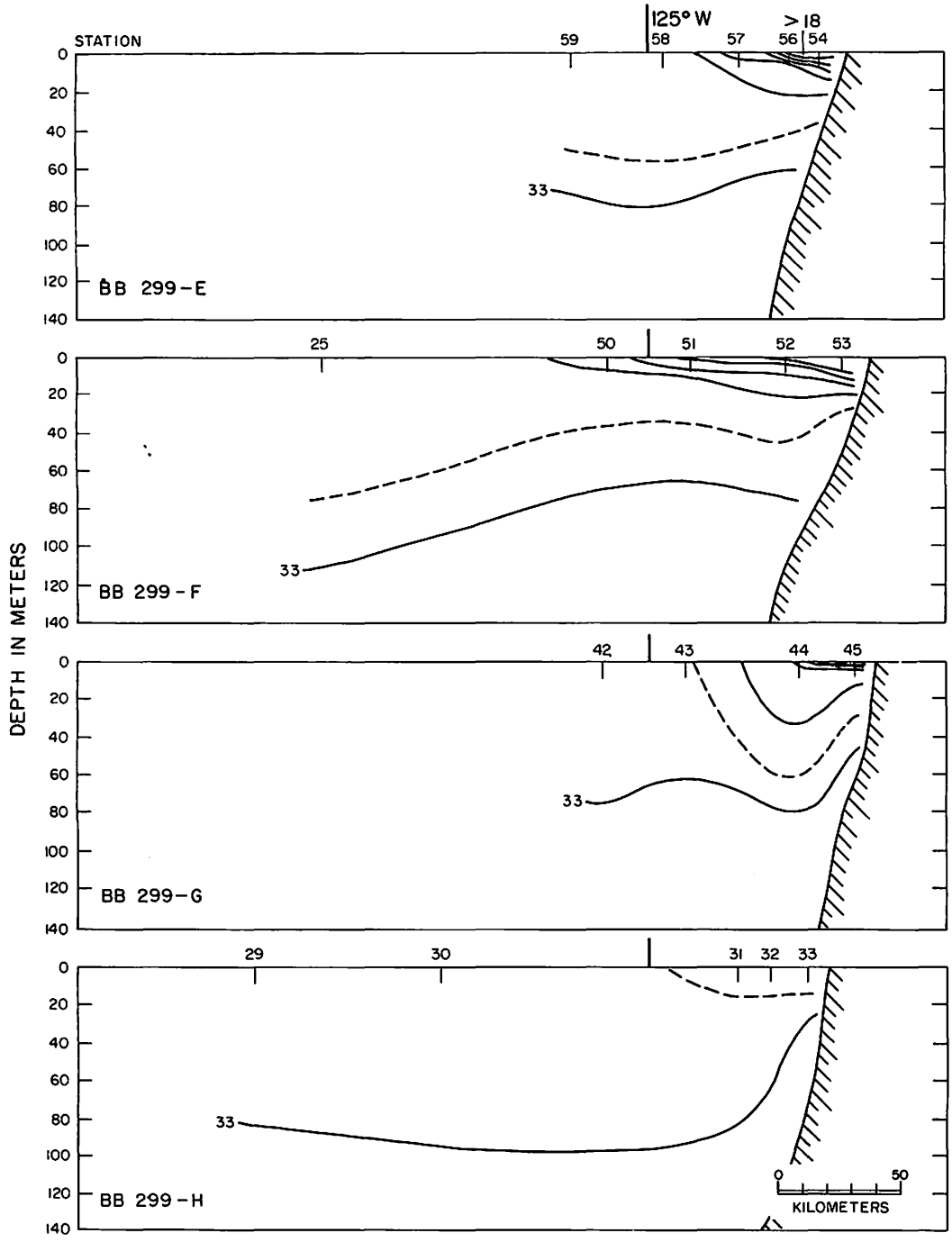

Fig. 79. Vertical distributions of salinity (—— ..., 31, 32, 33°/oo; --- 32.5°/oo) for Brown Bear Cruise 299, sections E-H.

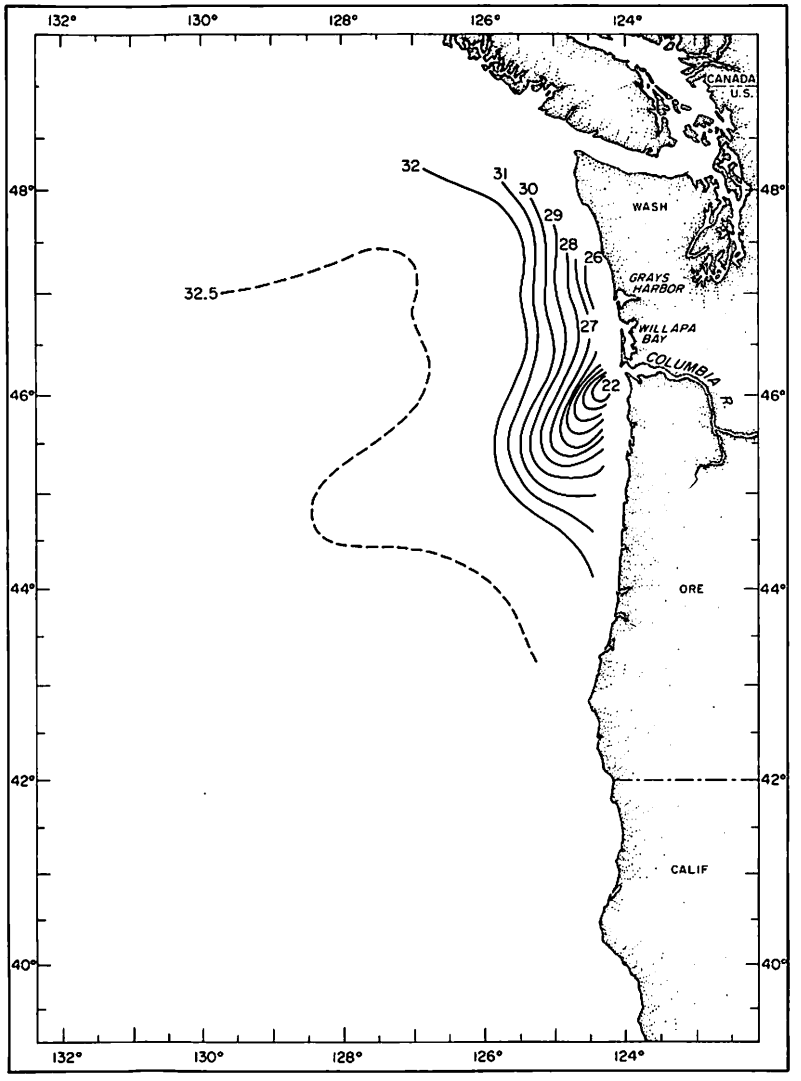

Fig. 80. Generalized spring surface salinity (°/oo) distribution.

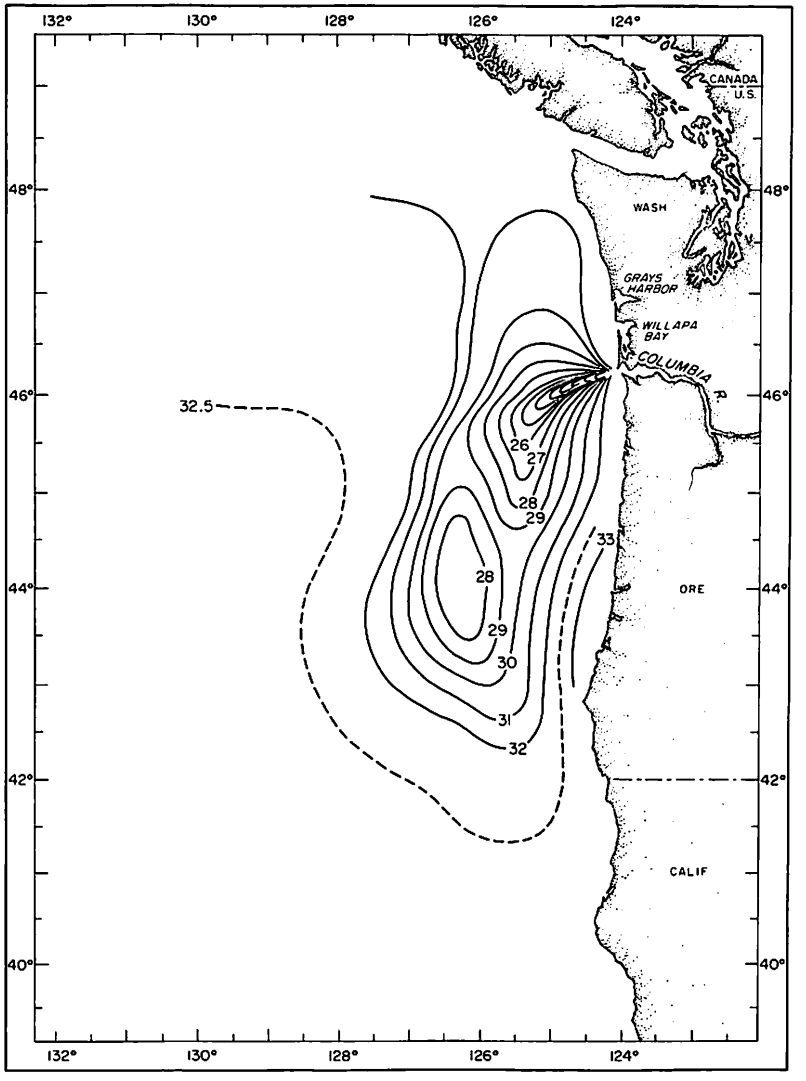

Fig. 81. Generalized summer surface salinity (°/oo) distribution.

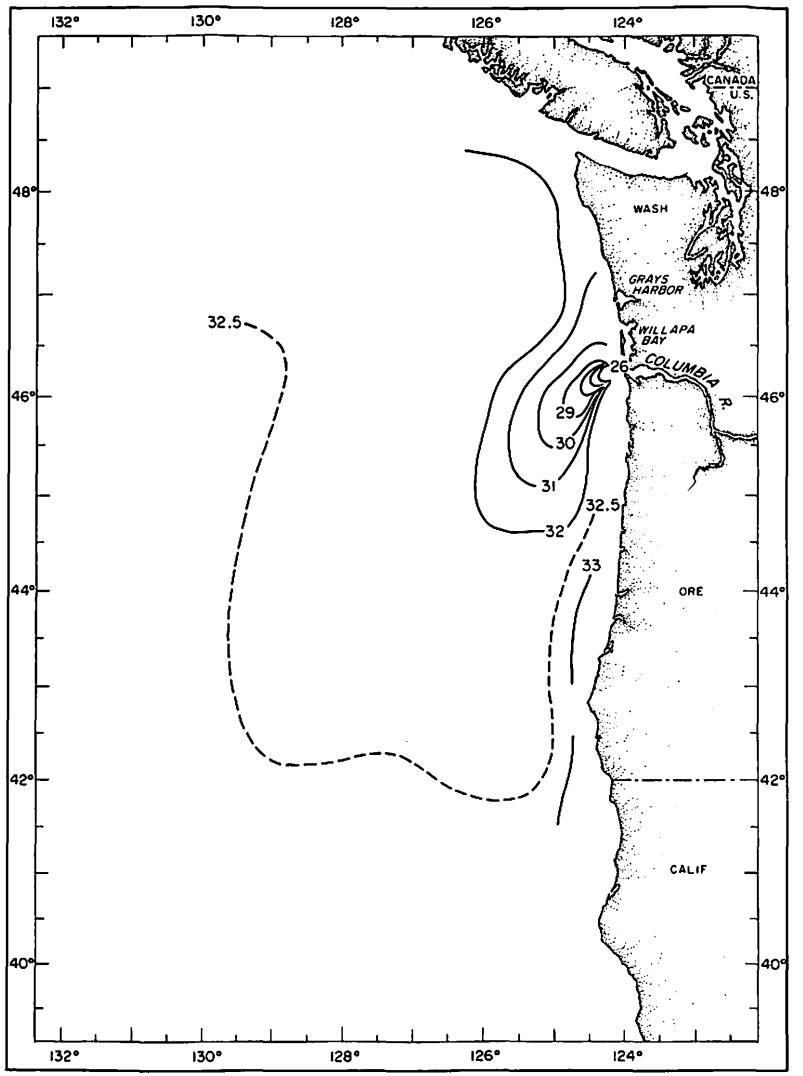

Fig. 82. Generalized autumn surface salinity (°/oo) distribution.

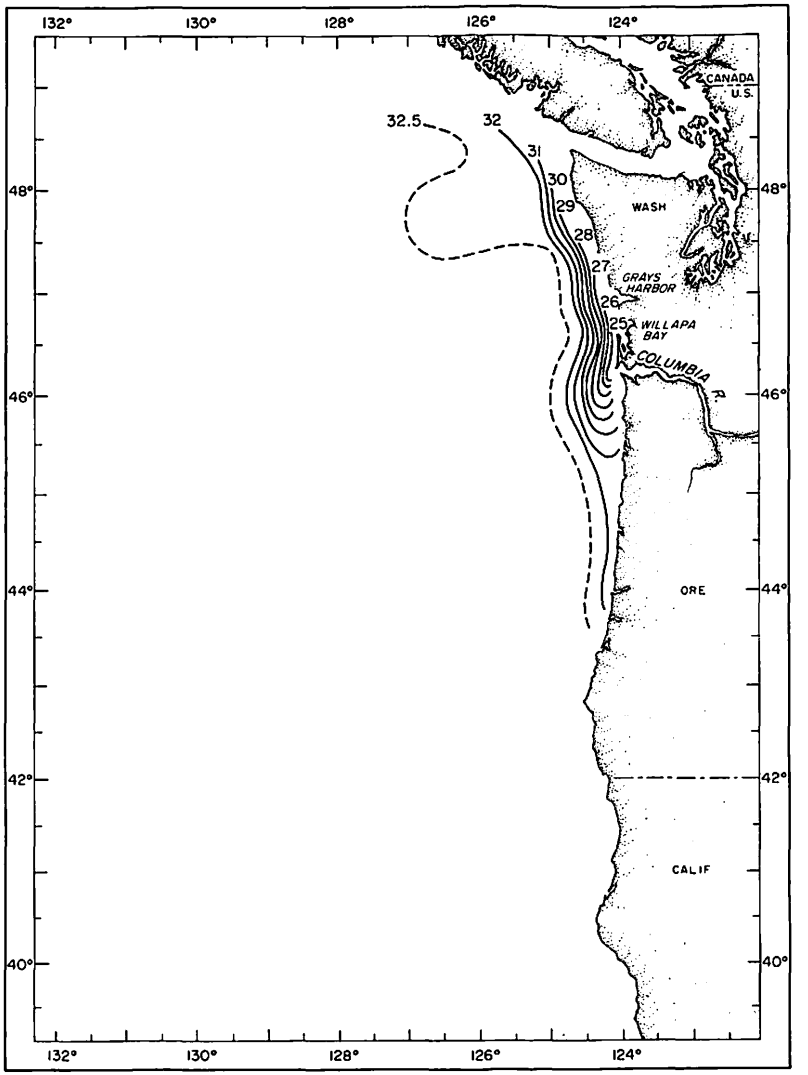

Fig. 83. Generalized winter surface salinity (°/oo) distribution.

SURFACE WINDS AND WATER TRANSPORT

Wind Program

Early in the program the considerable influence of the surface winds on the motion and distribution of the river's effluent at sea became evident. Consequently an attempt was made to determine the seasonal trends in the surface winds over the entire project area and to explore the association between the wind and the plume position and configuration. A summary of the techniques and data pertinent to the relationship between surface water motions and winds has been presented in T.R. 99. Some of the material is repeated here for clarification and updating.

Since January 1961 twice-daily pressures, based on the 0000 and 1200 GMT charts of atmospheric pressure prepared by the U.S. Weather Bureau at Seattle, have been determined for each of the eight grid points (Fig. 84). The meridional and zonal components of both the geostrophic and resultant surface winds, and the approximate surface motions of the water in response to these winds, were calculated by computer methods from these grid pressures. The computations entailed the determination of the geostrophic wind velocity aloft, rotation of this wind vector 15° to the left of its downwind direction (Montgomery, 1936), and a reduction of the speed by 30% (Gordon, 1950) to obtain a surface wind applicable to the standard height of 10 m above the sea surface.

These 10-m resultant winds were averaged in monthly groupings over the period 1961 through 1963 to produce a mean wind vector chart for the three offshore grid areas (Fig. 84). Each vector in this figure was determined by averaging separately the speeds and direction of their movement and therefore is not a true average resultant vector. The seasonal trends of the 10-m winds over the project area and the variations in direction and speed of these winds with latitude are apparent in this figure. Winter winds are predominantly from the southwest, while summer winds are northwest in the northern part of the area and north to north-northwest in the southern part. The average winds change in direction over a 180° arc from winter to summer and back to winter with no apparent abrupt shifts in speed or direction. The mean wind vectors reflect the character of the prevailing westerlies along this coast. The increase in the swing arc of the winds in the southern area is associated with the seasonal location of the predominant high-pressure ridge and the frontal activity that often intersects the coast between the northern and southern limits of the project area.

Figures 85-96 show the components of the monthly winds averaged over the period 1961 through 1963 for each 45° of arc centered on the cardinal and intercardinal points of the compass. Each wind rose is centered about the midpoint of the grid that was used to determine the wind values, and is divided into octants. The length of the bar represents the percentage of the month during which wind blows outward from the center of the rose in the direction of the bar. The concentric circles are both 5% of month frequency levels and 5-knot speed increments. The small numbers printed

along the bars represent the percentages of the monthly winds from the given direction that fall within the designated 5-knot increments of speed. The sum of these numbers should equal the total percentage indicated by each bar, and the sum of the percentages indicated by the eight bars equals approximately 100% of the month's winds. Any discrepancy here from a 100% level is caused by the rounding off of numbers in the computer program.

The bar graph with each wind rose shows the frequency, in percentage of month, of the wind in 5-knot speed increments without consideration of the direction. The frequency distribution of the wind strength through the yearly cycle and the latitudinal variation of this distribution are discernible from these bar graphs. The bar graphs show the annual shift in the frequency peak with the winds that normally increase in strength during the winter and decrease in summer, especially in the northern and central grids. The winds in the southern grid remain relatively strong in both winter and summer.

Wind Transport of Surface Water

The surface winds (10 m) and the associated surface stress have been used to estimate the transport of surface and near-surface waters. The driving stress of the wind on the sea surface causes a surface current that is directed approximately 45° to the right of the wind in the northern hemisphere (Ekman, 1902; Rossby and Montgomery, 1935). The stress and the surface water speed are expressed by the following:

$$|\vec{\tau}| = \rho_\alpha C_E \, |\vec{W}_{10}|^2 \tag{2}$$

where $\vec{\tau}$ is the surface wind stress, ρ_α is the density of air, C_D is the dimensionless drag coefficient (Wilson, 1960), and W_{10} is the 10-m wind speed; and by

$$V_s = \frac{0.0131}{\sqrt{\sin \phi}} W_{10} \tag{3}$$

where V_s is the speed of the surface current and ϕ is the latitude. The constant 0.0131 has been used in preference to 0.0127 erroneously reported in T.R. 99 and was chosen after evaluation of 77,000 observations involving equation (3) (T. F. Budinger, unpublished communication).

The zonal and meridional components of the net transports of the near-surface water, the Ekman transports, are determined from the surface stress through the equations

$$E_x = \tau_y / f$$

and

$$E_y = \tau_x / f \tag{4}$$

where τ_x and τ_y are the zonal and meridional components, respectively, of the surface stress and f is the Coriolis parameter. The net transport is

independent of any change in eddy viscosity with depth, and is directed approximately (in the northern hemisphere) 90° to the right of the wind direction if all conditions required for pure Ekman drift are met. The stresses are

$$\tau_x = \rho_\alpha C_D U\sqrt{U^2 + V^2}$$

and (5)

$$\tau_y = \rho_\alpha C_D V\sqrt{U^2 + V^2}$$

where U and V are the zonal and meridional components, respectively, of W_{10}. The Ekman transport, E, occurs from the surface down to a depth, D, the depth of frictional resistance. Therefore if D is known it is possible to determine an integrated transport velocity from E, since this transport is through an area of 1 m width and D m depth.

The twice-daily wind calculations were used to compute the Ekman transports for the project area using the above scheme. In accordance with equations (4) and (5), Fig. 97 represents a rotation of 90° and a change of scale of Fig. 84, and shows the appropriate seasonal oscillation in direction and magnitude of the mean Ekman transport as determined from the mean monthly winds. The remaining transport diagrams, Fig. 98-109, are counterparts of Fig. 85-96 in the wind section. These monthly mean Ekman transport figures indicate the frequency in percentage of time and magnitude of transport in the octants of the transport roses. The onshore transport of the coastal water during the winter months and the offshore transport to the south and southwest during the summer months are discernible in these figures. The actual transport onshore is strongly affected by the presence of the shoreline and is not truly of Ekman type, but to treat most of the transport as an Ekman type should give a good estimate.

The bar graphs accompanying the transport roses (Fig. 98-109) show the magnitude of the transports and the frequencies of their occurrence without regard to their direction, in the same manner as the wind diagrams. The nonlinearity between the scales of Fig. 85-96 and Fig. 98-109 is the result of the dependency of the transport on the square of the wind speed. The bar graphs are helpful in determining the differences in transport with respect to latitude over the yearly cycle. Larger transport occurs more frequently during the winter than in the summer. During the summer the transport in the southern section exceeds that in the northern section.

The importance of the wind effect on the effluent distribution is emphasized in Fig. 110, which shows the redistribution of near-surface salinities caused by moderately strong northerly winds and increased river discharge. These two distributions, based on data from the end of a Brown Bear cruise and the beginning of an Acona cruise, occurred within a 20-day period.

Currents in the Effluent Area

The sections in this report pertaining to wind-induced surface-water drift have been based on the assumption that transport by wind is the only mechanism available for producing surface currents. The dynamic

height anomalies referenced to the 1000-decibar surface and the geostrophic currents calculated relative to this surface were discussed in T.R. 99. In the region under study the topography of the anomalies is very flat with slopes of approximately 2 dynamic centimeters per 74 km (40 nautical miles). There is some doubt as to the reliability of currents determined from such flat topographies when the possible errors in determinations of salinity, temperature, depth, and position are considered (Reid, 1959; Leipper, 1959). The currents depicted by the topographies in T.R. 99 show the same seasonal trends that are displayed by the local wind-driven transports, and it is suspected that the geostrophic currents are manifestations of these long-term, generalized wind drifts in the local area superimposed upon drifts generated by the wind systems acting over the entire ocean. At present there are insufficient data to adequately separate the relatively weak geostrophic currents into their oceanic and locally produced components. The continuity of flow in the westward limits of the North Pacific West Wind Drift and the periodicity of the geostrophic currents in relationship to seasonal changes of oceanic and local scale would have to be considered to determine these components.

Since the wind-driven transport suffices to describe qualitatively the local geostrophic flow, only the Ekman transport has been considered in this report and other sources of movement have been excluded. Tidal currents and hydraulic flow from the Columbia River are important, but are mainly near shore and are not considered in the offshore effluent regions where detection of short-term variations is not possible because of the sampling techniques employed.

WATER-PARTICLE TRANSPORT

Water-Particle Displacement Due to Ekman Transport

Ekman transport is expressed in units of metric tons of water per second per 1 m width. Using 1.028×10^3 kg/m^3 as the density of seawater and dividing this into the transport, one obtains the number of cubic meters of water transported per second per 1 m width. This latter value divided by D, the depth of frictional resistance, yields an integrated transport velocity for the column, which may be considered the velocity of migration of the water if its only driving force is the wind. The monthly averages of integrated transport velocities for 1961 based on the above calculations are displayed in Fig. 36, page 56, T.R. 99. The value of D chosen for these calculations was 40 m as this depth approximated the lower boundary of the river effluent as defined by the 32.5°/oo isopleth. Further considerations suggest that over much of the plume area this depth is too great to sue in the velocity calculations.

The migration of water at the integrated transport velocity can be used to determine the direction and extent that a known surface salinity distribution will move with time. However, since this velocity is sensitive to the choice of D, several test cases involving actual shifts in the distributions of surface salinities were studied to determine if 40 m were a suitable D value to use in the analyses. Distributions

determined from one cruise were carefully compared with distributions from a successive cruise in an effort to trace distinct and definite features of the distributions that might be common to both cruises, but displaced by wind-induced transport. The displacement distance divided by the time between cruises yields an approximation of the lowest velocity required for the between-cruise migration, if it is assumed that the feature followed the shortest path. The migration velocity derived from the displacement and time between cruises is then equated to the average of the wind-derived Ekman transport divided by D for the same period. A first estimate of D is determined in this manner. This D is then used in calculating the integrated transport velocities from the twice-daily Ekman transports for the period. The twice-daily velocity vectors are plotted to determine the trajectory of discrete points from the original distribution. If the motions of the discrete points defining a particular feature were wind-driven only, then this feature should appear in the position determined from the second cruise. If this feature falls short of its goal in the allotted time interval, but travels in the correct direction, although not necessarily in a straight line, then integrated transport velocities are probably too small, indicating that the first estimate of D was too large. If the water particle exceeds its goal in the intervening time between cruises, then the velocities determined from Ekman transport are probably too large or D is too small. If enough suitable data are used, therefore, D can be evaluated as a best-fit variable to the problem.

A theoretical D in the area of the effluent waters can be estimated by another means. The D should be limited by the zone through which viscous stresses cannot be easily transmitted. Since stress is directly dependent upon the coefficient of eddy viscosity, it should reflect the variations of this coefficient and become less or greater with a smaller or larger coefficient. An empirical relationship between the coefficient of eddy viscosity and the stability of the water column was developed by Fjeldstad (Fjeldstad, 1936; Sverdrup, Johnson, and Fleming, 1942) and is expressed by the equations.

$$A = f(z)/(1 + \alpha E') \tag{6}$$

$$E' \doteq 10^{-3} \frac{d\sigma_t}{dz} \tag{7}$$

Equation (6) indicates that the coefficient of eddy viscosity, A, is inversely proportional to the stability of E'. In the Columbia River effluent area, station data indicate that $d\sigma_t/dz$ or E' has its maximum value at depths slightly less than 10 m in the nearshore area. This tends to make the coefficient of eddy viscosity and the stress small at very shallow depths rather than at the 40-m depth and imposes limits on the depth to which the Ekman transport penetrates.

The table of depths of frictional resistance derived from the stated cruise material (Table 4) shows the comparison of D values determined by two different methods. The D_A values are the depths determined by the depth of maximum stability, and D_B values are derived from the

migration of recognizable features under the influence of the surface winds over time periods separating two successive cruises. This latter D_B is the best-fit variable that causes the feature to move at the required velocity.

Table 4. Depths of Frictional Resistance

Data Source	D_A (m)	D_B (m)
Cruise Brown Bear 335 station 037	5	
Cruise Brown Bear 333 station H04	3	
Cruise Brown Bear 335 station 065	9	
Cruise Brown Bear 333 station H16	4	
Cruise Brown Bear 335 station 028	22	
Cruises Brown Bear 288 and Acona 6106		8
Cruises Brown Bear 287 and Brown Bear 288		20
Cruises Brown Bear 290 and Brown Bear 291		10

A dynamically valid relationship between D_A and the stability of the water column has not been established for the area in question as this would require detailed measurements for the coefficient of eddy viscosity, for velocity profiles, and of density in situ. The physical relationship between stability, eddy viscosity, and the transmittal of stress in the sea has been used as a guide in determining the zone beneath the sea surface through which surface-originating stresses have difficulty in passing. The depth of this zone, which corresponds to the zone of maximum stability, is considered synonomous with D, the depth of frictional resistance.

The area of investigations in the Columbia River project has two major factors that modify the general conditions under which the classical Ekman spiral is valid: the presence of a layer with great stability lying from 5 to 20 m under the river effluent during the late spring, summer and early autumn months; and the presence of the effluent as a nearly homogeneous water mass held against the coast in shallow water over the continental shelf during the winter months. Fjeldstad (1929) investigated data gathered by Sverdrup (1929) and determined that wind-induced currents in shallow water were affected by both stability and bottom friction. In the first case, where the coefficient of eedy viscosity decreases and stability increases with depth, the angles between the wind vectors and the water-current vectors increase at all depths as do the current velocities (Sverdrup, Johnson, and Fleming, 1942). Apparently this results from the compression of the Ekman spiral and the decrease of D. In the second case, applicable to the winter distribution of winds and river effluent, the coefficient of eddy viscosity remains nearly constant with depth as the total depth of water decreases toward the coastal boundary. Under these conditions the angles between the wind

vectors and water-current vectors, as well as the speed of the current, decrease with increasing depth more rapidly than in the classical Ekman spiral problem. The net transport of the effluent therefore is less than 90° to the right of the winter winds and produces a northward-setting flow along the coasts of Oregon and Washington.

Detailed measurements, as suggested by Rossby and Montgomery (1935) of winds, currents, and water properties are necessary to establish the seasonal dynamic interactions between wind stress and water movement for this particular area. An estimate of the integrated velocity from the Ekman transport can be made, however, subject to the selected value for D in the computations. The present data indicate that D increases going away from the mouth of the river during the summer effluent distribution pattern. At this season the equation approximating D in meters is as follows:

$$D = 5 + 0.067X \qquad (8)$$

where X is the distance from the river mouth in kilometers. This variable D gives transport-derived velocities reasonably consistent with observed migrations of identifiable parcels of water.

Prediction of Water-Particle Migration and Effluent Distribution During Summer Months

Reasonable estimates of the direction and extent of water-particle migration within the effluent for the period from spring to early autumn can be obtained from the surface-wind transport calculations. A field of points is selected within an area for which the surface salinity distribution is known and contoured. The mid-date of the cruise on which the isopleths are based represents a starting time. The trajectory of each point obtained from the twice-daily Ekman transport values divided by ρD, or from the surface current (equation 3), is determined and plotted. These trajectories are continued for a period of time ending on the date the new anticipated distribution is desired. The size of the wind grids (Fig. 84) in the present analysis tends to make the points move along similar path lines. A visual integration of these lines yields the stretching axis of the effluent, which has been referred to in T.R. 99. If the new salinity value at the terminal point of the trajectories is determined, then the new predicted plume configuration can be contoured through these terminal salinity values. The new distribution can be considered as representative of the effluent in its offshore margins after the migration, but not as a substitute for a new set of measurements in the area. This technique can serve as an aid in cruise planning, as the results indicate where to seek the effluent waters in the offshore regions. The method has not yielded information on the distribution of salinity adjacent to the river mouth, as no values or points from upriver have been available for prediction and the importance of tidal and hydraulic flow invalidates the assumed Ekman transport.

In order to facilitate this prediction scheme, data from successive cruises in the project area were analyzed for a method that would yield a reasonable estimate of the change in salinity of a migrating particle.

The mechanisms of dynamics of the system controlling the salinity change were not investigated. However, experience and familiarity with the data indicate that the surface salinity changes rapidly at first then more slowly as the effluent blends into the offshore background water. Thus the rate of change of salinity of the effluent depends upon the distance from the river mouth. This suggests that time and velocity of travel of the effluent might be used to estimate the salinity of a water particle as it moves seaward. A gross assumption, based on average conditions existing over considerable periods of time, can then be made that the mixing processes occur at a constant rate at all times in the area. The assumption requires that the salinity of the effluent water change as a function of time only while the velocity of migration determines its location.

Used with the above as a working concept, the following logarithmic equation was fitted to the data (Fig. 111):

$$S = 21.2^{\circ}/_{oo} + 6.7\ (\log_{10} T) \qquad (9)$$

where S is the surface salinity, $21.2^{\circ}/_{oo}$ is an average surface salinity near the river mouth, T is the transit time in days. The method for predicting the new salinity of a particle migrating under wind-induced motions requires that equation (9) be used for determining differences in both time and salinity. The original salinity value of the water to be wind-transported is found on the curve (Fig. 111). This salinity and associated time are considered S_o and T_o. The number of days allowed for the migration is then added to T_o to define a new T on the curve and the estimate of the transient water's new salinity, S.

This method, while lacking sophistication, yields a reasonable estimate for the change in salinity as determined from cruise data. A combined program of geostrophic winds, Ekman drift, and salinity change can be designed for computer analysis to give a simple first-order approximation of effluent distributions. Additional and definitive research into the areas of the dependency of wind-induced water motions upon the stratification and depth of water and the mechanics of mixing is needed to clarify the complex relationships involved and to provide a better basis for predicting the distribution of river effluent.

SUMMARY

Surveys off the Washington-Oregon coast by the Department of Oceanography, University of Washington, from 1961 through 1963 have provided salinity data for describing the Columbia River effluent in the Northeast Pacific Ocean. The data also have provided insight into the interactions between the observed distributions and the meteorological systems. Considerable variation in river discharge and local weather conditions occurs from year to year; however, four generalized seasonal distribution patterns of the wind- and discharge rate-controlled effluent emerge to form a cyclic pattern which is found in successive years: spring, increased river discharge and winds shifted from southerly to northerly

direction; summer, maximum river discharge followed by rapid reduction in flow and predominantly weak northerly winds; autumn, minimum river discharge and strong southerly winds; and winter, low to medium river discharge and predominantly southern winds. The 32.5°/oo salinity isopleth may be used to define the extent of the vertical and horizontal influence of the river effluent. The horizontal shift of this boundary is shown for the seasonal distributions.

The monthly trends and variations with latitude of the 10-m winds over the project area are presented. The effects of these surface winds on the motion and distribution of the river's effluent at sea are summarized in the average Ekman transport diagrams.

The cause-and-effect relationships between the effluent distribution and prevailing weather are not understood dynamically. Gross empirical relationships can be used, however, to determine changes in the distribution of the effluent at sea in response to changes in the atmospheric conditions.

Information from the wind analysis can be used to determine the direction and extent of the shift of a known distribution pattern in response to surface winds. Related to this shift of the water in response to the winds is the change in salinity as the outflow mixes with the oceanic water. An empirical relationship indicates that a time base and original salinity may be used to estimate the salinity of the water as it moves along its wind-driven course. The water particle's movement in response to the wind and its change in salinity with time enable investigators to construct a new distribution pattern for the effluent from an earlier distribution pattern and winds during the intervening time.

Only a few questions concerning the distribution of the Columbia River effluent at sea are answered by this report. The span of time covered by the data is brief and data coverage is not uniform over space and time. However, the material is sufficient to give considerable insight into the seasonal trends in distribution and can aid those pursuing more detailed studies in the area.

ACKNOWLEDGMENTS

This research was supported by the U.S. Atomic Energy Commission, Contracts AT(45-1)-1385 and AT(45-1)-1725 and the Office of Naval Research, Contracts Nonr-477(10) and Nonr-477(37), Project NR 083 012. The authors wish to express their appreciation to the ship and scientific field personnel for large expenditures of time and effort in gathering the material for the study. The contributions of Misses Patricia Dinkins, Charlotte MacEwan, Carol Rautenberg, Messrs. John Watson, Robert Hamilton, Douglas Evans, Donald Doyle and the cartographic section to the production of this report are gratefully adcknwledged. To these people and many more the authors are greatly indebted.

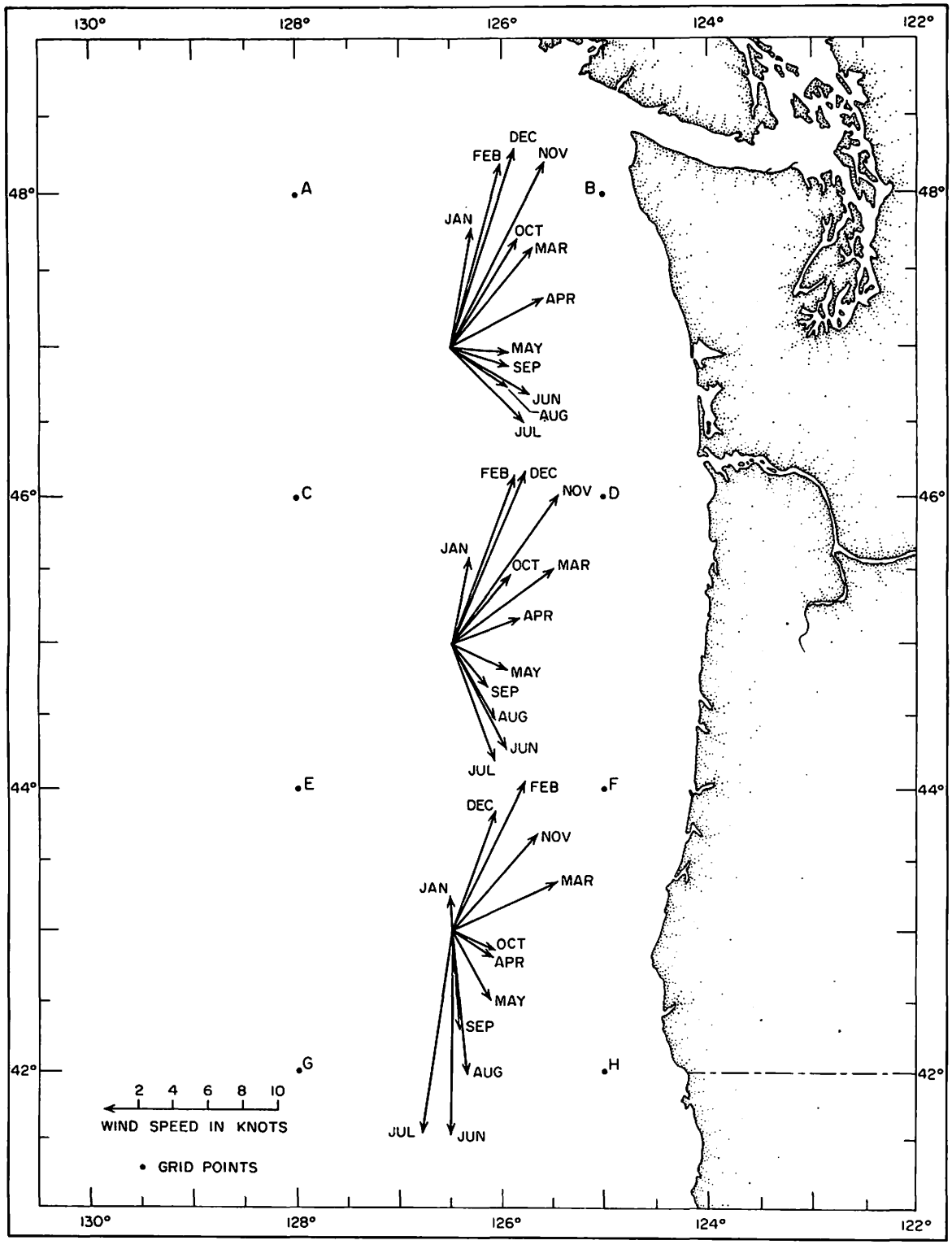

Fig. 84. Average direction and velocity of monthly winds for 1961-1963.

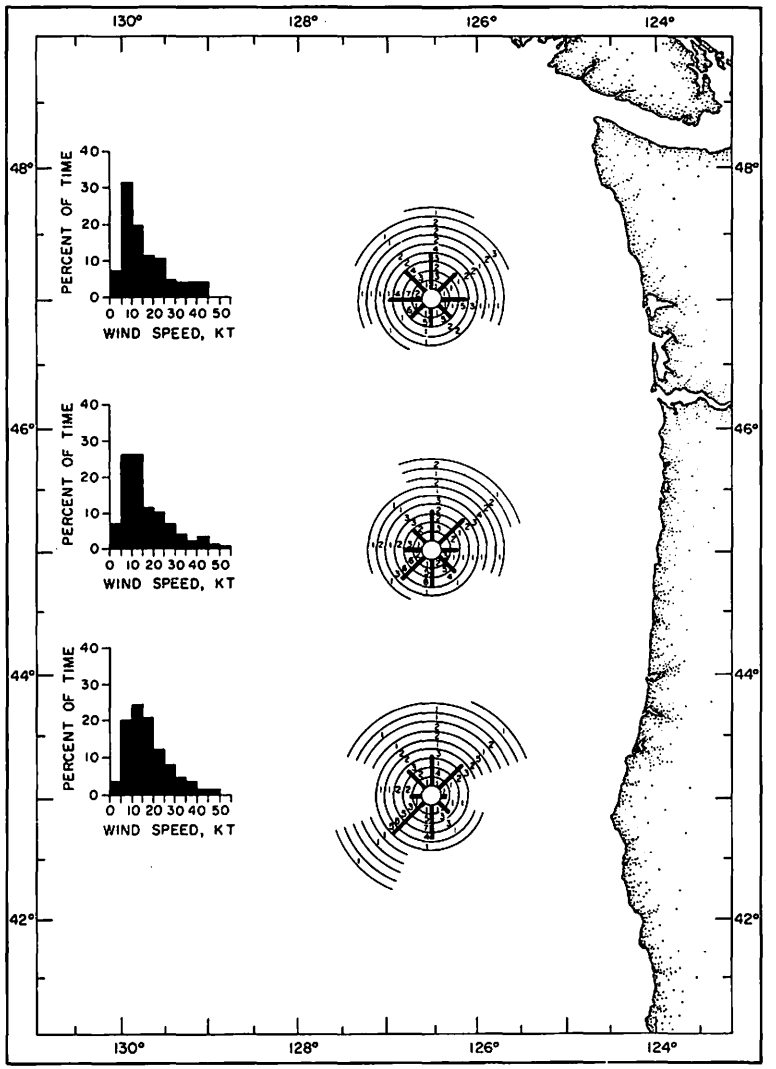

Fig. 85. Average direction and velocity of January winds for 1961-1963.

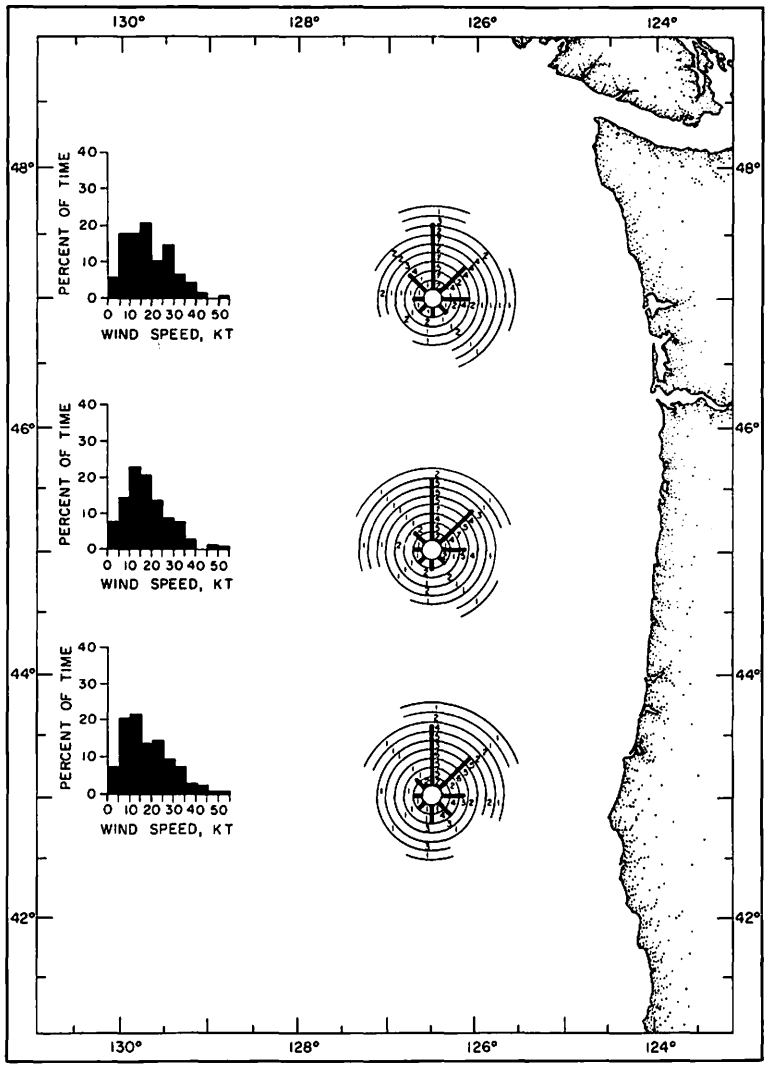

Fig. 86. Average direction and velocity of February winds for 1961-1963.

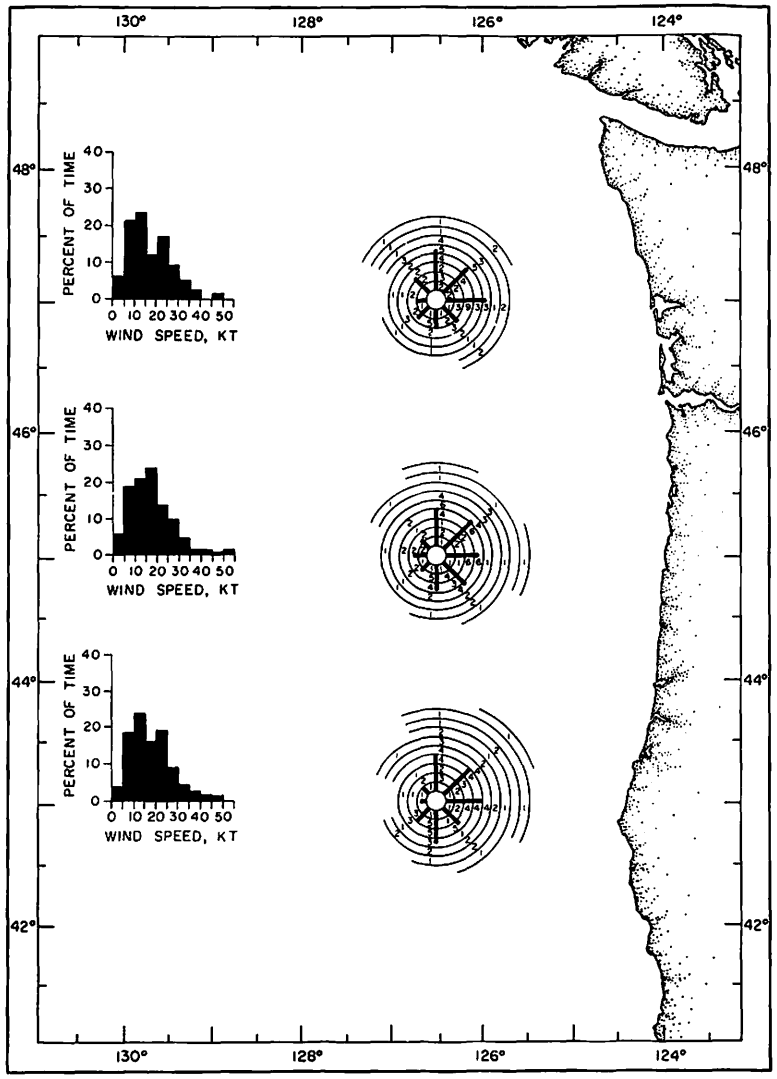

Fig. 87. Average direction and velocity of March winds for 1961-1963.

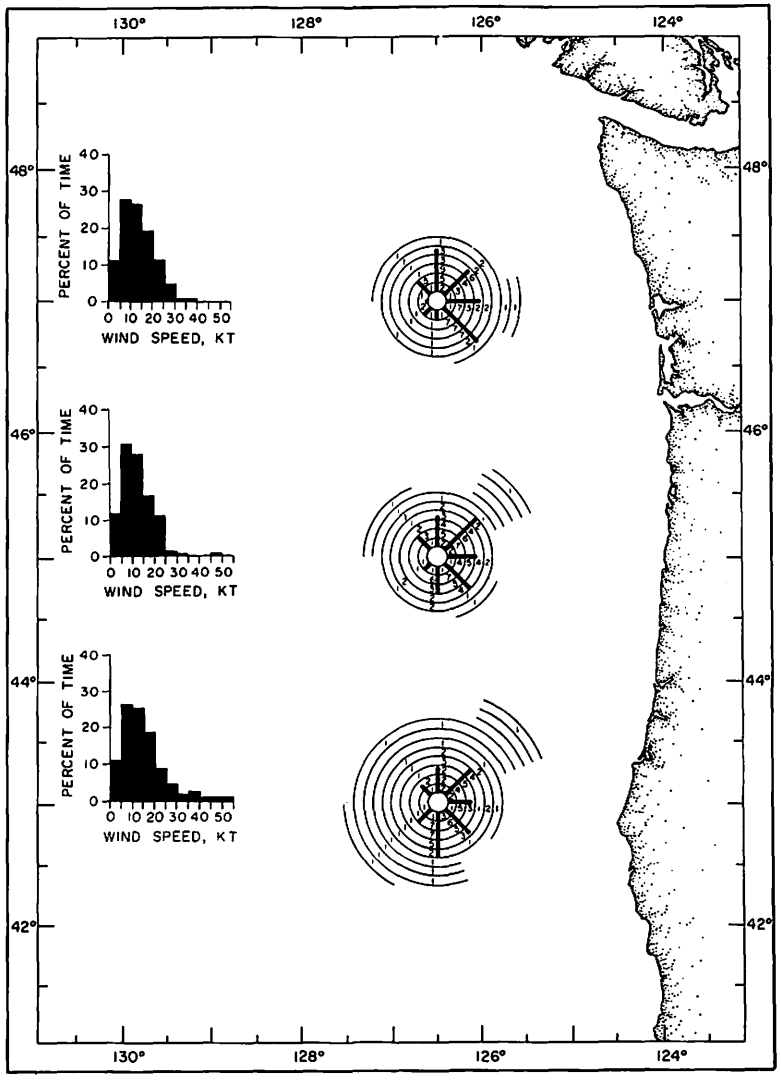

Fig. 88. Average direction and velocity of April winds for 1961-1963.

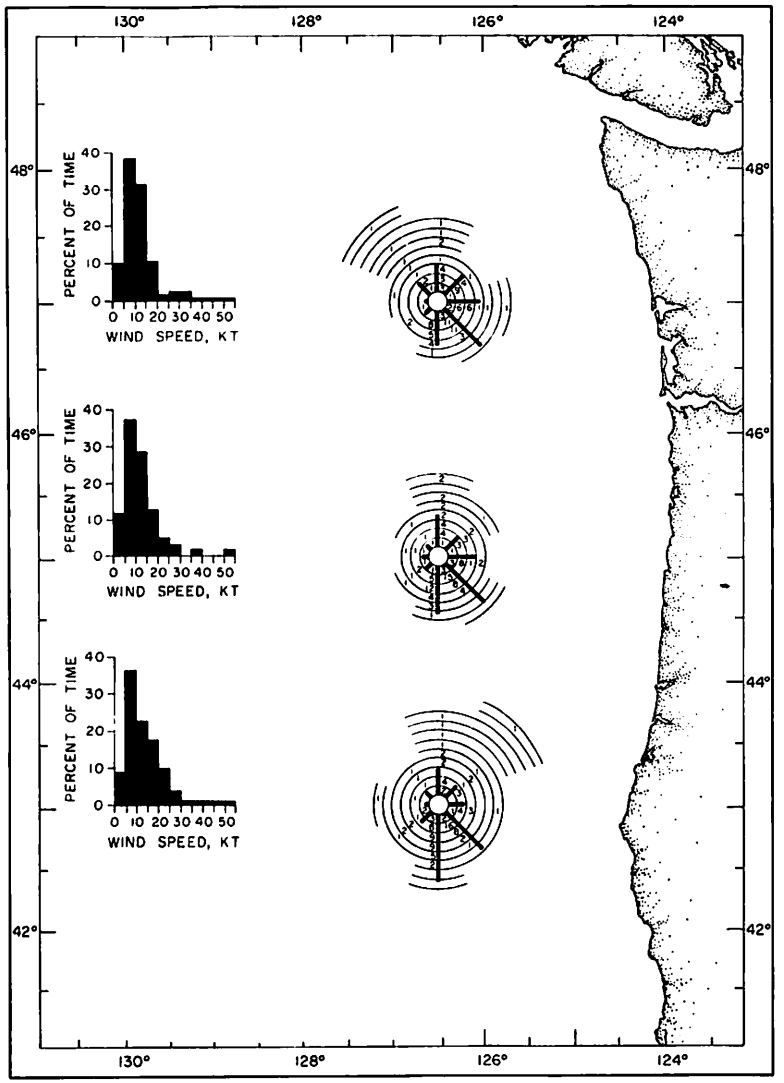

Fig. 89. Average direction and velocity of May winds for 1961-1963.

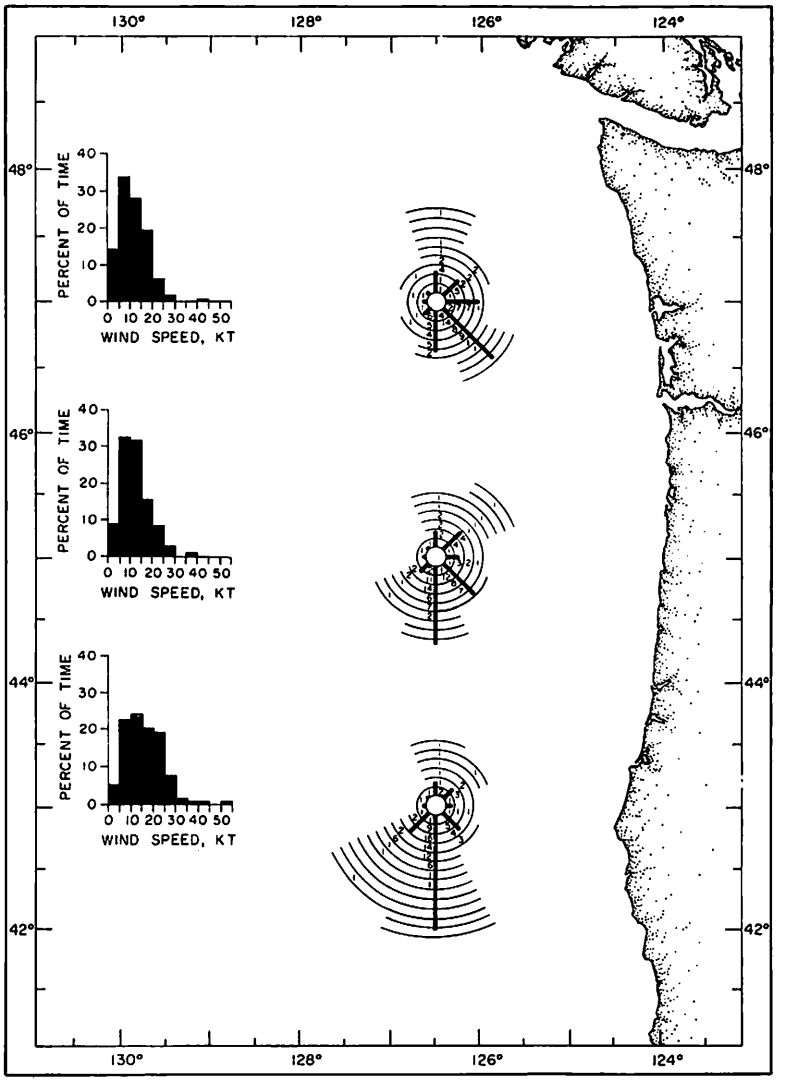

Fig. 90. Average direction and velocity of June winds for 1961-1963.

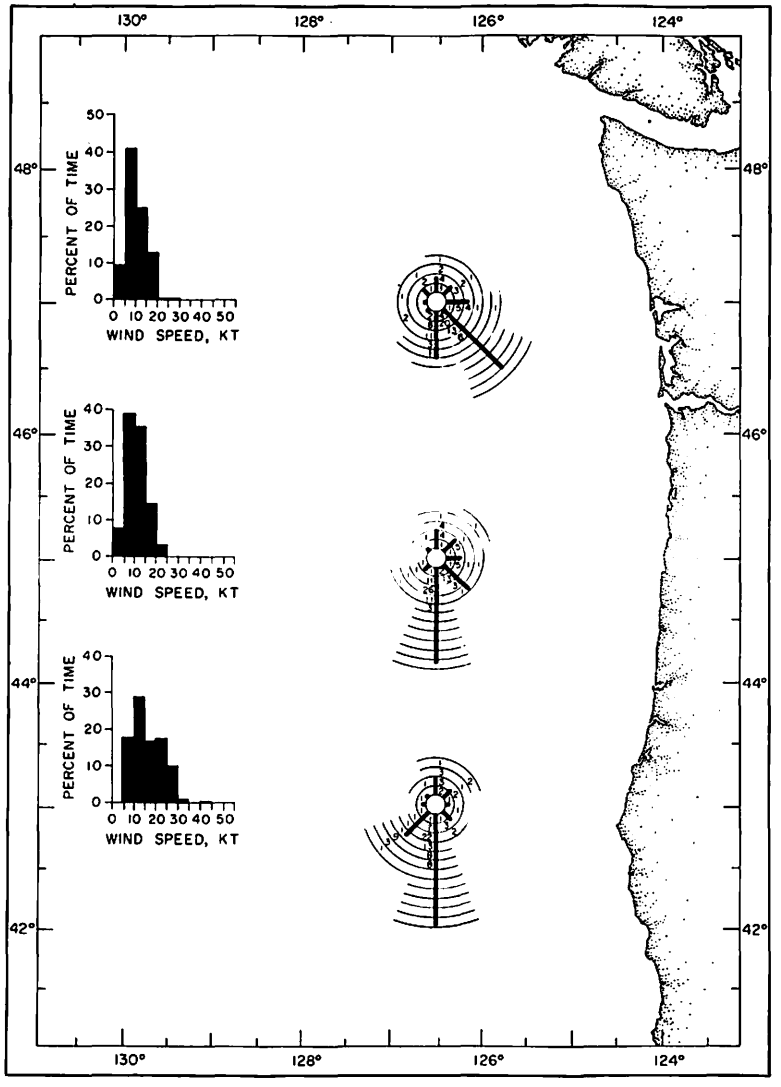

Fig. 91. Average direction and velocity of July winds for 1961-1963.

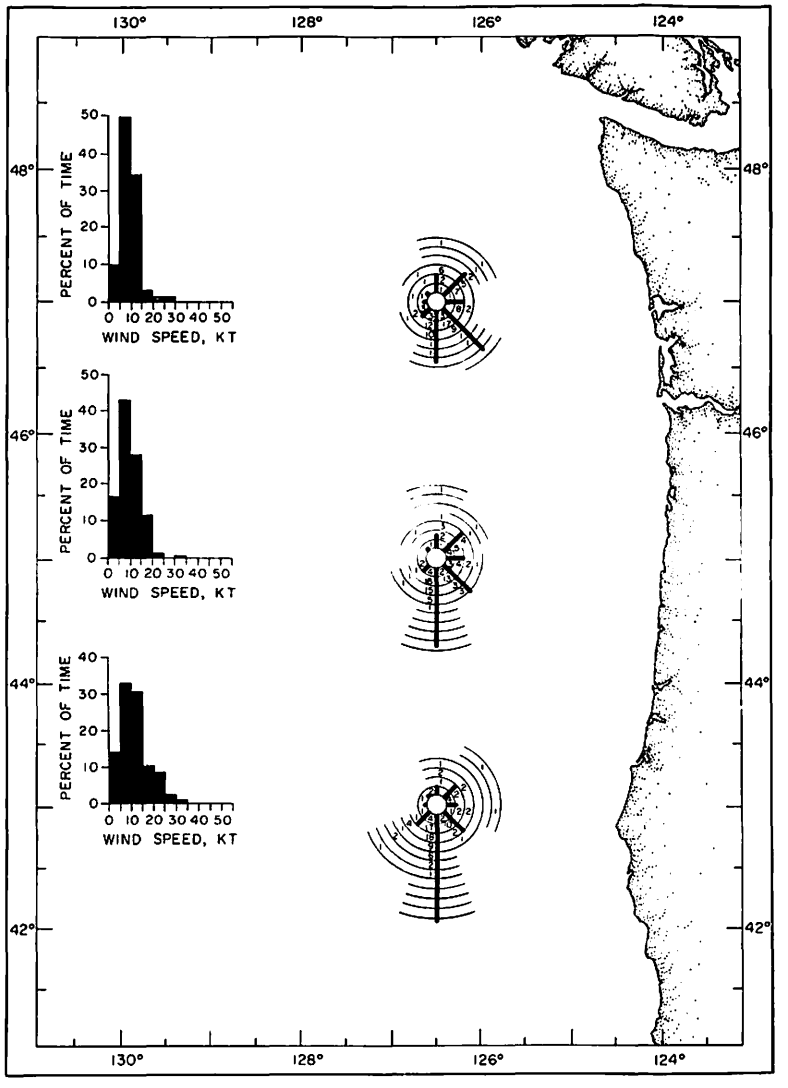

Fig. 92. Average direction and velocity of August winds for 1961-1963.

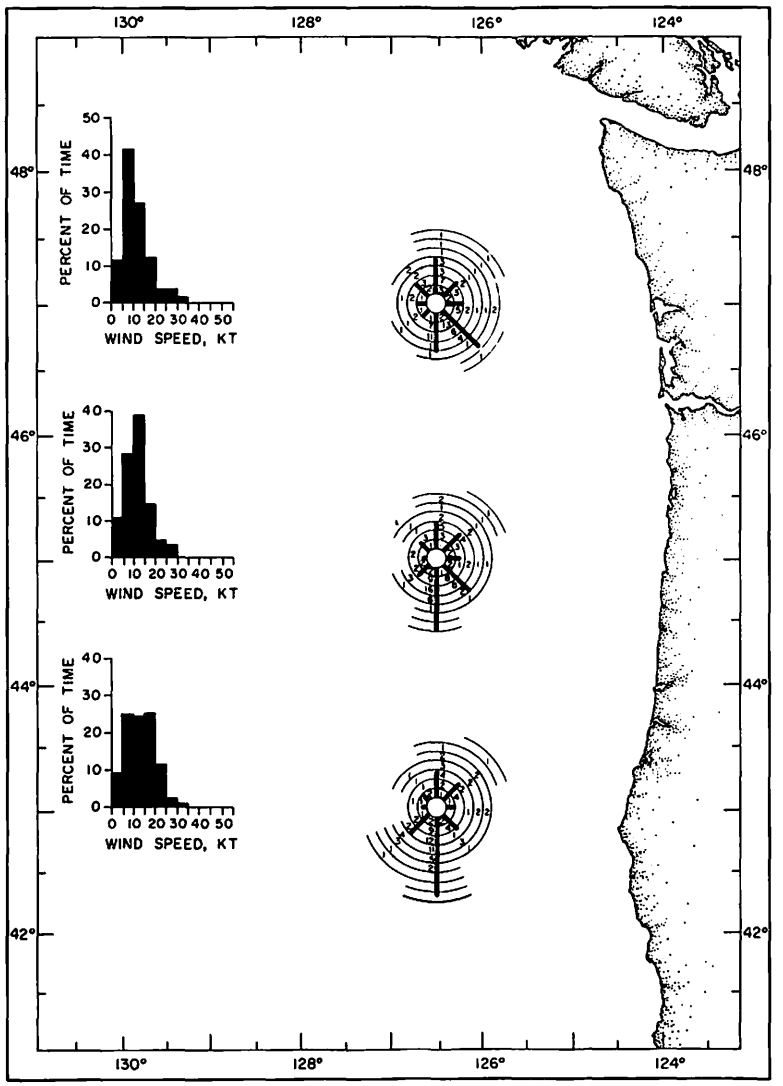

Fig. 93. Average direction and velocity of September winds for 1961-1963.

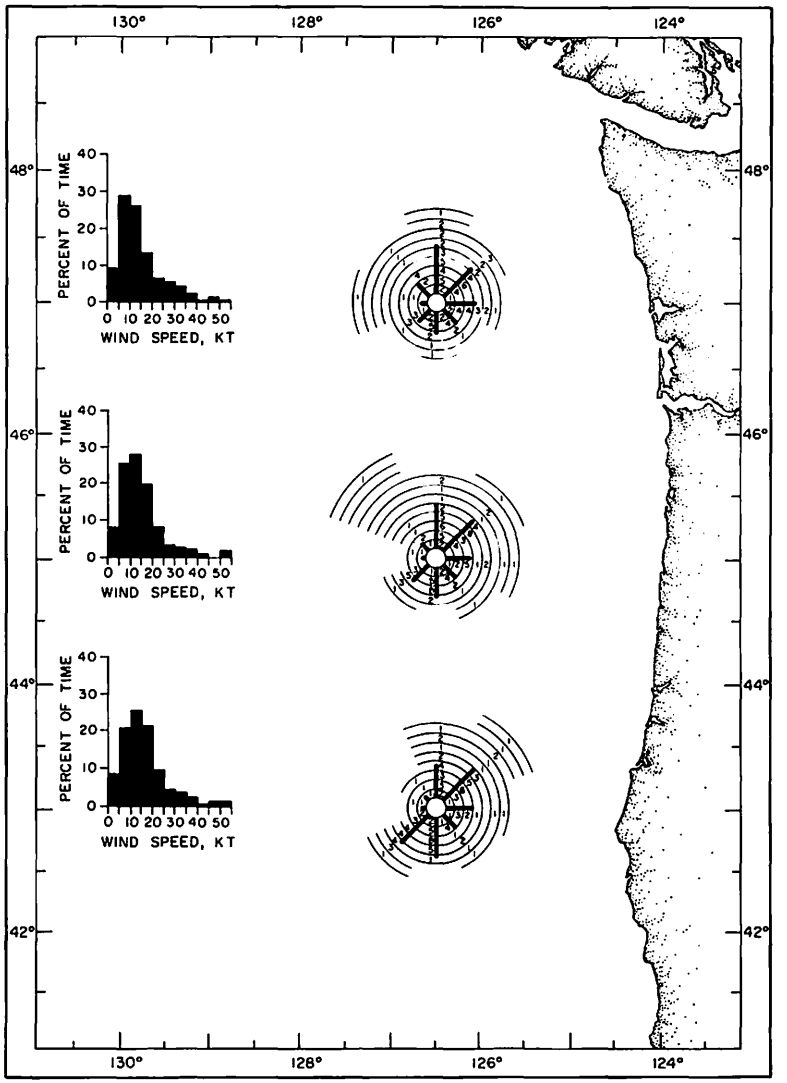

Fig. 94. Average direction and velocity of October winds for 1961-1963.

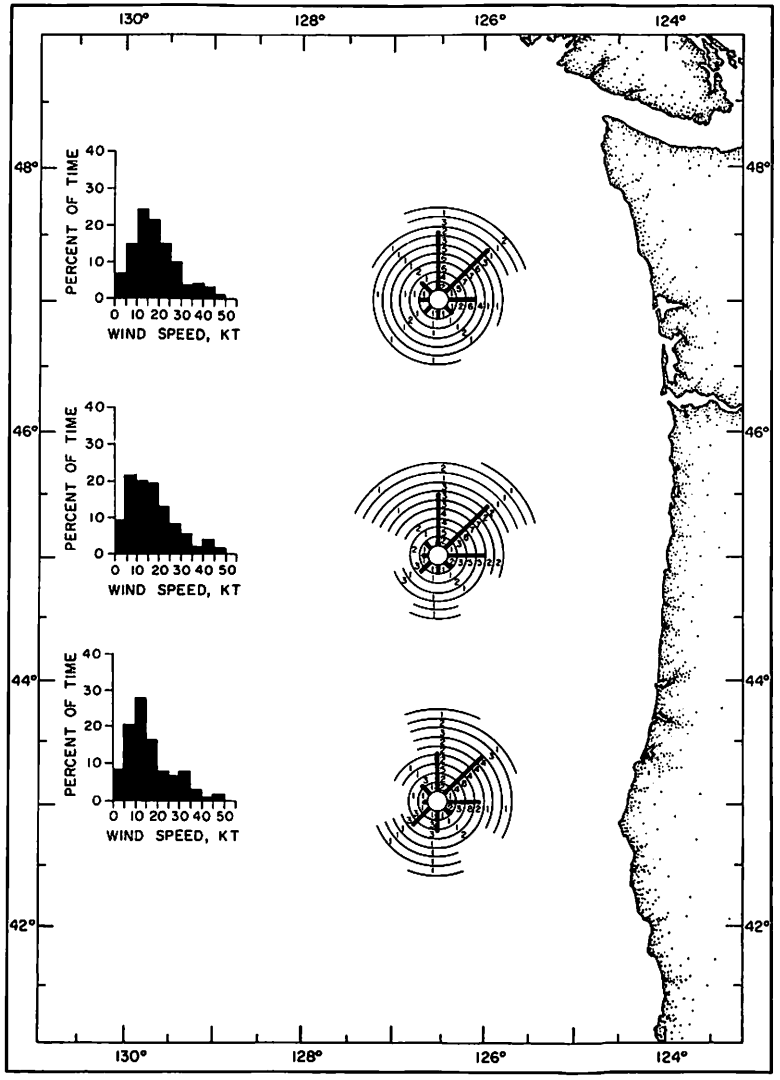

Fig. 95. Average direction and velocity of November winds for 1961-1963.

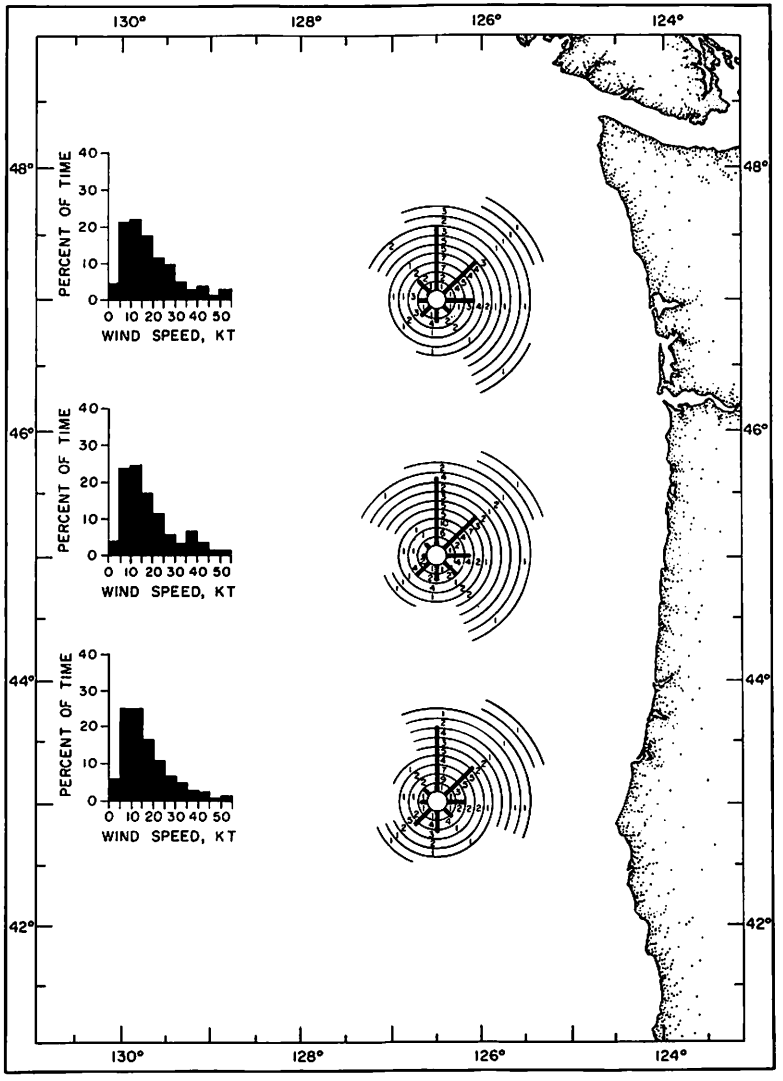

Fig. 96. Average direction and velocity of December winds for 1961-1963.

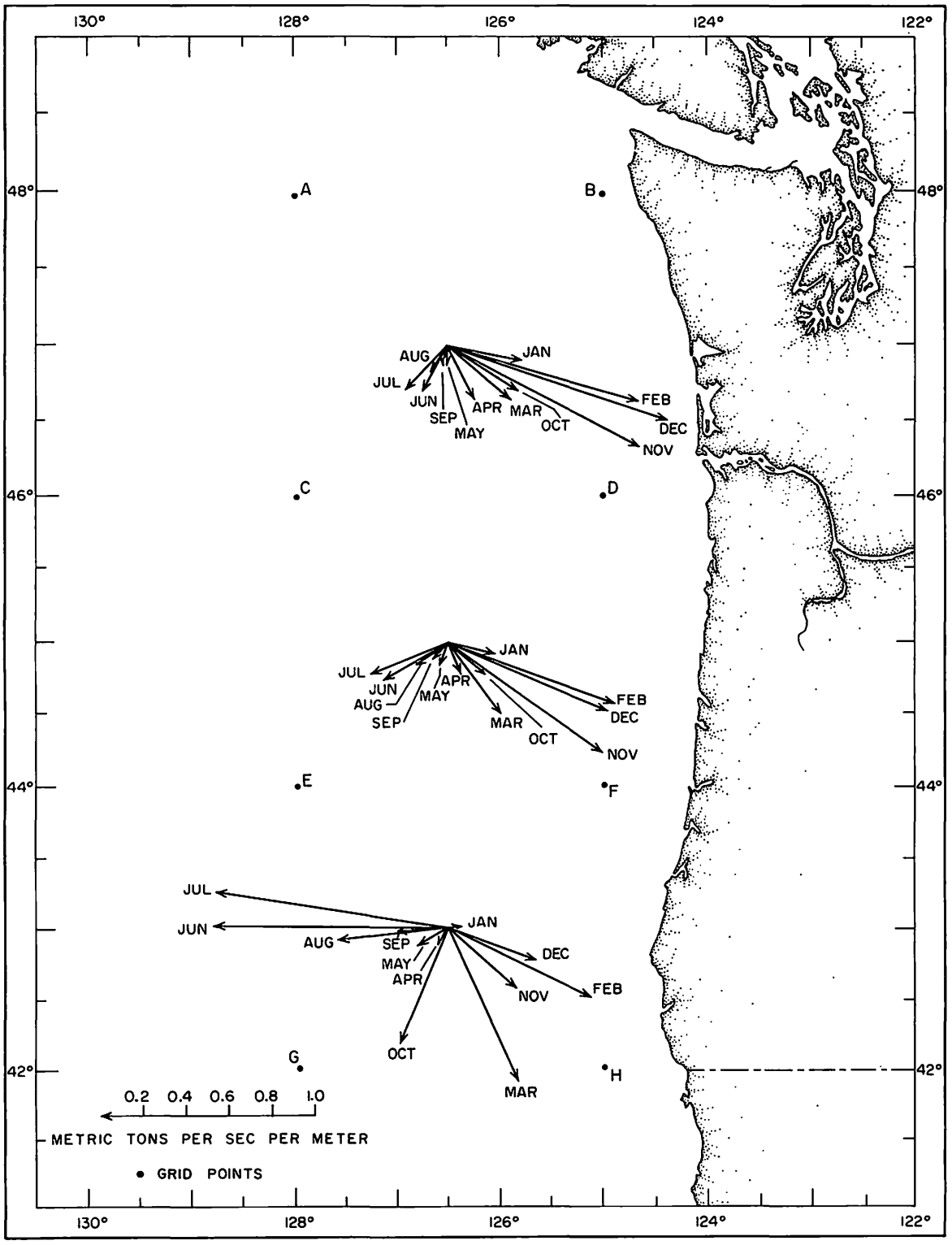

Fig. 97. Average direction and magnitude of monthly Ekman transports for 1961-1963.

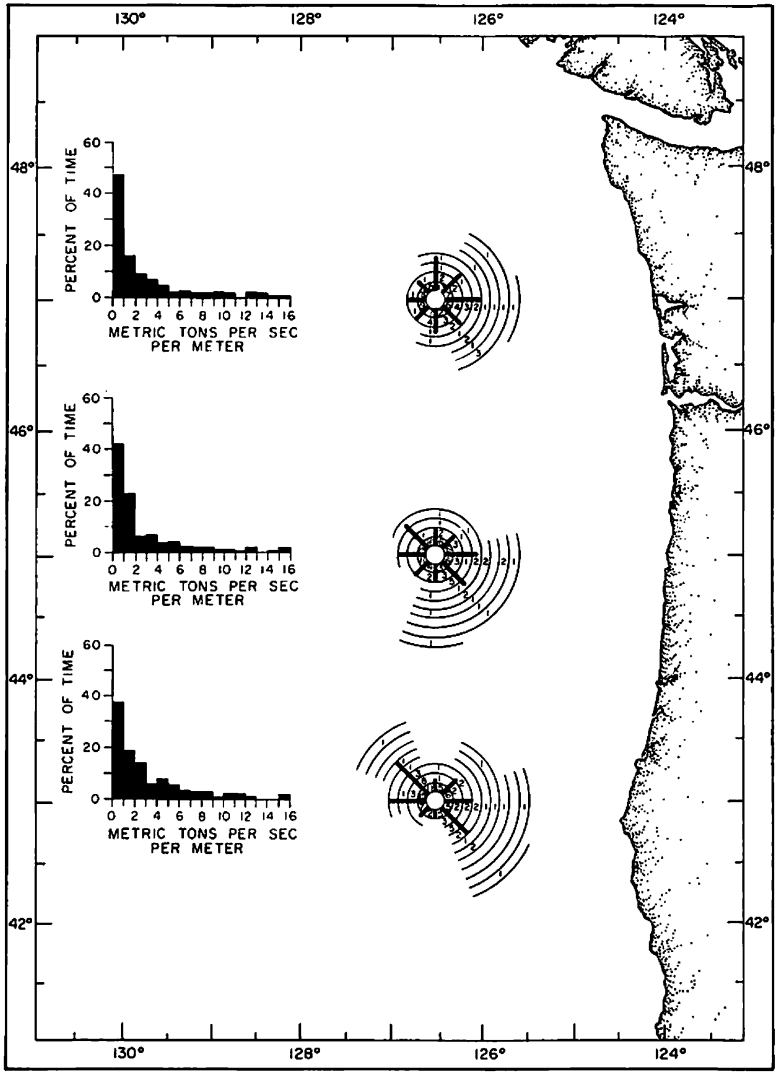

Fig. 98. Average direction and magnitude of Ekman transport for January 1961-1963.

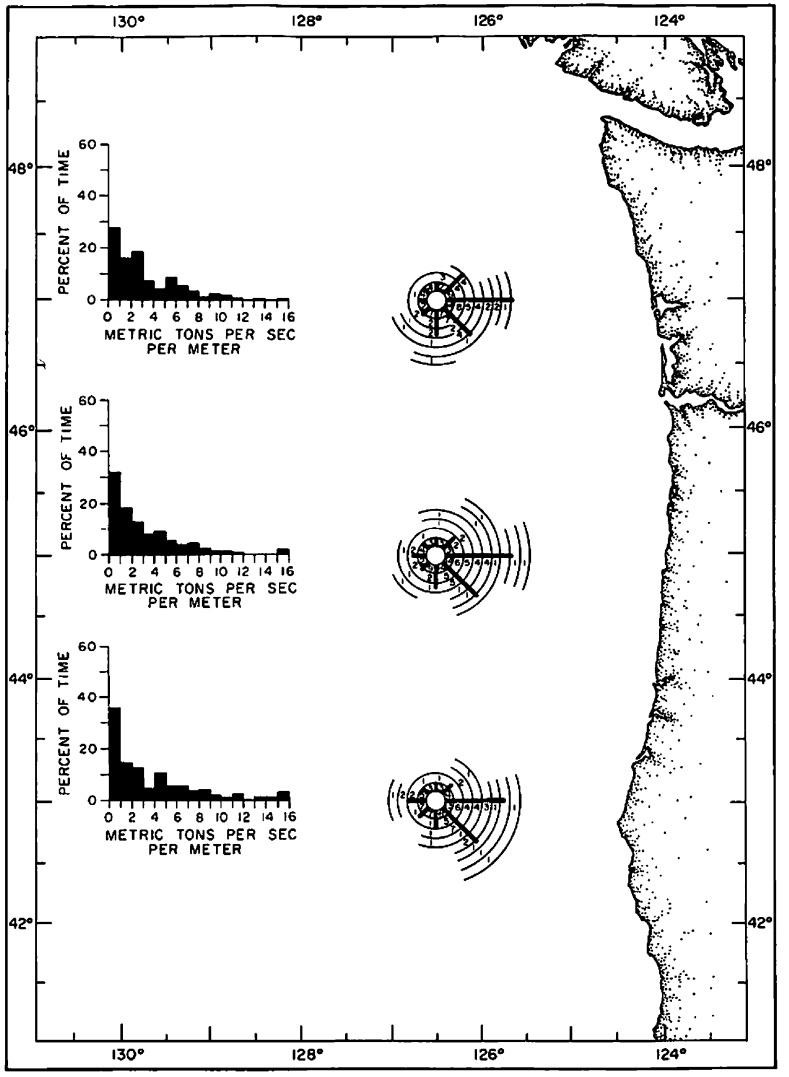

Fig. 99. Average direction and magnitude of Ekman transport for February 1961-1963.

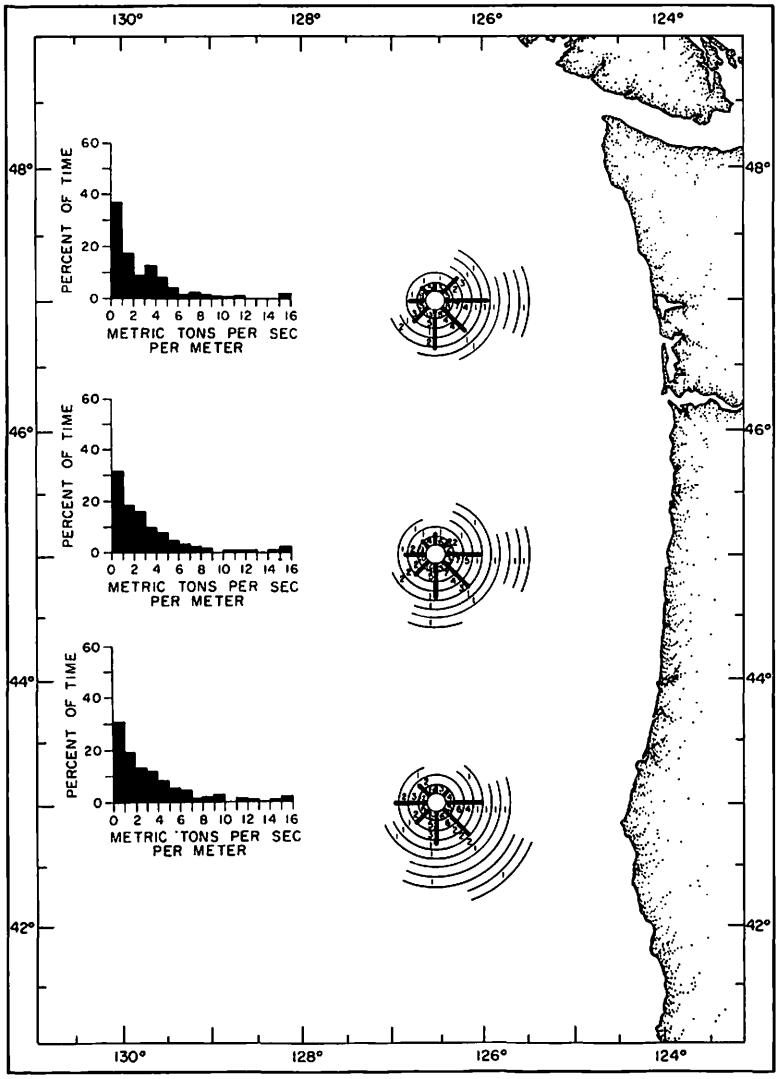

Fig. 100. Average direction and magnitude of Ekman transport for March 1961-1963.

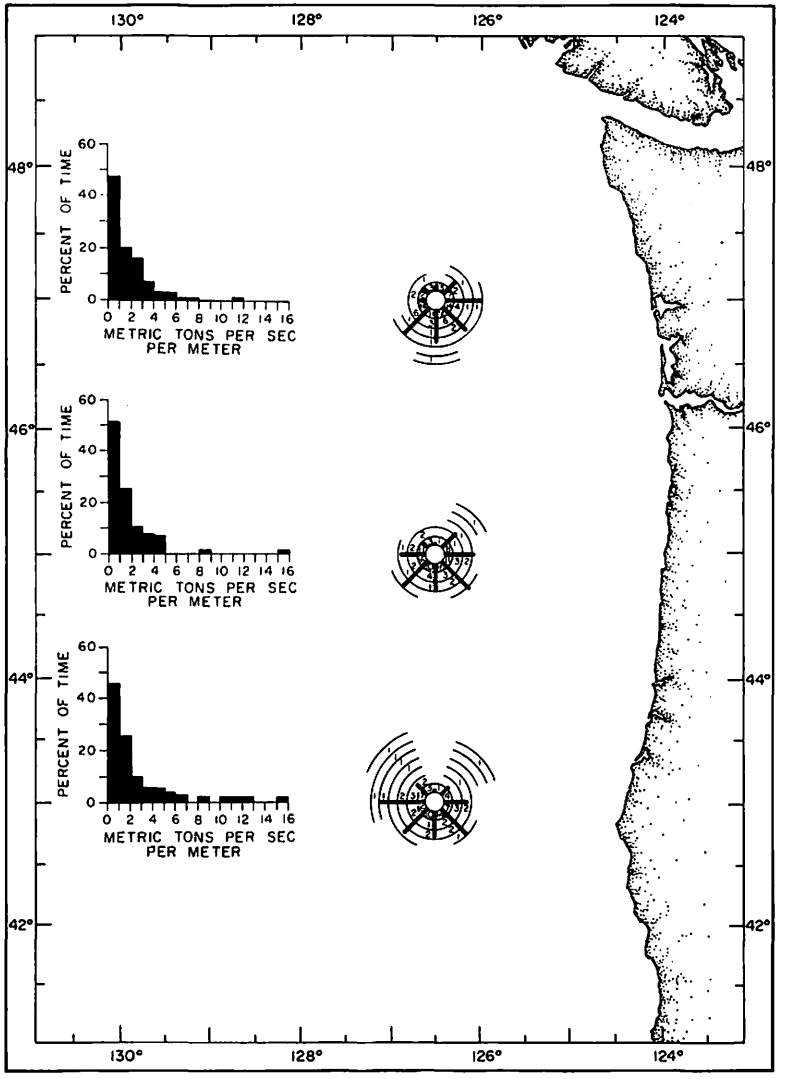

Fig. 101. Average direction and magnitude of Ekman transport for April 1961-1963.

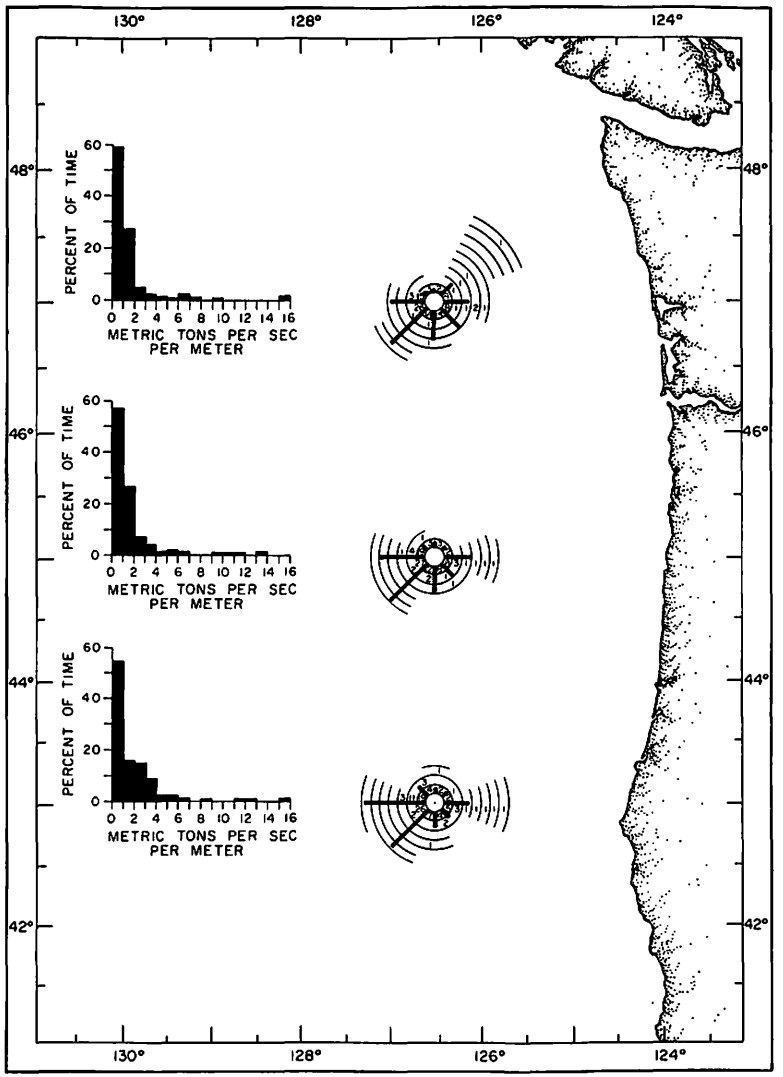

Fig. 102. Average direction and magnitude of Ekman transport for May 1961-1963.

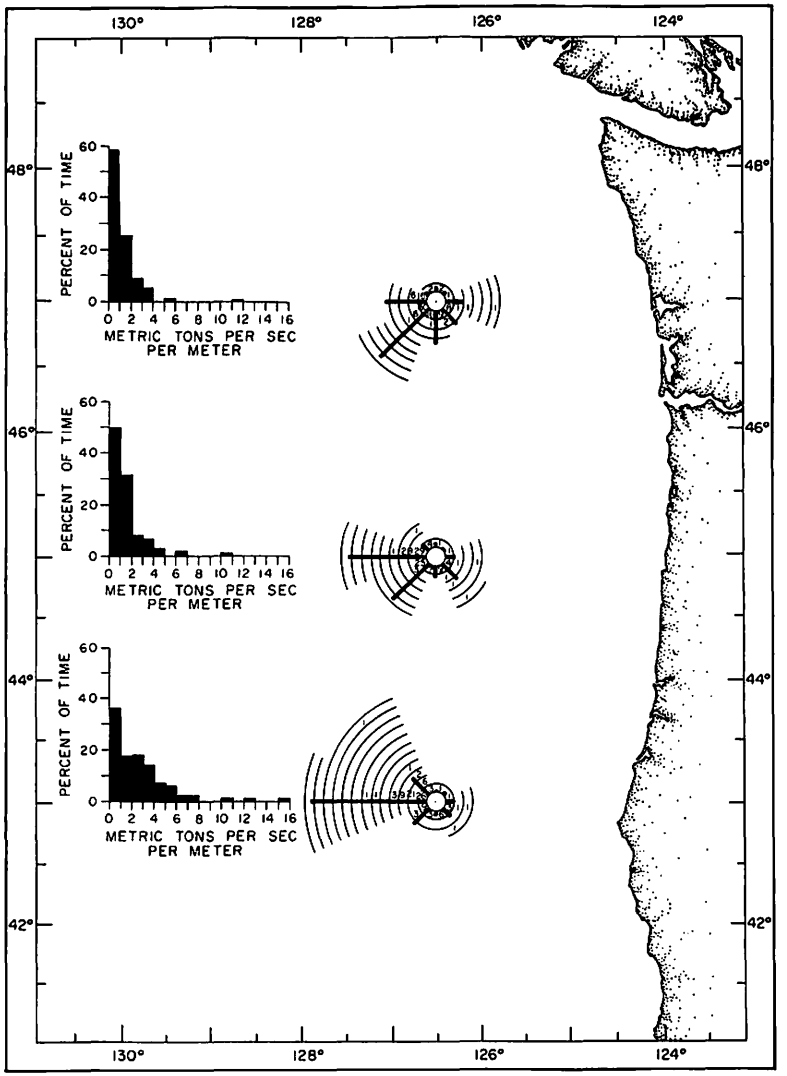

Fig. 103. Average direction and magnitude of Ekman transport for June 1961-1963.

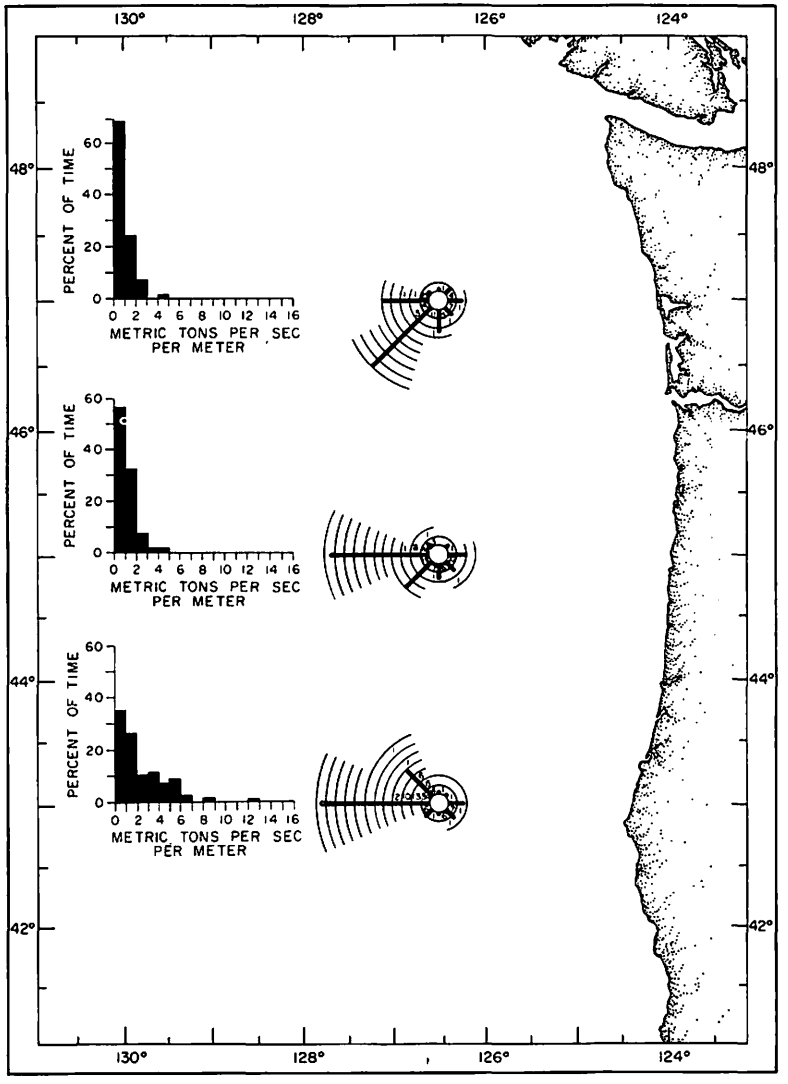

Fig. 104. Average direction and magnitude of Ekman transport for July 1961-1963.

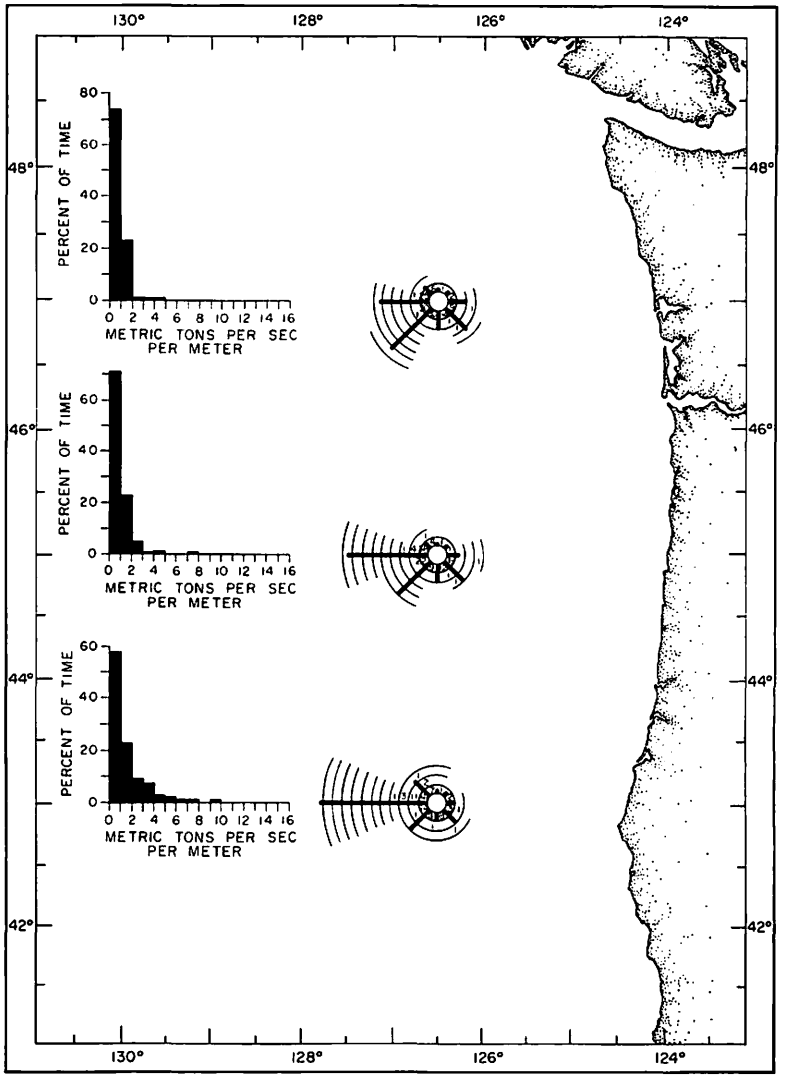

Fig. 105. Average direction and magnitude of Ekman transport for August 1961-1963.

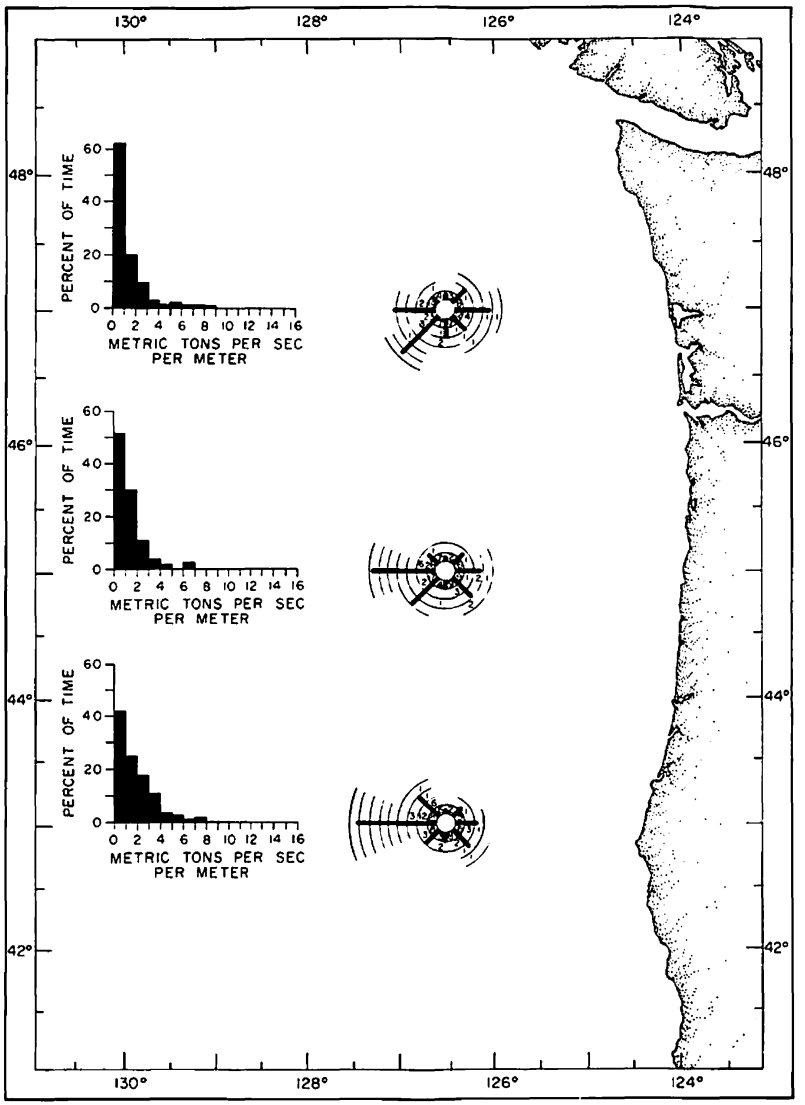

Fig. 106. Average direction and magnitude of Ekman transport for September 1961-1963.

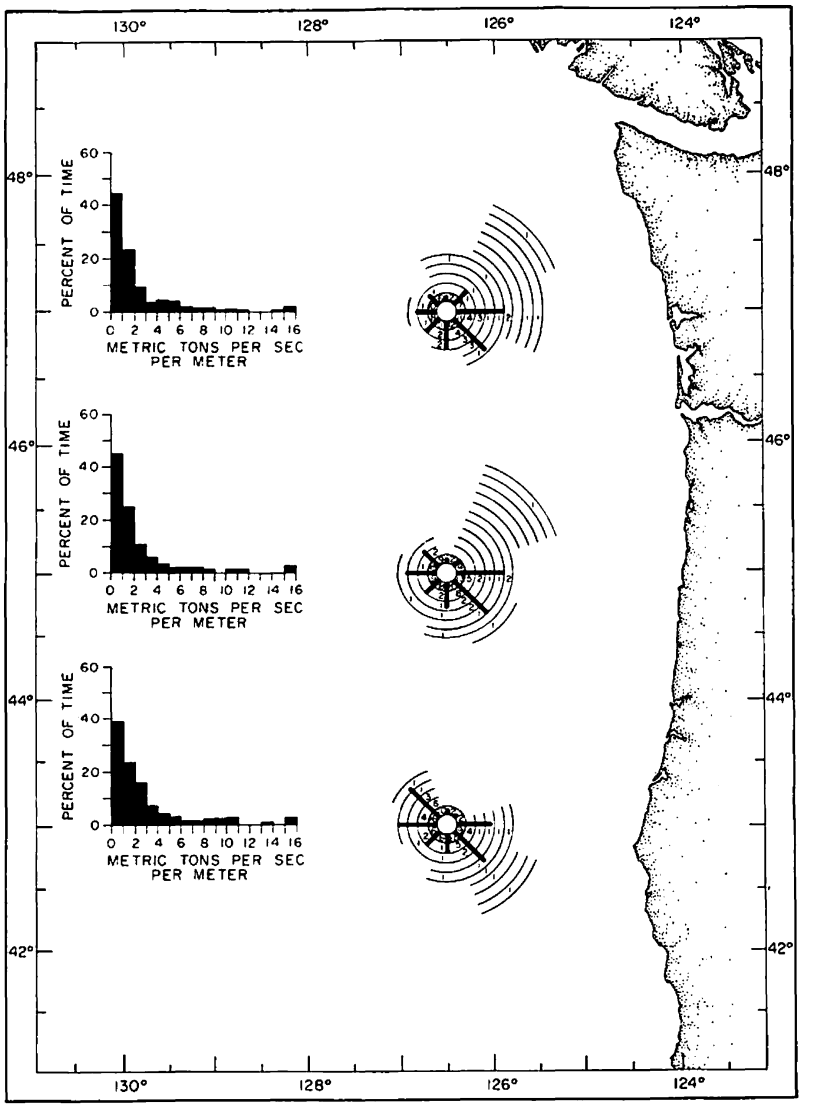

Fig. 107. Average direction and magnitude of Ekman transport for October 1961-1963.

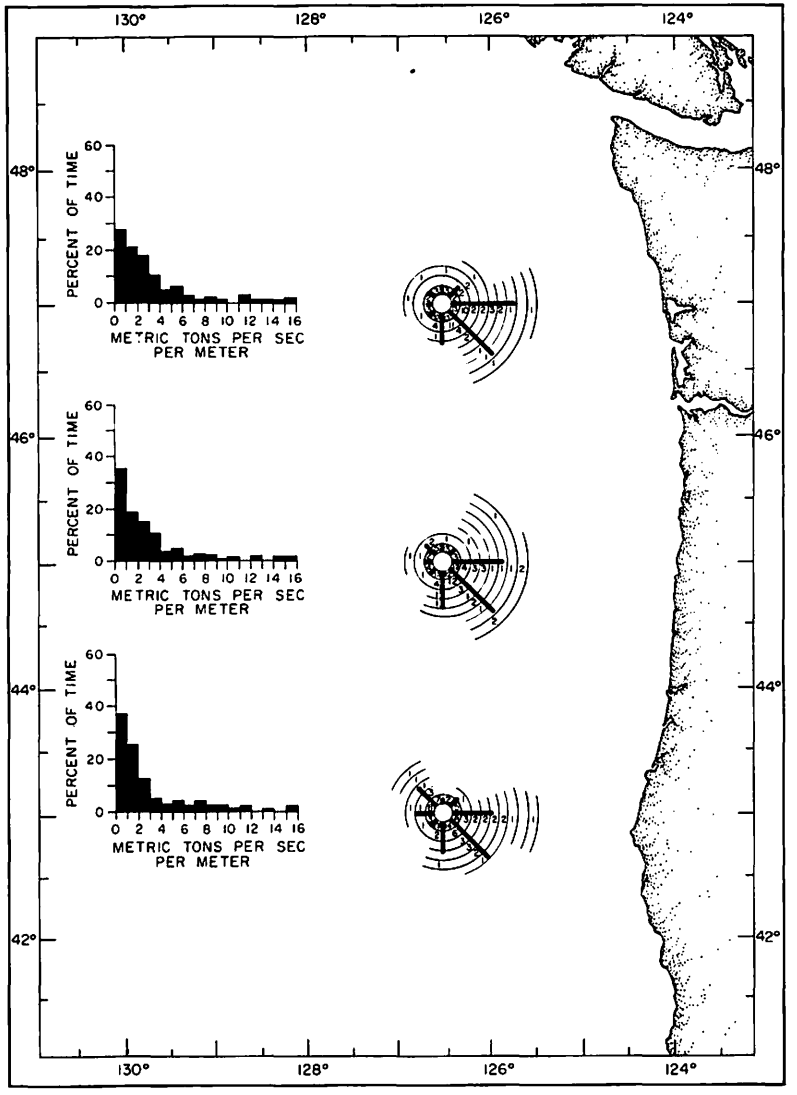

Fig. 108. Average direction and magnitude of Ekman transport for November 1961-1963.

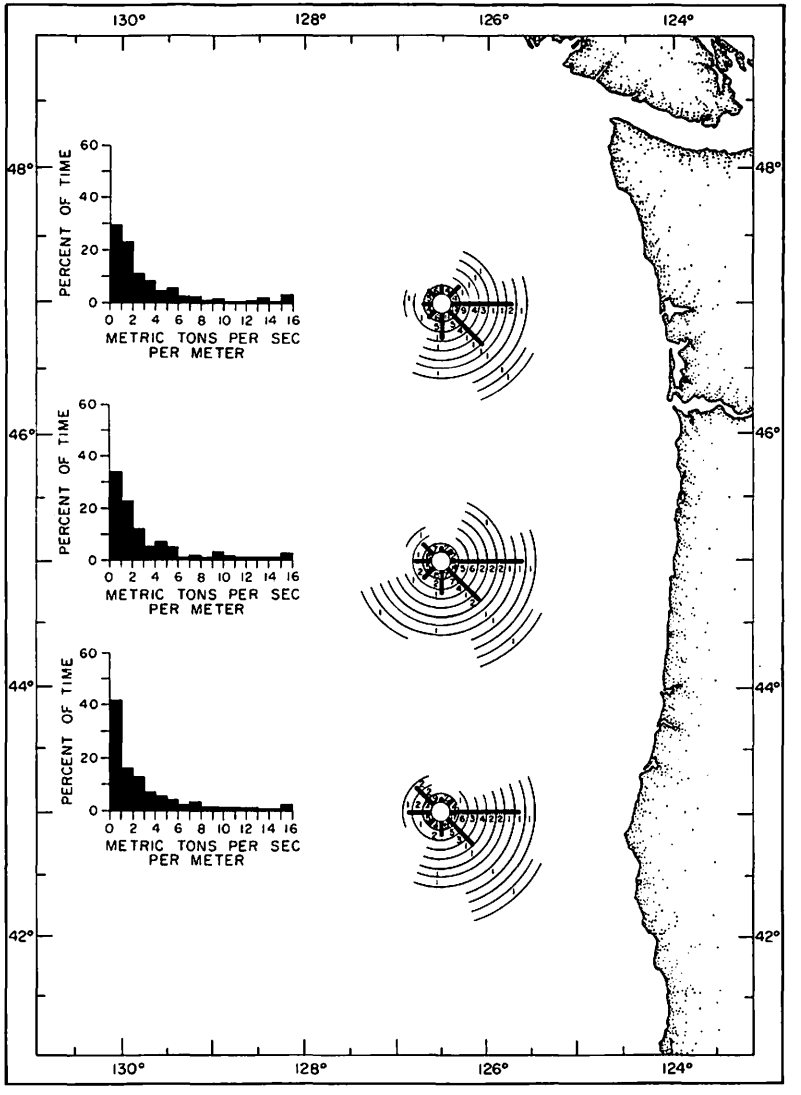

Fig. 109. Average direction and magnitude of Ekman transport for December 1961-1963.

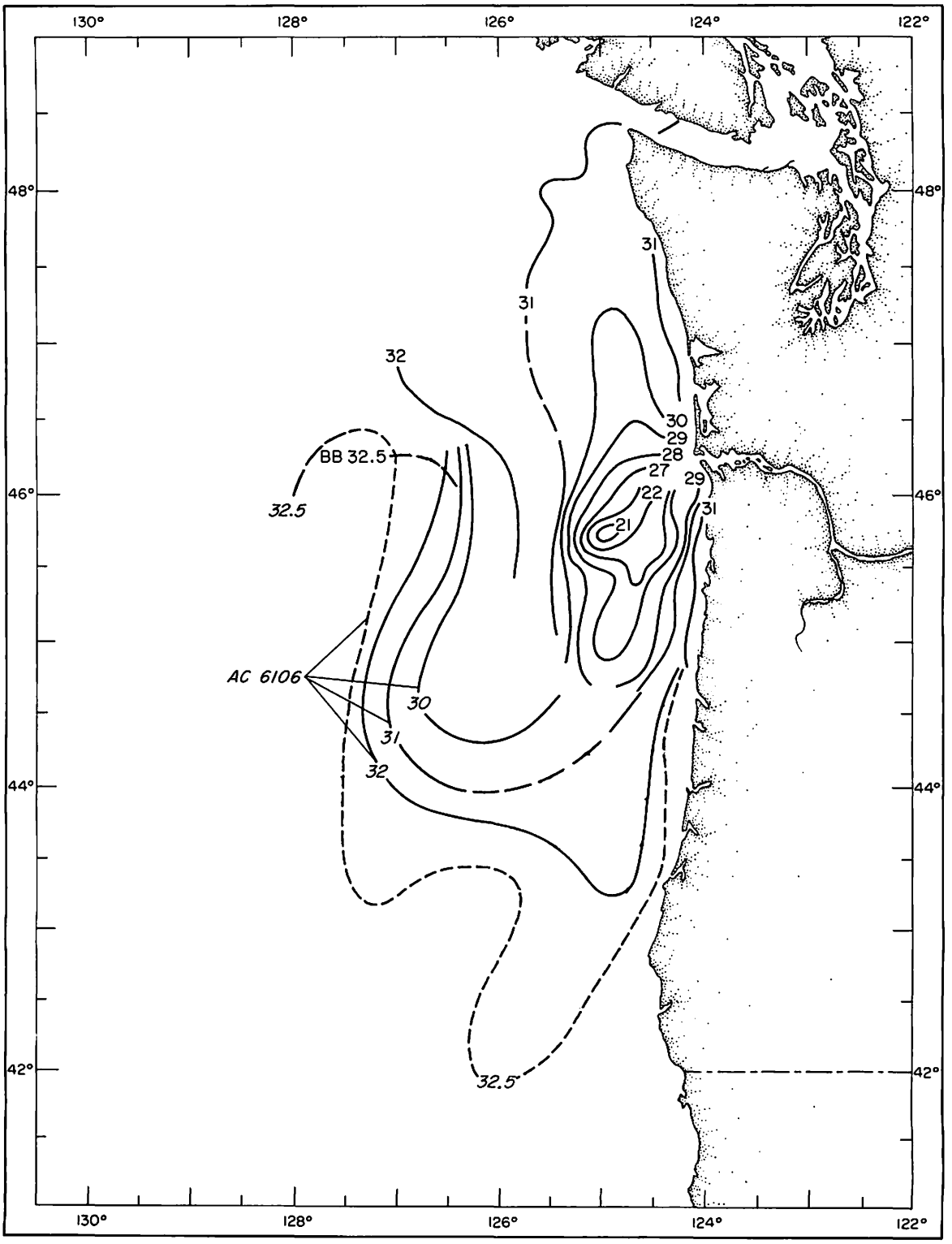

Fig. 110. Response of surface salinity patterns to the wind.

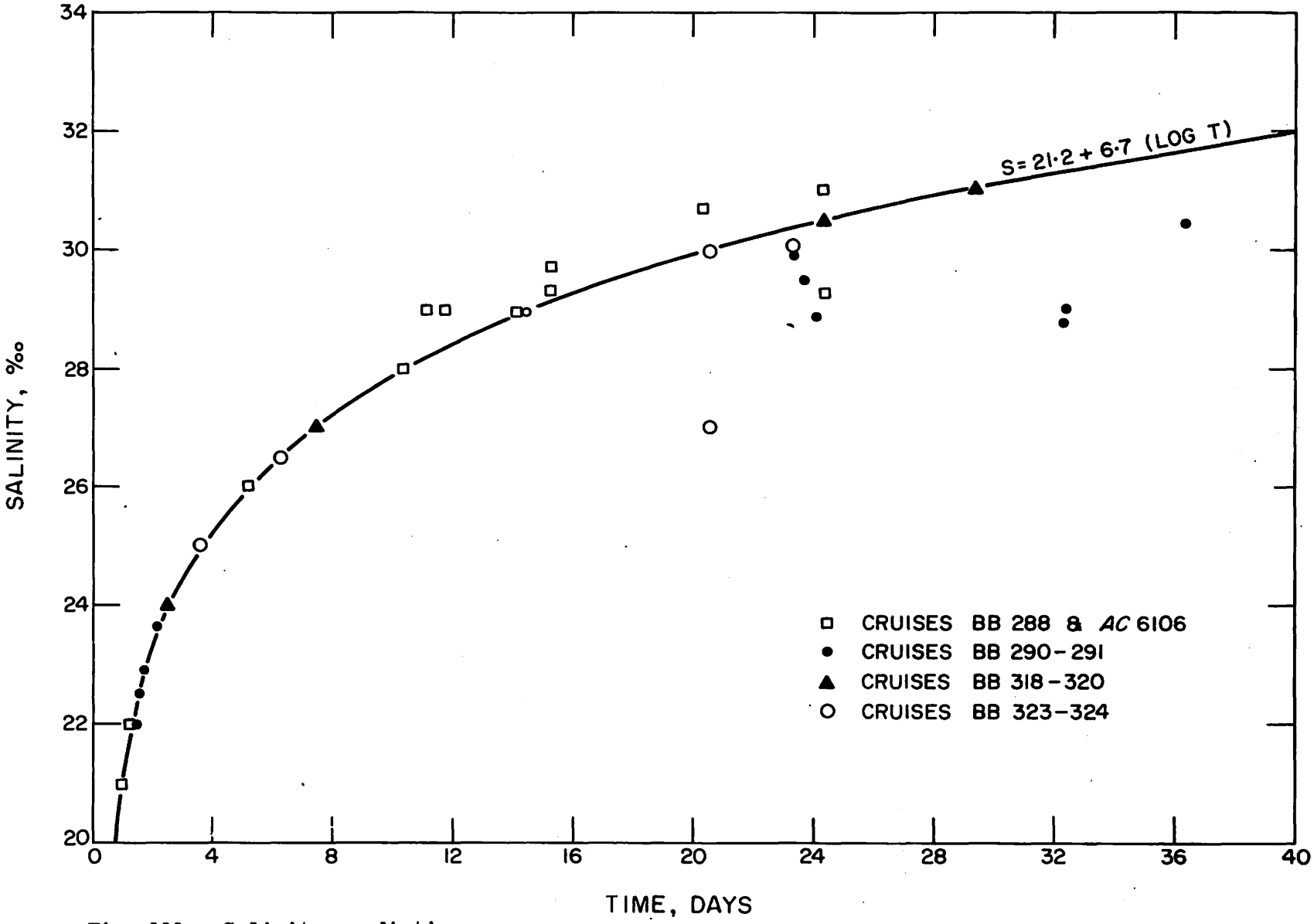

Fig. 111. Salinity prediction curve.

REFERENCES

Budinger, T. F., L. K. Coachman, and C. A. Barnes
1964. Columbia River effluent in the Northeast Pacific Ocean, 1961, 1962: Selected aspects of physical oceanography. Univ. Washington, Dept. Oceanography Tech. Rept. no. 99 (ref. M63-18). 78 p.

Ekman, V. W.
1902. Om jordrotationens inverkan på vindströmmar i hafvet. Nyt Magazin for Naturvidenskaberne 40:37.

Fjeldstad, J. E.
1929. Ein Beitrag zur Theorie der winderzeugten Meeresströmungen. Beit. Geophysik 23:237-247.

Fjeldstad, J. E.
1936. Results of tidal observations. Scientific results of the Norwegian north polar expedition with the Maud, 1918-1925, vol. 4, no. 4. 88 p.

Gordon, A. H.
1950. The ratio between observed velocities of the wind at 50 ft. and 2000 ft. over the North Atlantic Ocean. Quart. J. Roy. Meteorol. Soc. 76:344-348.

Leipper, D. F.
1959. The classical hydrographic procedure and its relation to the physical and chemical properties of sea water. In Physical and Chemical Properties of Sea Water. Publ. no. 600, National Academy of Sciences, National Research Council. p. 1-9.

Montgomery, R. B.
1936. Transport of surface water due to the wind system over the North Atlantic. Papers Phys. Oceanog. Meteorol. 4(3):23-30.

Reid, R. O.
1959. Influence of some errors in the equation of state or in observations on geostrophic currents. In Physical and Chemical Properties of Sea Water. Publ. no. 600, National Academy of Sciences, National Research Council. p. 10-29.

Rossby, C. G. and R. B. Montgomery
1935. The layer of frictional influence in wind and ocean currents. Papers Phys. Oceanog. Meteorol. 3(3):12-14.

Sverdrup, H. U.
1929. The waters on the North Siberian Shelf. Scientific results of the Norwegian north polar expedition with the Maud, 1918-1925, vol. 4, no. 2. 131 + 175 p.

Sverdrup, H. U., M. W. Johnson, and R. H. Fleming
1942. The oceans: Their physics, chemistry, and general biology. Prentice-Hall, Englewood Cliffs, New Jersey. 1087 p.

U.S. Army Corps of Engineers
1960. Interim report on 1959 current measuring program--Columbia River at mouth, Oregon and Washington, vol. I-IV. U.S. Army Engineer District, Portland, Oregon.

U.S. Geological Survey, Water Resources Division
1961- Weekly runoff report, Pacific Northwest water resources.
1963. Current Records Center, Portland, Oregon.

Wilson, G. W.
1960. Note on surface wind stress over water at low and high wind speeds. J. Geophys. Res. 65:3377-3382.

APPENDIX

Publications

Anderson, George C.

1963. Effects of the distribution of Columbia River water on certain aspects of the biology of the area. Trans. Am. Geophys. Union 44(1):207-208. (Abstr.)

1964. The seasonal and geographic distribution of primary productivity off the Washington and Oregon coasts. Limnol. Oceanog. 9:284-302. (Contribution no. 315 of the Department of Oceanography, University of Washington)

1965. Fractionation of phytoplankton populations off the Washington and Oregon coasts. Limnol. Oceanog. 10:477-480. (Contribution no. 348 of the Department of Oceanography, University of Washington and AEC rept. no. RLO-1725-46)

Anderson, George C. and Karl Banse

1963. Hydrography and phytoplankton production. In Proceedings of the Conference on Primary Productivity Measurement, Marine and Freshwater (M. S. Doty, ed.). U.S. Atomic Energy Commission, TID-7633. p. 61-71. (Contribution no. 251 of the Department of Oceanography, University of Washington. Also distributed as Tech. Rept. no. 95)

1965. Chlorophylls in marine phytoplankton: Correlations with carbon uptake. Deep-Sea Res. 12:531-533. (Contribution no. 350 of the Department of Oceanography, University of Washington and AEC rept. no. RLO-1725-47)

Budinger, Thomas F., Lawrence K. Coachman, and Clifford A. Barnes

1963. Description of the Columbia River plume and certain aspects of the mixing of river water in the sea. Trans. Am. Geophys. Union 44(1):208-209. (Abstr.)

Duxbury, Alyn C.

1965. The union of the Columbia River and the Pacific Ocean--General features. In Ocean Science and Ocean Engineering 1965, vol. II. p. 914-922. Marine Technology Society, Washington, D.C. Oral presentation at Ocean Science and Ocean Engineering Conference, June 1965, Washington, D.C. (Contribution no. 358 of the Department of Oceanography, University of Washington and AEC rept. no. RLO-1725-5)

Gross, M. Grant

1963. Radioactivity of marine sediments near the Columbia River in 1962. Trans. Am. Geophys. Union 44(1):68. (Abstr.)

1963. Radioactivity of marine sediments near the Columbia River. Trans. Am. Geophys. Union 44(1):210. (Abstr.)

Gross, M. Grant (continued)
1965. Carbonate contents of surface sediments from the Northeast Pacific Ocean. Northwest Sci. 39(3):85-92. (Contribution no. 343 of the Department of Oceanography, University of Washington and AEC rept. no. RLO-1725-44)

1966. Distribution of radioactive marine sediment derived from the Columbia River. J. Geophys. Res. 71(8):2017-2021. (Contribution no. 366 of the Department of Oceanography, University of Washington and AEC rept. no. RLO-1725-14)

Gross, M. Grant, Clifford A. Barnes, and Gordeon K. Riel
1964. Radioactivity of the Columbia River discharge in the Northeast Pacific Ocean in August 1963. Trans. Am. Geophys. Union 45(1): 65. (Abstr.)

1965. Radioactivity of the Columbia River effluent. Science 149(3688): 1088-1090. (Contribution no. 344 of the Department of Oceanography, University of Washington and AEC rept. no. RLO-1725-45)

Hansen, Donald V.
1965. Currents and mixing in the Columbia River estuary. In Ocean Science and Ocean Engineering 1965, vol. II. p. 943-955. Marine Technology Society, Washington, D.C. Oral presentation at Ocean Science and Ocean Engineering Conference, June 1965, Washington, D.C. (Contribution no. 357 of the Department of Oceanography, University of Washington and AEC rept. no RLO-1725-4)

Hobson, Louis A.
1966. Some influences of the Columbia River effluent on marine phytoplankton during January 1961. Limnol. Oceanog. 11(2):223-234. (Contribution no. 367 of the Department of Oceanography, University of Washington and AEC rept. no. RLO-1725-50)

Ling, Hsin-Yi
1965. The tintinnid Parafavella gigantea (Brandt), Kofoid & Campbell, 1929, in the North Pacific Ocean. J. Paleontol. 39(4):721-723. (Contribution no. 329 of the Department of Oceanography, University of Washington and AEC rept. no. RLO-1725-43)

1966. The radiolarian Protocystis thomsoni (Murray) in the Northeast Pacific Ocean. Micropaleontology 12(2):203-214. (Contribution no. 340 of the Department of Oceanography, University of Washington and AEC rept. no. RLO-1725-54)

McManus, Dean A.
1963. A criticism of certain usage of the phi-notation. J. Sediment. Petrol. 33(3):670-674. (Contribution no. 266 of the Department of Oceanography, University of Washington)

McManus, Dean A. (continued)

1964. Major bathymetric features near the coast of Oregon, Washington and Vancouver Island. Northwest Sci. 38(3):65-82. (Contribution no. 299 of the Department of Oceanography, University of Washington and AEC rept. no. RLO-1725-25)

1965. A large-diameter coring device. Deep-Sea Res. 12(2):227-232. (Contribution no. 332 of the Department of Oceanography, University of Washington and AEC rept. no. RLO-1725-28)

1966. A study of maximum load for small-diameter sieves. J. Sediment. Petrol. 35(4):792-796. (Contribution no. 322 of the Department of Oceanography, University of Washington and AEC rept. no. RLO-1725-55)

Morse, Betty-Ann and Noel McGary

1965. Graphic representation of the salinity distribution near the Columbia River mouth. In Ocean Science and Ocean Engineering 1965, vol. II. Marine Technology Society, Washington, D.C. Oral presentation at Ocean Science and Ocean Engineering Conference, June 1965, Washington, D.C. (Contribution no. 356 of the Department of Oceanography, University of Washington and AEC rept. no. RLO-1725-3)

Nayudu, Y. Rammohanroy and Betty J. Enbysk

1964. Bio-lithology of Northeast Pacific surface sediments. Marine Geology, 2(4):310-342. (Contribution no. 282 of the Department of Oceanography, University of Washington and AEC rept. no. RLO-1725-42)

Sanger, Gerald A.

1965. Observations of wildlife off the coast of Washington and Oregon in 1963, with notes on the Laysan albatross (Diomedea immutabilis) in this area. The Murrelet 46(1):1-6. (Contribution no. 331 of the Department of Oceanography, University of Washington and AEC rept. no. RLO-1725-27)

Stefánsson, Unnsteinn and Francis A. Richards

1963. Silicate-salinity relationships in the Columbia River effluent. Trans. Am. Geophys. Union 44(1):213. (Abstr.)

1963. Processes contributing to the nutrient distribution of the Columbia River and Strait of Juan de Fuca. Limnol. Oceanog. 8(4):394-410. (Contribution no. 292 of the Department of Oceanography, University of Washington)

1964. Distribution of dissolved oxygen, density, and nutrients off the Washington and Oregon coasts. Deep-Sea Res. 11(3):355-380. (Contribution no. 314 of the Department of Oceanography, University of Washington and AEC rept. no. RLO-1725-26)

Whetten, John T.
1966. Sediments from the Lower Columbia River and the origin of graywacke. Science 152(3725):1057-1058. (Contribution no. 382 of the Department of Oceanography, University of Washington and AEC rept. no. RLO-1725-49)

Abstracts

Barnes, Clifford A. and M. Grant Gross
1966. Distribution at sea of Columbia River water and its load of radionuclides. In Abstracts of Papers for Symposium on the Disposal of Radioactive Wastes into Seas, Oceans and Surface Waters. Vienna, 16-20 May 1966. International Atomic Energy Agency SM-72/17. (AEC rept. no. RLO-1725-41)

Embysk, Betty J. and Susan C. Cooper
1964. Biogenic elements in surface sediments of Cascadia Basin, Northeast Pacific. Geological Society of America, Cordilleran Section, 60th Annual Meeting, Seattle. p. 31-32.

Gross, M. Grant
1966. Organic carbon in surface sediment from the Northeast Pacific Ocean. Oral presentation at the American Society of Limnology and Oceanography, Seattle, 13-18 June 1966. (AEC rept. no. RLO-1725-56)

Hanson, L. G. and J. T. Whetten
1965. Particle size distribution of Lower Columbia River reservoir sediments. Oral presentation at the Geological Society of America, Kansas City, Kansas, 5 November 1965. (AEC rept. no. RLO-1725-51)

McManus, Dean A.
1964. Bottom sediment types in Cascadia Basin, Northeast Pacific Ocean. Geological Society of America, Cordilleran Section, 60th Annual Meeting, Seattle. p. 44-45.

Whetten, John T.
1966. Modern graywacke-type sediments from the Columbia River. Oral presentation at the Geological Society of America, Reno, 8 April 1966. (AEC rept. no. RLO-1725-53)

Whetten, J. T. and L. G. Hanson
1965. Mineral and chemical composition of Lower Columbia River reservoir sediments. Oral presentation at the Geological Society of America, Kansas City, Kansas, 5 November 1965. (AEC rept. no. RLO-1725-52)

Literature Survey

Anderson, George C., Clifford A. Barnes, Thomas F. Budinger, Cuthbert M. Love, and Dean A. McManus.
1961. The Columbia River discharge area of the Northeast Pacific Ocean: A literature survey. University of Washington, Department of Oceanography (Ref. M61-25)

Technical Reports

Anderson, George C.
1963. Columbia River effluent in the Northeast Pacific Ocean, 1961, 1962: Selected aspects of phytoplankton distribution and production. Univ. Washington, Dept. Oceanography Tech. Rept. no. 96. 77 p.

Anderson, George C. and Karl Banse
1963. Hydrography and phytoplankton production. Univ. Washington, Dept. Oceanography Tech. Rept. no. 95. 21 p. (Also contribution no 251 of the Department of Oceanography, University of Washington--see Publications)

Andrews, Robert S.
1965. Modern sediments of Willapa Bay, Washington: A coastal plain estuary. Univ. Washington, Dept. Oceanography Tech. Rept. no. 118. 43 p. (AEC rept. no. RLO-1725-6)

Ballard, Ronald L.
1964. Distribution of beach sediment near the Columbia River. Univ. Washington, Dept. Oceanography Tech. Rept. no. 98. 82 p.

Budinger, Thomas F., Lawrence K. Coachman, and Clifford A. Barnes
1964. Columbia River effluent in the Northeast Pacific Ocean, 1961, 1962: Selected aspects of physical oceanography. Univ. Washington, Dept. Oceanography Tech. Rept. no. 99. 78 p.

Gross, M. Grant
1963. Preliminary report on the sediments and radioactivity in the vicinity of the Columbia River effluent. Univ. Washington, Dept. Oceanography Tech. Rept. no. 84. 32 p.

Hobson, Louis A.
1964. Some influences of the Columbia River effluent on marine phytoplankton during January 1961. Univ. Washington, Dept. Oceanography Tech. Rept. no. 100. 46 p.

Love, Cuthbert M.
1963. Physical, chemical, and biological data from the Northeast Pacific Ocean: Columbia River effluent area, January - June 1961. Univ. Washington, Dept. Oceanography Tech. Rept. no. 86. 405 p.

Love, Cuthbert M. with the Data Analysis Staff
1964. Physical, chemical, and biological data from the Northeast Pacific Ocean: Columbia River effluent area, July - August 1961. Univ. Washington, Dept. Oceanography Tech. Rept. no. 112. 260 p.

1964. Physical, chemical, and biological data from the Northeast Pacific Ocean: Columbia River effluent area, September - December 1961. Univ. Washington, Dept. Oceanography Tech. Rept. no. 115, vol. I-II.

1965. Physical, chemical, and biological data from the Northeast Pacific Ocean: Columbia River effluent area, January - October 1962. Univ. Washington, Dept. Oceanography Tech. Rept. no. 119, vol. I-V. (AEC rept. no. RLO-1725-15 through 19)

1966. Physical, chemical, and biological data from the Northeast Pacific Ocean: Columbia River effluent area, January - June 1963. Univ. Washington, Dept. Oceanography Tech. Rept. no 134, vol. I-VI. (AEC rept. no. RLO-1725-32 through 37)

Royse, Chester F., Jr.
1964. Sediments of Willapa submarine canyon. Univ. Washington, Dept. Oceanography Tech. Rept. no. 111. 62 p.

Unclassified
Security Classification

DOCUMENT CONTROL DATA · R&D

(Security classification of title, body of abstract and indexing annotation must be entered when the overall report is classified)

1. ORIGINATING ACTIVITY (Corporate author)
University of Washington, Department of Oceanography, Seattle, Washington 98105

2a. REPORT SECURITY CLASSIFICATION
Unclassified

2b. GROUP

3. REPORT TITLE
THE COLUMBIA RIVER EFFLUENT AND ITS DISTRIBUTION AT SEA, 1961-1963

4. DESCRIPTIVE NOTES (Type of report and inclusive dates)
Interim Report 1961-1963

5. AUTHOR(S) (Last name, first name, initial)
Duxbury, Alyn C.
Morse, Betty-Ann
McGary, Noel

6. REPORT DATE	7a. TOTAL NO. OF PAGES	7b. NO. OF REFS
June 1966	111	14

8a. CONTRACT OR GRANT NO.
Nonr-477(10) AT(45-1)-1385
Nonr-477(37) AT(45-1)-1725

b. PROJECT NO.
NR 083 012

c.

d.

9a. ORIGINATOR'S REPORT NUMBER(S)
Technical Report No. 156

9b. OTHER REPORT NO(S) (Any other numbers that may be assigned this report)
Reference M66-31
AEC-RLO-1725-62

10. AVAILABILITY/LIMITATION NOTICES
This report has been furnished to the OTS and DDC. Copies may be requested through these agencies.

11. SUPPLEMENTARY NOTES

12. SPONSORING MILITARY ACTIVITY
Office of Naval Research
San Francisco, California

13. ABSTRACT

Surveys off the Washington-Oregon coast by the Department of Oceanography, University of Washington, from 1961 through 1963 have provided salinity data for describing the Columbia River effluent in the Northeast Pacific Ocean. The data also have provided insight into the interactions between the observed distributions and the meteorological systems. Each salinity distribution is categorized into one of four distinct seasonal patterns, mainly influenced by river discharge and winds. The salinity distributions delineate the extent of the influence of the Columbia River effluent in the Northeast Pacific Ocean both horizontally with distance and vertically with depth. Also shown and discussed are the mean wind patterns for the area during this time period, their influence on the river outflow and their role in the transport of the dilute surface waters. A method is described for the prediction of the salinity distribution of the effluent from surface wind data.

DD FORM 1 JAN 64 1473

Unclassified
Security Classification

14. KEY WORDS	LINK A		LINK B		LINK C	
	ROLE	WT	ROLE	WT	ROLE	WT
Salinity distribution						
Effluent water						
Columbia River						
Northeast Pacific Ocean						
Washington–Oregon coast						
RV *Brown Bear*						
CNAV *Oshawa*						
RV *Acona*						
Columbia River discharge						
Surface winds						
Water transport						
Salinity prediction						
Seasonal variation						

INSTRUCTIONS

1. ORIGINATING ACTIVITY: Enter the name and address of the contractor, subcontractor, grantee, Department of Defense activity or other organization *(corporate author)* issuing the report.

2a. REPORT SECURITY CLASSIFICATION: Enter the overall security classification of the report. Indicate whether "Restricted Data" is included. Marking is to be in accordance with appropriate security regulations.

2b. GROUP: Automatic downgrading is specified in DoD Directive 5200.10 and Armed Forces Industrial Manual. Enter the group number. Also, when applicable, show that optional markings have been used for Group 3 and Group 4 as authorized.

3. REPORT TITLE: Enter the complete report title in all capital letters. Titles in all cases should be unclassified. If a meaningful title cannot be selected without classification, show title classification in all capitals in parenthesis immediately following the title.

4. DESCRIPTIVE NOTES: If appropriate, enter the type of report, e.g., interim, progress, summary, annual, or final. Give the inclusive dates when a specific reporting period is covered.

5. AUTHOR(S): Enter the name(s) of author(s) as shown on or in the report. Enter last name, first name, middle initial. If military, show rank and branch of service. The name of the principal author is an absolute minimum requirement.

6. REPORT DATE: Enter the date of the report as day, month, year; or month, year. If more than one date appears on the report, use date of publication.

7a. TOTAL NUMBER OF PAGES: The total page count should follow normal pagination procedures, i.e., enter the number of pages containing information.

7b. NUMBER OF REFERENCES: Enter the total number of references cited in the report.

8a. CONTRACT OR GRANT NUMBER: If appropriate, enter the applicable number of the contract or grant under which the report was written.

8b, 8c, & 8d. PROJECT NUMBER: Enter the appropriate military department identification, such as project number, subproject number, system numbers, task number, etc.

9a. ORIGINATOR'S REPORT NUMBER(S): Enter the official report number by which the document will be identified and controlled by the originating activity. This number must be unique to this report.

9b. OTHER REPORT NUMBER(S): If the report has been assigned any other report numbers *(either by the originator or by the sponsor)*, also enter this number(s).

10. AVAILABILITY/LIMITATION NOTICES: Enter any limitations on further dissemination of the report, other than those imposed by security classification, using standard statements such as:

(1) "Qualified requesters may obtain copies of this report from DDC."

(2) "Foreign announcement and dissemination of this report by DDC is not authorized."

(3) "U. S. Government agencies may obtain copies of this report directly from DDC. Other qualified DDC users shall request through _____."

(4) "U. S. military agencies may obtain copies of this report directly from DDC. Other qualified users shall request through _____."

(5) "All distribution of this report is controlled. Qualified DDC users shall request through _____."

If the report has been furnished to the Office of Technical Services, Department of Commerce, for sale to the public, indicate this fact and enter the price, if known.

11. SUPPLEMENTARY NOTES: Use for additional explanatory notes.

12. SPONSORING MILITARY ACTIVITY: Enter the name of the departmental project office or laboratory sponsoring *(paying for)* the research and development. Include address.

13. ABSTRACT: Enter an abstract giving a brief and factual summary of the document indicative of the report, even though it may also appear elsewhere in the body of the technical report. If additional space is required, a continuation sheet shall be attached.

It is highly desirable that the abstract of classified reports be unclassified. Each paragraph of the abstract shall end with an indication of the military security classification of the information in the paragraph, represented as *(TS)*, *(S)*, *(C)*, or *(U)*.

There is no limitation on the length of the abstract. However, the suggested length is from 150 to 225 words.

14. KEY WORDS: Key words are technically meaningful terms or short phrases that characterize a report and may be used as index entries for cataloging the report. Key words must be selected so that no security classification is required. Identifiers, such as equipment model designation, trade name, military project code name, geographic location, may be used as key words but will be followed by an indication of technical context. The assignment of links, roles, and weights is optional.

UNCLASSIFIED TECHNICAL REPORTS DISTRIBUTION LIST
for OCEANOGRAPHIC CONTRACTORS
of the OCEAN SCIENCE AND TECHNOLOGY GROUP
of the OFFICE OF NAVAL RESEARCH
(Revised April 1966)

DEPARTMENT OF DEFENSE

Director of Defense Research
& Engineering
Office of Secretary of Defense
Washington, D.C. 20301
1 Attn: Office, Assistant Director
(Research)

Navy

2 Office of Naval Research
Ocean Science & Technology Group
(Code 408P)
Office of Naval Research
Washington, D.C. 20360
1 Attn: Surface Branch (Code 463)
1 Attn: Undersea Programs (Code 446)
1 Attn: Field Projects (Code 418)
1 Attn: Geography Branch (Code 414)

1 Commanding Officer
Office of Naval Research Branch
495 Summer Street
Boston, Massachusetts 02110

1 Commanding Officer
Office of Naval Research Branch
207 West 24th Street
New York, New York 10011

1 Commanding Officer
Office of Naval Research Branch
219 S. Dearborn Street
Chicago, Illinois 60604

1 Commanding Officer
Office of Naval Research Branch
1000 Geary Street
San Francisco, California 94109

1 Commanding Officer
Office of Naval Research Branch
1030 East Green Street
Pasadena, California 91101

5 Commanding Officer
Office of Naval Research Branch
Navy #100, Fleet Post Office
New York, New York 09510

6 Director
Naval Research Laboratory
Attn: Code 5500
Washington, D.C. 20390

(Note: 3 copies are forwarded by the above addressee to the British Joint Services Staff for further distribution in England and Canada.)

2 Commander
U.S. Naval Oceanographic Office
Washington, D.C. 20390
Attn: Library (Code 1640)

Chief, Bureau of Naval Weapons
Department of the Navy
Washington, D.C. 20360
1 Attn: FASS
1 Attn: RU-222

1 Office of the U.S. Naval Weather
Service
U.S. Naval Station
Washington, D.C. 20390

1 Chief, Bureau of Yards & Docks
Office of Research
Department of the Navy
Washington, D.C. 20390
Attn: Code 70

U.S. Navy Electronics Laboratory
San Diego, California 92152

1 Attn: Code 3102

1 Attn: Code 3060C

1 Commanding Officer & Director
U.S. Naval Civil Engineering Laboratory
Port Hueneme, California 93401

1 Commanding Officer
Pacific Missile Range
Pt. Mugu, California

1 Commander, Naval Ordnance Laboratory
White Oak
Silver Spring, Maryland 20910

1 Commanding Officer
Naval Ordnance Test Station
China Lake, California 93557

1 Commanding Officer
Naval Radiological Defense Laboratory
San Francisco, California 94135

1 Commanding Officer
U.S. Naval Underwater Ordnance Station
Newport, Rhode Island 02844

Chief, Bureau of Ships
Department of the Navy
Washington, D.C. 20360

1 Attn: Code 1622B

1 Officer-in-Charge
U.S. Navy Weather Research Facility
Naval Air Station, Bldg. R-48
Norfolk, Virginia 23511

1 Commanding Officer
U.S. Navy Air Development Center
Johnsville, Pennsylvania
Attn: NADC Library

1 U.S. Fleet Weather Central Joint Typhoon Warning Center
COMNAVMARIANAS Box 12
San Francisco, California

1 Superintendent
U.S. Naval Academy
Annapolis, Maryland 21402

2 Department of Meteorology & Oceanography
U.S. Naval Postgraduate School
Monterey, California 93940

1 Commanding Officer
U.S. Naval Underwater Sound Laboratory
New London, Connecticut 06321

1 Commanding Officer
U.S. Navy Mine Defense Laboratory
Panama City, Florida 32402

1 Officer-in-Charge
U.S. Fleet Numerical Weather Facility
U.S. Naval Postgraduate School
Monterey, California 93940

Air Force

1 Hdqtrs., Air Weather Service
(AWSS/TIPD)
U.S. Air Force
Scott Air Force Base, Illinois

1 ARCRL (CRZF)
L. G. Hanscom Field
Bedford, Massachusetts

Army

1 Army Research Office
Office of the Chief of R & D
Department of the Army
Washington, D.C. 20310

1 U.S. Army Beach Erosion Board
5201 Little Falls Road, N.W.
Washington, D.C. 20016

OTHER U.S. GOVERNMENT AGENCIES

20 Defense Documentation Center
Cameron Station
Alexandria, Virginia 20305

2 National Research Council
2101 Constitution Avenue, N.W.
Washington, D.C. 20418
Attn: Committee on Undersea Warfare
Attn: Committee on Oceanography

1 Laboratory Director
California Current Resources Laboratory
Bureau of Commercial Fisheries
P.O. Box 271
La Jolla, California 92038

1 Commanding Officer
Coast Guard Oceanographic Unit
Bldg. 159, Navy Yard Annex
Washington, D.C. 20390

Environmental Sciences Services Admin.
U.S. Department of Commerce
Washington, D.C. 20235
1 Attn: Institute of Oceanography
1 Attn: Institute of Atmospheric Sciences

1 Geological Division
Marine Geology Unit
U.S. Geological Survey
Washington, D.C. 20240

1 Director
U.S. Army Engineers Waterways Experiment Station
Vicksburg, Mississippi 49097
Attn: Research Center Library

1 Laboratory Director
California Current Resources Laboratory
Bureau of Commercial Fisheries
P.O. Box 271
La Jolla, California 92038

1 Laboratory Director
Bureau of Commercial Fisheries
Biological Laboratory
450-B Jordon Hall
Stanford, California 94305

1 Bureau of Commercial Fisheries
U.S. Fish & Wildlife Service
Post Office Box 3830
Honolulu, Hawaii 96812

1 Laboratory Director
Biological Laboratory
Bureau of Commercial Fisheries
P.O. Box 3098, Fort Crockett
Galveston, Texas 77552

1 Laboratory Director
Biological Laboratory
Bureau of Commercial Fisheries
P.O. Box 1155
Juneau, Alaska 99801

1 Laboratory Director
Biological Laboratory
Bureau of Commercial Fisheries
P.O. Box 6
Woods Hole, Massachusetts 02543

1 Laboratory Director
Biological Laboratory
Bureau of Commercial Fisheries
P.O. Box 280
Brunswick, Georgia 31521

1 Laboratory Director
Tuna Resources Laboratory
Bureau of Commercial Fisheries
P.O. Box 271
La Jolla, California 92038

1 Bureau of Sport Fisheries & Wildlife
U.S. Fish and Wildlife Service
Librarian
Sandy Hook Marine Laboratory
P.O. Box 428
Highlands, New Jersey 07732

1 Laboratory Director
Biological Laboratory
Bureau of Commercial Fisheries
#75 Virginia Beach Drive
Miami, Florida 33149

1 Director, Bureau of Commercial Fisheries
U.S. Fish & Wildlife Service
Department of Interior
Washington, D.C. 20240

1 Bureau of Commercial Fisheries
Biological Laboratory, Oceanography
2725 Montlake Boulevard East
Seattle, Washington 98102

1 Director
National Oceanographic Data Center
Washington, D.C. 20390

1 Library, U.S. Weather Bureau
Washington, D.C. 20235

1 Director, Bureau of Commercial Fisheries
U.S. Fish & Wildlife Service
Department of Interior
Washington, D.C. 20240

1 Dr. Gene A. Rusnak
U.S. Geological Survey
Marine Geology and Hydrology
345 Middlefield Road
Menlo Park, California 94025

1 Assistant Director
Oceanography Museum of Natural History
Smithsonian Institution
Washington, D.C. 20560

1 Advanced Research Projects Agency
Attn: Nuclear Test Detection Office
The Pentagon
Washington, D.C. 20310

1 Chief, Marine Science Center
Coast & Geodetic Survey
U.S. Department of Commerce
Lake Union Base
1801 Fairview Avenue East
Seattle, Washington 98102

RESEARCH LABORATORIES

2 Director
Woods Hole Oceanographic Institution
Woods Hole, Massachusetts 02543

1 Director
Narragansett Marine Laboratory
University of Rhode Island
Kingston, Rhode Island 02881

1 Bingham Oceanographic Laboratories
Yale University
New Haven, Connecticut 06520

1 Gulf Coast Research Laboratory
Ocean Springs, Mississippi 39564
Attn: Librarian

1 Chairman, Department of Meteorology & Oceanography
New York University
New York, New York 10453

1 Director
Lamont Geological Observatory
Columbia University
Palisades, New York 10964

1 Director
Hudson Laboratories
145 Palisade Street
Dobbs Ferry, New York 10522

1 Great Lakes Research Division
Institute of Science & Technology
University of Michigan
Ann Arbor, Michigan

1 Director
Chesapeake Bay Institute
Johns Hopkins University
Baltimore, Maryland 21218

1 Director, Marine Laboratory
University of Miami
#1 Rickenbacker Causeway
Miami, Florida 33149

1 Lieutenant Nestor C. L. Granelli
Montevideo 459
Buenos Aires, Argentina

2 Head, Department of Oceanography
& Meteorology
Texas A & M University
College Station, Texas 77843

1 Director
Scripps Institution of Oceanography
La Jolla, California 92083

1 Allan Hancock Foundation
University Park
Los Angeles, California 90007

1 Head, Department of Oceanography
Oregon State University
Corvallis, Oregon 97331

1 Director, Artic Research Laboratory
Pt. Barrow, Alaska 99723

1 Head, Department of Oceanography
University of Washington
Seattle, Washington 98105

1 Geophysical Institute of the
University of Alaska
College, Alaska 99735

1 Director
Bermuda Biological Station
for Research
St. Georges, Bermuda

1 Director, Hawaiian Marine Laboratory
University of Hawaii
Honolulu, Hawaii 96825

1 President
Osservatorio Geofisico Sperimentale
Trieste, Italy

1 Department of Engineering
University of California
Berkeley, California 94720

1 Applied Physics Laboratory
University of Washington
1013 N.E. Fortieth Street
Seattle, Washington 98105

1 Director
Ocean Research Institute
University of Tokyo
Tokyo, Japan

1 Marine Biological Association of
the United Kingdom
The Laboratory
Citadel Hill
Plymouth, England

1 New Zealand Oceanographic Institute
Department of Scientific and
Industrial Research
P.O. Box 8009
Wellington, New Zealand
Attn: Librarian

1 Mr. J. A. Gast
Wildlife Building
Humboldt State College
Arcata, California 95521

1 Department of Geodesy & Geophysics
Cambridge University
Cambridge, England

1 Institute of Geophysics
University of Hawaii
Honolulu, Hawaii 96825

1 Division of Engineering & Applied
Physics
Harvard University
Cambridge, Massachusetts 02138

1 Underwater Warfare Division
of the Norwegian Defense Research
Establishment
Karljohansvern, Horten, Norway

1 Department of Geology & Geophysics
Massachusetts Institute of Technology
Cambridge, Massachusetts 02139

1 Marine Science Center
Lehigh University
Bethlehem, Pennsylvania 18015